Staphylococcus aureus and Fatty Acids: Impact on Membrane Function and Signaling

By

Zachary DeMars
B.Sc. Kansas State University, 2016

Submitted to the graduate degree program in Microbiology and the Graduate Faculty of the University of Kansas in partial fulfilment of the requirements for the degree of Doctor of Philosophy.

_____

Advisor: Jeffrey Bose, Ph.D.

_____

Wolfram Zueckert, Ph.D.

_____

Indranil Biswas, Ph.D.

_____

Joseph Lutkenhaus, Ph.D.

_____

Aron Fenton, Ph.D.

Date Defended: April 9, 2021

The dissertation committee for Zachary DeMars certifies that this is the approved version of the following dissertation:

Staphylococcus aureus and Fatty Acids: Impact on Membrane Function and Signaling

_____

Advisor: Jeffrey Bose, Ph.D.

_____

Graduate Director: Jianming Qiu, Ph.D.

Date Approved: April 12, 2021

Abstract

Staphylococcus aureus can utilize exogenous fatty acids for phospholipid synthesis. The fatty acid kinase FakA is essential for this utilization by phosphorylating exogenous fatty acids for incorporation into lipids. How exogenous fatty acid utilization from the environment via FakA affects the composition and function of the phospholipid membrane, central metabolism, and virulence factor regulation is not well understood. We found that inactivation of the exogenous fatty acid utilization system through genetic deletion of *fakA* resulted in a membrane that is more rigid than membranes of wild-type *S. aureus*. Central metabolism, particularly the production and consumption of acetate, was significantly altered resulting in a more oxidized cellular environment when *fakA* was deleted. Both the accumulation of free fatty acids within the cell of a *fakA* mutant and the presence of exogenous fatty acids in the growth medium decrease virulence factor production through the transmembrane domains of the two-component system SaeRS. In summary, we identified previously unknown roles for the exogenous fatty acid utilization system in maintaining membrane and metabolic homeostasis in addition to expanding our mechanistic understanding of how fatty acids negatively influence virulence factor expression.

Acknowledgements

Thank you to my wife, Shelby, for understanding and supporting me throughout my graduate school career. You have kept me focused and motivated to be successful and without you, I wouldn't have made it this far. To my parents, thank you for always supporting me in whatever I wanted to do in my life. Whether it be my love of sports or wanting to go to graduate school, you were always telling me I could do it and instilling a belief in me that has driven me to this day. Thank you to my grandparents, especially my Grandpa Jim. I still remember you telling me to go to school for as long as I possibly could. I have taken that literally. Without that, I probably wouldn't have thought about graduate school and science as an option for my career.

To Dr. Bose, thank you for helping me learn how to become a productive and critically thinking scientist. I'm glad you were willing to take a chance on me as a graduate student and allowed me to have the freedom to follow the path directed by the data. I appreciate you supporting my goals. I really appreciate the casual conversations we have about life, the science, and our hobbies. Without your mentorship, I would not have had the opportunities that I have today, and I am grateful for that.

To the Bose lab, thanks for dealing with me on a day-to-day basis. Thank you all for your willingness to help me with questions and helping me formulate my ideas. We persevered through the grind of doing research. Having you as companions made it much more manageable, enjoyable, and worthwhile. Thank you!

This research was supported by funding from the National Institute of Allergy and Infectious Diseases (NIAID) award R01AI121073 to Dr. Bose and a pilot project grant through award P20GM112117. I would like to thank Miranda Ridder for the help in harvesting mouse skin for

the mouse skin homogenate experiments. The lipid analyses described in this work were performed at the Kansas Lipidomics Research Center Analytical Laboratory and would not have been possible without Dr. Ruth Welti and Mary Roth. Instrument acquisition and lipidomics method development were supported by the National Science Foundation (including support from the Major Research Instrumentation program; current award DBI-1726527), K-IDeA Networks of Biomedical Research Excellence (INBRE) of National Institute of Health (P20GM103418), USDA National Institute of Food and Agriculture (Hatch/Multi-State project 1013013), and Kansas State University. I am grateful to Dr. Tim Garrett at the Southeast Center for Metabolomics the free fatty acid analysis done for this research (NIH grant #U24 DK097209). Thanks to Dr. Paul Fey at the University of Nebraska Medical Center for providing strains and Dr. Kelly Rice at the University of Florida for thoughtful discussion. In addition, thanks to Dr. Christopher Petucci along with members of the Southeast Center for Integrated Metabolomics for mass spectrometry analysis. Thank you to Dr. Taeok Bae at the University of Indiana Medical School of Medicine, Dr. Jovanka Voyich at the University of Montana, and Dr. Martin McGavin at Western University for their generosity and donation of strains and plasmids used in this study.

Table of Contents

List of Tables and Figures

Chapter 1

Chapter 2

Chapter 3

Chapter 4

Chapter 1: Literature Review

History and epidemiology of *Staphylococcus aureus*

When setting out to understand the cause of suppuration in humans in 1880, Sir Alexander Ogston identified and named the causal microorganism *Staphylococcus* [1]. Despite being discovered over 140 years ago, *Staphylococcus aureus* remains responsible for a large portion of infections in nearly all anatomical sites of the human body [2]. These infections became treatable upon the serendipitous discovery of penicillin by Sir Alexander Fleming [3]. Resistance of *S. aureus* to penicillin was rapidly identified in the clinic, foreshadowing the ability of many types of bacteria to rapidly become resistant to antibiotics. As new antibiotics were discovered in the following years, so to was resistance to these new antibiotics, including vancomycin and methicillin. In response to this multidrug resistance, the Centers for Disease Control and Prevention (CDC) identified *S. aureus* as a serious threat to human health.

This Gram-positive bacterium owes its name to the way it grows in grape-like clusters (*Staphyl-*) and typically has a golden pigment (*aureus*) when grown on laboratory media. It is a coagulase-positive organism, which separates this organism from coagulase-negative staphylococci (CoNS) and this difference is often used for clinical identification. *S. aureus* asymptomatically colonizes approximately 30% of the human population and colonizes up to 60% of the population intermittently, predominantly in the anterior nares and the skin [4]. Given the asymptomatic nature of most colonized individuals, *S. aureus* has historically been classified as an opportunistic pathogen, commonly causing disease in compromised individuals. Recently the idea of *S. aureus* being an opportunistic pathogen has been challenged because an increase in infections caused by *S. aureus* has been reported in healthy individuals within the general community (or community-associated) [5-9]. The increase in infections of healthy individuals, along with the keen ability of *S. aureus* to become resistant to antibiotics, particularly methicillin, requires a deeper and thorough

understanding of mechanisms used by *S. aureus* to cause infection. Additionally, alternative antibiotics are needed to both treat infections and alleviate the rise in antibiotic resistance.

S. aureus can establish infections in nearly any anatomical site of the human body, each representing a unique environment for the bacteria to survive in. Despite *S. aureus*' ability to infect different parts of the body, this bacterium prefers to colonize and cause skin and soft tissue infections (SSTIs), commonly resulting in abscess formation. Community-associated MRSA (CA-MRSA) caused a significant increase of skin infections in relatively healthy people during the 1990's, despite methicillin-resistance being present decades prior [5]. After the identification of CA-MRSA, the number of hospital emergency visits in the United States presenting with SSTI's nearly doubled from the early 1990's to the 2000's [10]. In particular, CA-MRSA strain USA300 is commonly considered to be the most dominant strain in the U.S. [9, 11, 12]. Why CA-MRSA is such a prolific pathogen is not fully understood. Evidence suggests that these strains overproduce virulence factors. For example, CA-MRSA clones often encodes Panton-Valentine leukocidins (PVL) [13] and phenol-soluble modulins (PSMs) [14] that are highly toxic to host cells and play roles in different stages of infection. These toxins, as well as other virulence determinants, will be covered in subsequent sections.

Central carbon metabolism and regulation

Central carbon metabolism

For an overview of central metabolism in *S. aureus*, see Figure 1.1. Carbon flow is greatly influenced by the presence of preferred carbon sources, such as glucose. *S. aureus* uses glycolysis to produce pyruvate. That pyruvate can be converted into multiple metabolites depending on the environment. Under aerobic conditions and in the presence of glucose, the TCA cycle is repressed

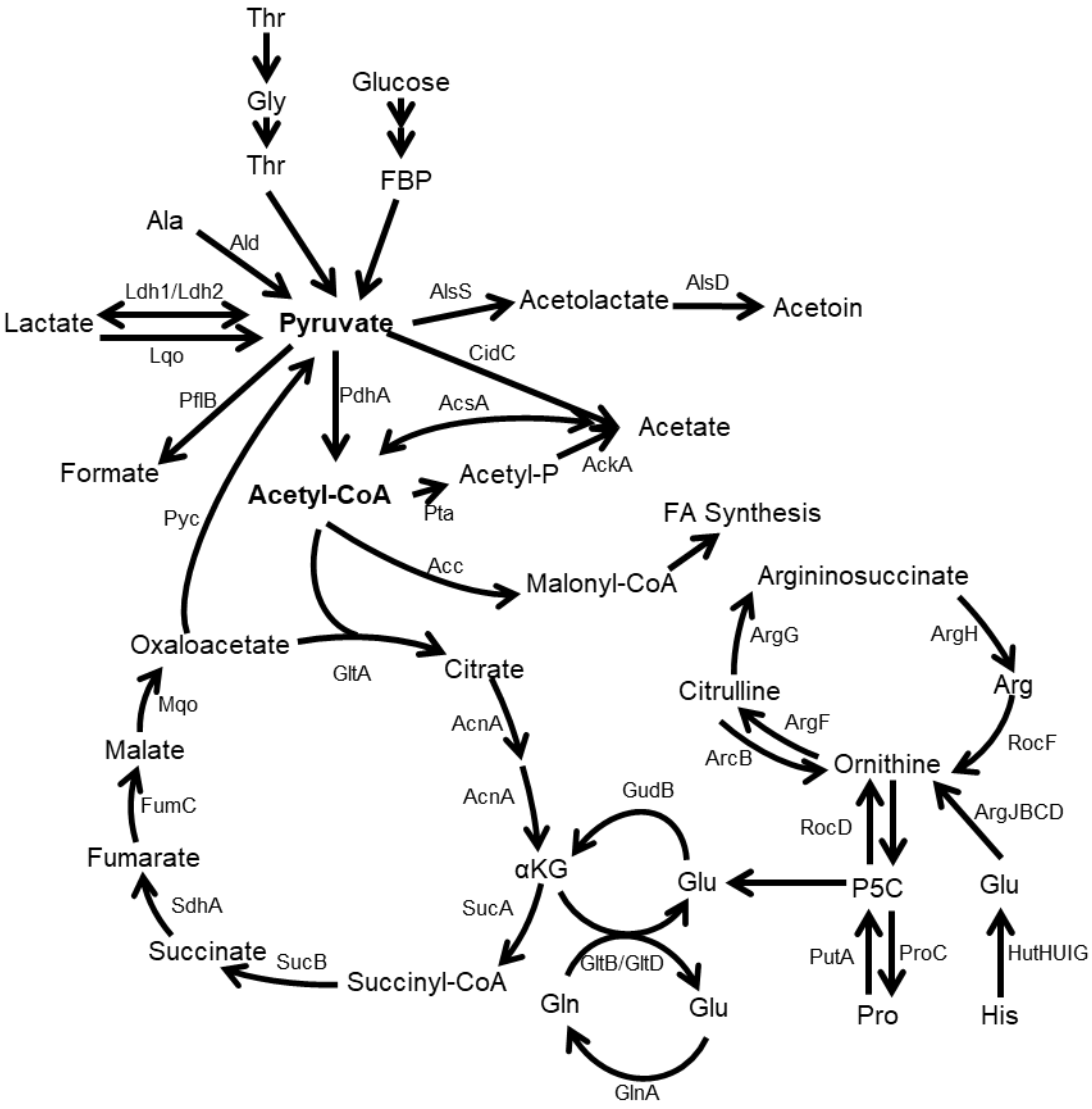
Thr
Gly
Thr
Glucose
FBP
Ala
Ald
Ldh1/Ldh2
Lactate
Lqo
Pyruvate
AlsS
Acetolactate
AlsD
Acetoin
CidC
PflB
PdhA
AcsA
Acetate
Formate
Acetyl-P
AckA
Acetyl-CoA
Pta
Pyc
FA Synthesis
Acc
Malonyl-CoA
Argininosuccinate
ArgG
ArgH
Oxaloacetate
GltA
Citrate
Citrulline
Arg
Mqo
AcnA
ArgF
RocF
Malate
ArcB
Ornithine
AcnA
GudB
RocD
ArgJBCD
FumC
Fumarate
αKG
Glu
P5C
Glu
SdhA
SucA
PutA
ProC
HutHUIG
Succinate
SucB
Succinyl-CoA
GltB/GltD
Gln
Glu
Pro
His
GlnA

Figure 1. 1

Figure 1.1. Overview of central metabolism in *S. aureus*. Enzyme abbreviations are as follows, including open reading frames from SAUSA300_FPR3757 genome. Ald- alanine dehydrogenase (SAUSA300_1331 and 1655), AlsS- α-acetolactate synthase (SAUSA300_2166), AlsD- α-acetolactate decarboxylase (SAUSA300_2165), CidC- pyruvate oxidase (SAUSA300_2477), PdhA- Pyruvate dehydrogenase E1 component (SAUSA300_0993), PflB- formate acetyltransferase (SAUSA300_0220), Pyc- pyruvate carboxylase (SAUSA300_1014), Pta-phostphate acetyltransferase (SAUSA300_0570), AckA- acetate kinase (SAUSA300_1657), Acetyl-CoA synthetase (SAUSA300_1679), Acc- acetyl-CoA carboxylase complex (AccA-SAUSA300_1646, AccD- SAUSA300_1647), Lqo- lactate:quinone oxidoreductase (SAUSA300_2541), Ldh1- lactate dehydrogenase 1 (SAUSA300_0235), Ldh2- lactate dehydrogenase 2 (SAUSA300_2537), GltA- citrate synthase (SAUSA300_1641), AcnA-aconitase hydratase (SAUSA300_1246). SucA- 2-oxoglutarate dehydrogenase complex E1 unit (SAUSA300_1306), SucB- 2-oxoglutarate dehydrogenase complex E2 unit (SAUSA300_1305), SdhA- succinase dehydrogenase (SAUSA300_1047), FumC- fumarate hydratase (SAUSA300_1801), Mqo- malate:quinone oxidoreductase (SAUSA300_2541 and 2312), GudB-glutamate dehydrogenase (SAUSA300_0861), GltB- glutamate synthase, large subunit (SAUSA300_0445), GltD- glutamate synthase, small subunit (SAUSA300_0446), GlnA-glutamine synthetase (SAUSA300_1201), PutA- proline dehydrogenase (SAUSA300_1711), ProC- pyrroline-5-carboxylate reductase (SAUSA300_1452), RocD/ArgD- ornithine aminotransferase (SAUSA300_0187 and 0860), HutH- hisitidine ammonia lyase (SAUSA300_0008), HutU- urocanate hydratase (SAUSA300_2278), HutI-imidazolonepropionase (SAUSA300_2277), HutG- formimidoylglutamase (SAUSA300_2281), ArgF- ornithine carbamoyltransferase (SAUSA300_1062), ArgG- argininosuccinate synthase (SAUSA300_0864), ArgH- argininiosuccinase lyase (SAUSA300_0863), ArgJ- arginine biosynthesis bifunctional protein (SAUSA300_0185), ArgB- acetylglutamate kinase (SAUSA300_0184), ArgC- N-acetyl-γ -glutamyl-phosphate reductase (SAUSA300_0186), and RocF- arginase (SAUSA300_2114).

[15] and much of the pyruvate is converted to acetyl-CoA and then acetate. That metabolism is accompanied with ATP being formed with substrate-level phosphorylation by the phosphotransacetylase-acetate kinase (Pta-AckA) pathway [16, 17]. Pyruvate is also converted to lactate to maintain redox balance via lactate dehydrogenases 1 and 2 (Ldh1 and Ldh2) [18, 19]. Once glucose and glycolytic intermediates are depleted from the environment, repression of the TCA cycle is relieved and acetate is re-assimilated to acetyl-CoA [20] for progression through the TCA cycle. This switch from glucose consumption and acetate production to acetate consumption is known as the "acetate switch" [21]. The acetyl-CoA produced from the consumption of acetate is then oxidized by the TCA cycle and results in the production of reduced electron carriers NADH and $FADH_2$.

The exhaustion of glucose from the environment relieves repression of the TCA cycle and allows carbon flow to proceed through this oxidative pathway. Energy produced by the TCA cycle is stored by the reduction of dinucleotide electron carriers with the reduction NAD^+ to NADH and FAD^+ to $FADH_2$. The reduced electron carriers are then oxidized by the electron transport chain which results in recycled NAD^+. The transfer of electrons from carriers (NADH) to acceptors (menaquinone) is coupled to the export of protons outside of the cell. This results in the formation of a membrane potential across the membrane with the exterior of the cell being more positive than the inside of the cell. The formation of a membrane potential is essentail for driving the production of ATP via the F_0F_1 ATPase. The first step in the generation of membrane potential and ATP production is the oxidation of NADH by the type II NADH dehydrogenases. The type II NADH dehydrogenases are responsible for accepting and transferring electrons to menaquinone in the membrane without translocating protons across the membrane [22-26]. The reduced menaquinones can then be oxidized by three different cytochromes depending on the growth

environment. Cytochrome aa_3 (QoxDCBA) and cytochrome bo_3 are primarily responsible for oxidizing reduced menaquinones under aerobic growth conditions using oxygen as the terminal electron acceptor [27]. In contrast, cytochrome *bd* (CydAB) is more active when oxygen is scarce [27]. The presence of the different cytochromes and their activity under different environmental conditions highlight the capacity of *S. aureus* to grow under varying environments.

NADH and $FADH_2$ are not the only electron carriers in *S. aureus*. This bacterium can also utilize nitrate as an alternative electron carrier for use during anaerobic respiration. This is mediated via the nitrate reductase system [28]. The process involves endogenously produced nitric oxide (NO^-) that is converted to nitrate by the flavohaemoprotein Hmp [29]. This nitrate can then be used to reduce menaquinone and allow ions to drive ATP production via the F_0F_1 ATPase. Both the cytochromes and nitrate reductase systems are responsible for establishing membrane potential. The different ways *S. aureus* can respire and produce ATP using a variety of different electron donors from different pathways of metabolism is key for the ability of this bacterium to cause infections. In addition to full metabolic pathways for glycolysis, pentose-phosphate pathway, and the TCA cycle, genes are present in *S. aureus* to support synthesis of nearly all amino acids. Despite their presence, *S. aureus* is still auxotrophic for the amino acid arginine and thus cannot be grown in a minimal media [30]. The ability of *S. aureus* to endogenously synthesize arginine is due to the repression of the biosynthetic genes [31]. This repression is mediated by global metabolic regulatory proteins, which are discussed below.

Regulation of metabolism in S. aureus

Metabolic pathways in *S. aureus* are under the control of metabolic regulatory proteins [32-35]. One of these regulatory proteins is carbon catabolite protein A, or CcpA. CcpA is a DNA-binding protein that has been shown to regulate multiple branches of metabolism. CcpA's DNA-binding

activity is activated by binding to fructose-1,6-bisphosphate, which results in CcpA-mediated regulation of target genes. CcpA represses the TCA cycle in the presence of glucose or other glycolytic carbohydrates that generate fructose-1,6-bisphosphate [15, 36-39]. In addition, CcpA controls the expression of genes encoding key enzymes in amino acid metabolism [34, 40, 41]. For example, active CcpA represses the ability of *S. aureus* to synthesize arginine from proline [31]. Deletion of *ccpA* from *S. aureus* also impacts the transcription of virulence factors [42].

CodY is a another metabolic regulatory protein which directly responds to the intracellular concentrations of branch-chained amino acids (BCAAs) as well as levels of cellular GTP [43, 44]. Accordingly, CodY has been shown to regulate BCAA biosynthesis pathways and control the expression of a multitude of virulence factors (e.g., repressing toxins and activating Microbial Surface Components Recognizing Adhesive Matrix Molecules (MSCRAMMs)) [33, 45-47]. Similar to CcpA, CodY has also been shown to alter transcription of virulence factor expression [33, 48, 49]. Other metabolic regulatory systems, such as the AirSR and SrrAB two-component systems, sense the presence or absence of oxygen in the environment [50-55]. Other metabolic regulatory systems, while playing important roles in modulating metabolism and virulence, will be not be discussed here and are reviewed in depth by Richardson *et al.* [32]. Because of the variety of metabolic regulatory systems that respond to different stimuli, both the availability of nutrients and oxygen can induce both metabolic changes and alter virulence factor production.

Fatty acid and lipid metabolism

Fatty acid metabolism

Fatty acids are synthesized from acetyl-CoA or branched-chain amino acids (BCAAs) and are the building blocks for phospholipid synthesis. These phospholipids make up the phospholipid

membrane of the cell. *S. aureus* endogenously produces fatty acids via the fatty acid synthesis type II (FASII) system [56]. Fatty acids can be saturated (no double bonds) or unsaturated (acyl chain containing double bonds). They can also be straight-chain fatty acids (SCFA) or branched-chain fatty acids (BCFA). The pathway for fatty acid synthesis in *S. aureus* is reviewed in Figure 1.2A. The synthesis of SCFA primarily utilizes the precursor acetyl-CoA, which is converted to malonyl-CoA via acetyl-CoA carboxylase. Malonyl-CoA is converted to malonyl-ACP by the malonyl-CoA ACP transacylase, FabD. The 3-oxoacyl-ACP synthase III enzyme, FabH, can utilize both acetyl-CoA and malonyl-ACP to produce β-ketoacyl-ACP. This molecule is then elongated by 3-oxoacyl-ACP reductase, FabG, 3-hydroxacyl-ACP dehydratase, FabZ, and enoyl-ACP synthase II, FabI. These enzymatic steps ultimately result in the production of an acyl-ACP molecule. The acyl-ACP molecule is elongated by 3-oxoacyl-ACP synthase II, FabF, using malonyl-ACP. Acyl-ACP is then converted to acyl-phosphate by the acyl–acyl carrier protein:phosphate transacylase, PlsX [57]. One interesting caveat when studying phospholipids in *S. aureus* is the organism's inability to endogenously synthesize unsaturated fatty acids (USFAs). The production of USFAs is mediated by the enzymatic activity 3-hydroxacyl-ACP dehydratases. There are at least two different isoforms of 3-hydroxacyl-ACP dehydratase: FabA and FabZ [58]. *S. aureus* only possesses the FabZ isoform of 3-hydroxacyl-ACP dehydratase. This isoform is thought to be unable to accommodate unsaturated fatty acids during elongation [59].

In other microorganism and higher order organisms, USFAs are incorporated into phospholipids and aid in the modulation of phospholipid membrane fluidity. Instead, *S. aureus* utilizes BCFAs to help modulate membrane fluidity, depending on growth conditions (Figure 1.2B) [60]. Most fatty acids in *S. aureus* phospholipid membranes are comprised of BCFAs [61]. BCFAs are derived from the BCAAs leucine, isoleucine and valine. The BCAAs are converted to acyl-CoA

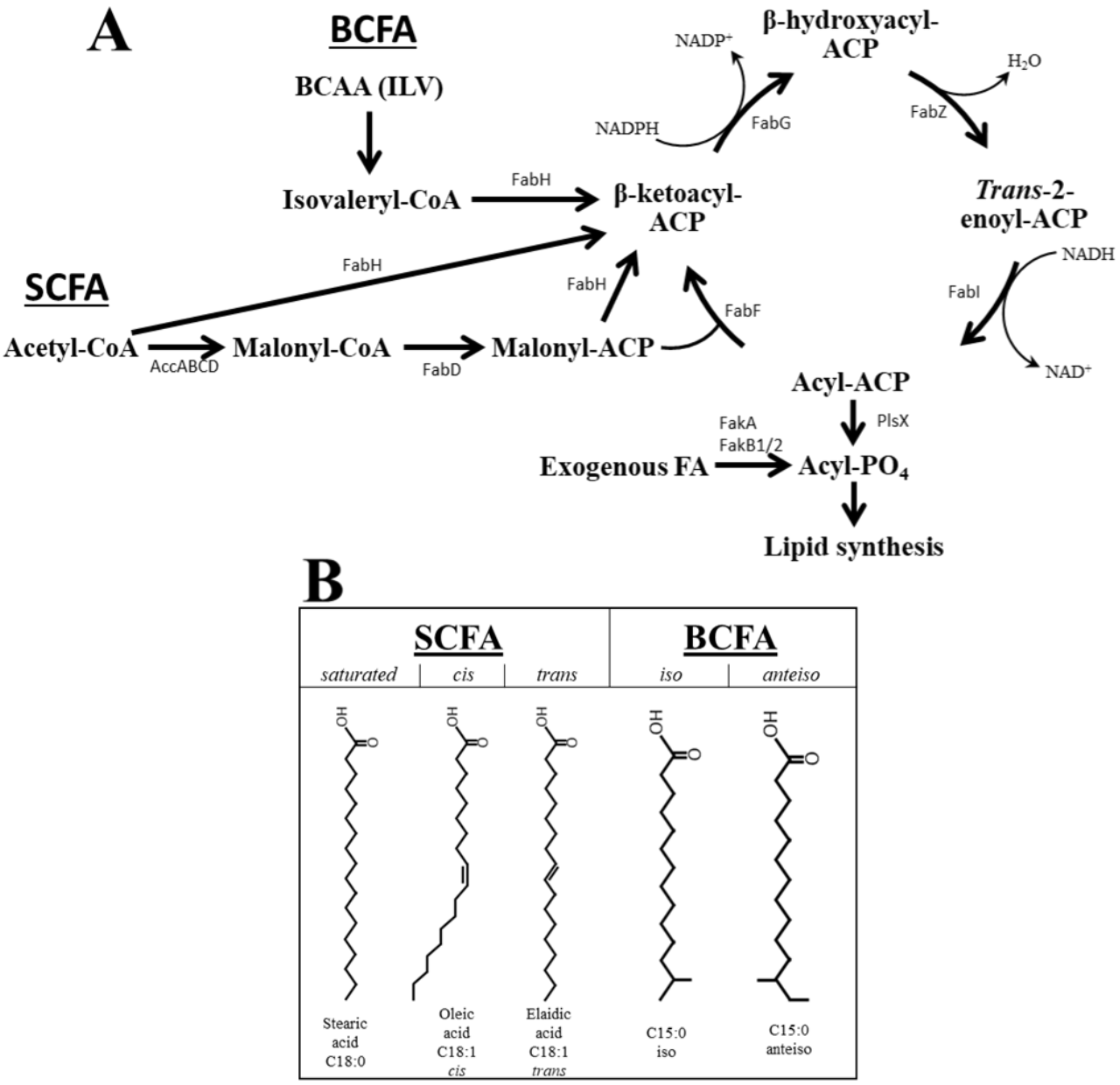
A
BCFA
BCAA (ILV)
Isovaleryl-CoA
FabH
β-ketoacyl-ACP
NADP+
β-hydroxyacyl-ACP
NADPH
FabG
H2O
FabZ
Trans-2-enoyl-ACP
NADH
FabI
NAD+
SCFA
FabH
FabH
FabF
Acetyl-CoA
AccABCD
Malonyl-CoA
FabD
Malonyl-ACP
Acyl-ACP
PlsX
FakA
FakB1/2
Exogenous FA
Acyl-PO4
Lipid synthesis
B
SCFA
BCFA
saturated
cis
trans
iso
anteiso
Stearic acid C18:0
Oleic acid C18:1 cis
Elaidic acid C18:1 trans
C15:0 iso
C15:0 anteiso

Figure 1. 2

Figure 1.2 A) Overview of fatty acid synthesis in *Staphylococcus aureus*. Enzyme abbreviations are as follows, including open reading frames from SAUSA300_FPR3757 genome. AccABCD- acetyl-CoA carboxylase complex (SAUSA300_1646-7, AccA and D, SAUSA300_1563-4, AccC and B), FabD- malonyl-CoA ACP transacylase (SAUSA300_1123), FabH- 3-oxoacyl-ACP synthase III (SAUSA300_0885), FabF- 3-oxoacyl-ACP synthase II (SAUSA300_0886), FabG- 3-oxoacyl-ACP reductase (SAUSA300_1124), FabZ- 3-hydroxyacyl-ACP dehydratase (SAUSA300_2054), FabI- enoyl-ACP reductase I (SAUSA300_0912), PlsX- acyl–acyl carrier protein:phosphate transacylase (SAUSA300_1122), FakA- fatty acid kinase A (SAUSA300_1119), FakB1- saturated fatty acid-binding protein (SAUSA300_0733), FakB2- unsaturated fatty acid-binding protein (SAUSA300_1318). This figure has been adapted from Progress in Lipid Research, 52(3), Parsons, J. B., & Rock, C. O. Bacterial lipids: metabolism and membrane homeostasis, 249-276, (©2013) with permission from Elsevier. **B)** Structures of select fatty acids to highlight important differences.

derivatives (isoleucine to 2-methylbutyrl-CoA, leucine to isovaleryl-CoA, and valine to isobutyryl-CoA), which enter the FASII pathway by conversion to β-ketoacyl-ACP via 3-oxoacyl-ACP synthase III enzyme, FabH. BCFAs are in one of two different conformations: iso and anteiso (Figure 1.2B). Most fatty acids found in the phospholipid membrane of *S. aureus* are anetiso-C15:0.

The FASII system is different from the mammalian fatty acid synthesis machinery and thus, it has been a target of antimicrobial research [62-64]. Recently, an exogenous fatty acid (exoFA) utilization system was identified in *S. aureus* [65, 66]. Questions about the inhibiton of FASII immediately followed the discovery of the exoFA utilization system. It was argued whether inhibition of bacterial FASII as a viable therapeutic target, since exoFAs would allow the bacterium to overcome the inhibition of endogenous fatty acid production [67, 68]. Endogenous fatty acid metabolism begins with acetyl-CoA. Thus, supplementation of fatty acids from exogenous sources could be a way *S. aureus* avoids competing for acetyl-CoA with central metabolism. This exoFA utilization system consists of the fatty acid kinase, FakA, and the fatty acid binding proteins FakB1 and FakB2. Originally identified as VfrB for its role in impacting protease and hemolytic activity [66], FakA was later identified to be a fatty acid kinase and renamed as such [65]. ExoFAs are predicted to passively enter the phospholipid membrane. FakB1 and FakB2 then bind to and remove them from that membrane. Current data suggests that FakB1 prefers to bind saturated fatty acids and FakB2 prefers to bind unsaturated fatty acids [65]. Once removed from the membrane, the carboxyl end of the fatty acid is phosphorylated by FakA. This acyl-phosphate is then either elongated via FASII or incorporated into phospholipids. The discovery of the exoFA utilization system represents a supplement to FASII production of fatty acids for phospholipid synthesis.

Phospholipid synthesis in S. aureus

Phospholipids are synthesized using the acyl-phosphate molecules produced via FASII or the exoFA utilization system [69]. Phospholipid synthesis in *S. aureus* is presented in Figure 1.3A. Regardless of its origin, acyl-phosphate is converted to phosphatidic acid by glycerol-3-phosphate acyltransferase, PlsY, and 1-acyl-sn-glycerol-3-phosphate acyltransferases, PlsC. Phosphatidic acid is then converted to phosphatidylglycerol (PG) (Figure 1.3B). PG is the most abundant phospholipid found in *S. aureus* membranes [70] and serves as the central phospholipid from which all other phospholipids are derived. PG can by lysinalyated via the transmembrane enzyme multipeptide resistance factor, MprF, forming the positively charged phospholipid lysyl-PG (LPG) (Figure 1.3B) [71]. Additionally, two PG molecules can be condensed to form cardiolipin (CL) via cardiolipin synthase 1 and 2 (Cls1 and Cls2) (Figure 1.3B) [72, 73]. Under normal growth conditions, Cls2 is the dominant synthase [73]. Cardiolipin is important for growth in the presence of high salt concentrations [73].

Phospholipids play an important role in the interaction between host and pathogen. Membrane associated products, such as lipopolysaccharides, lipoteichoic acids, and lipoproteins are sensed during infection by the host encoded pattern-recognition receptors that induce the activity of numerous host immune cells [74, 75]. In addition to these membrane products, phospholipids themselves can play a role in evading the immune system. For example, increased concentrations LPG in the membrane of *S. aureus* has been shown to be important for evading neutrophils and antimicrobial peptides [76]. The composition of the phospholipid membranes of bacteria can also dictate whether antimicrobial treatment during infection is successful. Resistance to daptomycin, a lipopeptide antimicrobial, as well as altered trafficking of neutrophils, can result from the mutation of cardiolipin synthase (*cls2*) and increased abundance of membrane cardiolipin [77].

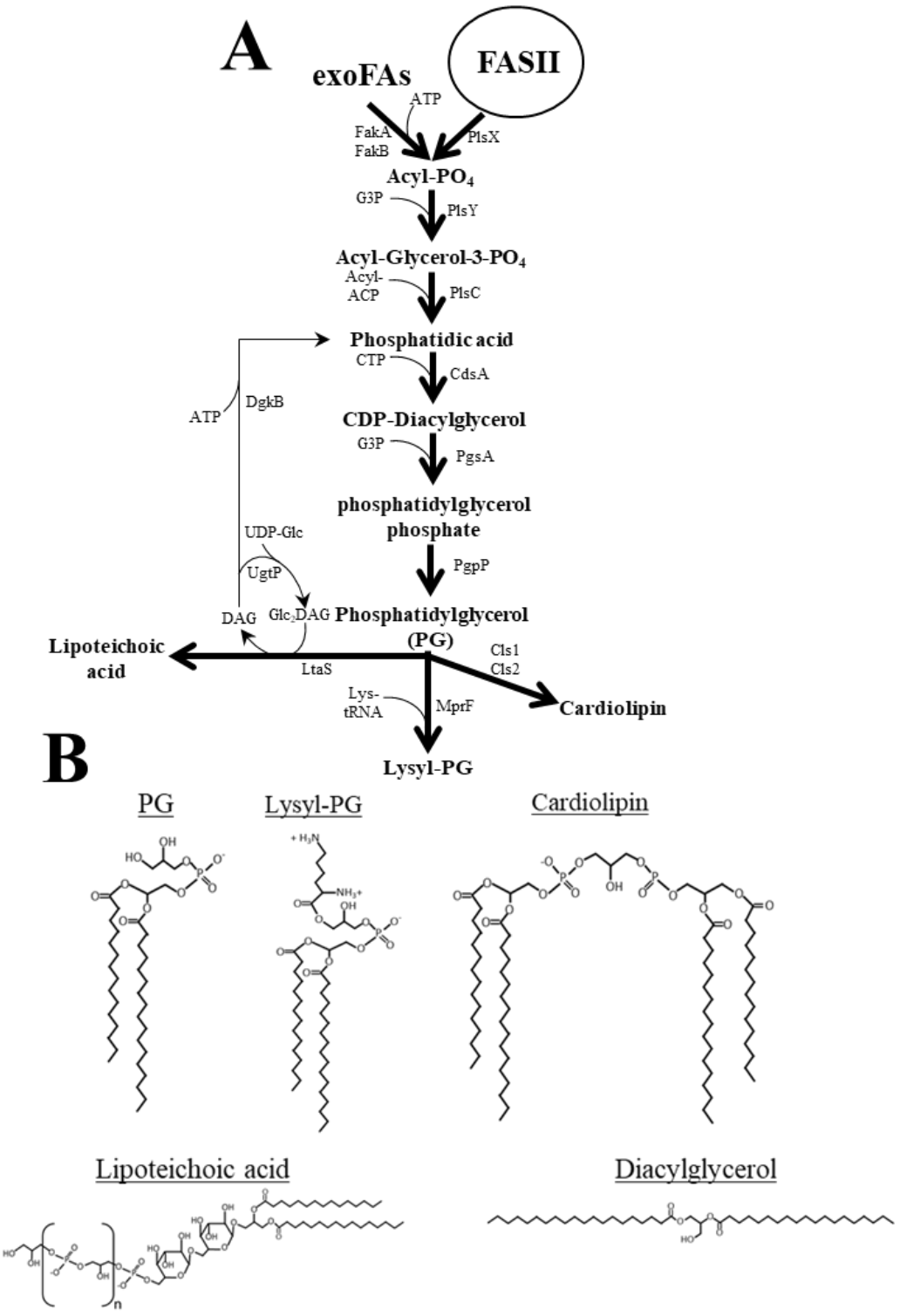
A
exoFAs
FASII
ATP
FakA
FakB
PlsX
Acyl-PO4
G3P
PlsY
Acyl-Glycerol-3-PO4
Acyl-ACP
PlsC
Phosphatidic acid
CTP
CdsA
ATP
DgkB
CDP-Diacylglycerol
G3P
PgsA
phosphatidylglycerol phosphate
UDP-Glc
UgtP
PgpP
DAG
Glc2DAG
Phosphatidylglycerol (PG)
Lipoteichoic acid
LtaS
Cls1
Cls2
Cardiolipin
Lys-tRNA
MprF
Lysyl-PG
B
PG
Lysyl-PG
Cardiolipin
Lipoteichoic acid
Diacylglycerol

Figure 1. 3

Figure 1.3 A) Overview of phospholipid synthesis in *S. aureus*. Enzyme abbreviations are as follows, including open reading frame designations from SAUSA300_FPR3757 genome. PlsX- phosphate acyltransferase (SAUSA300_1122), PlsY- glycerol-3-phosphate acyltransferase (SAUSA300_1249), CdsA- phosphatidate cytidylyltransferase (SAUSA300_1154), PgsA- CDP-diacylglycerol—glycerol-3-phosphate phosphatidyltransferase (SAUSA300_1176), PgpP- unidentified phosphatidylglycerophosphatase (predicted ORF SAUSA300_1557), MprF- , phosphatidylglycerol lysyltransferase (SAUSA300_1255), LtaS- lipoteichoic acid synthase (SAUSA300_0703), Cls1- cardiolipin synthase 1 (SAUSA300_1216), Cls2- cardiolipin synthase 2 (SAUSA300_2044), UgtP- diacylgclyerol β-glucosyltransferase (SAUSA300_0918), DgkB- diacylglycerol kinase (SAUSA300_1529). This figure was adapted from Internationl Journal of Medical Microbiology, 305(2), Kuhn, S., Slavetinsky, C. J., & Peschel, A, Synthesis and function of phospholipids in *Staphylococcus aureus*, 196-202, (©2015) with permission from Elsevier. **B.** Structure of the molecules phosphatidylglycerol (PG), lysyl-PG, cardiolipin, lipoteichoic acid, and diacylglycerol. This figure was adapted from Molecular Microbiology, 80(2), Broad-spectrum antimicrobial peptide resistance by MprF-mediated aminoacylation and flipping of phospholipids, Ernst and Peschel, (©2011) with permission John Wiley and Sons.

Microbial lipids can also serve as antigens for the immune system [78], further emphasizing the role that lipids play during the infection process. More recently, the identification of bacterial extracellular vesicles has also become a topic of interest and could contribute to host-pathogen interactions [79]. These observations clearly suggest that the composition of the phospholipid membrane is a vital component of the host-pathogen interface.

In addition to being building blocks for membranes, free fatty acids are a part of the mammalian innate immune system [80]. They are typically secreted via sebaceous glands in the skin and have antimicrobial capabilities [80]. The most prevalent fatty acids found in sebum on human skin include the saturated fatty acids palmitic acid (16:0), stearic acid (C18:0) and myristic acid (C14:0) and the unsaturated fatty acids palmitoleic acid (C16:1), oleic acid (C18:1), and linoleic acid (C18:2) [81]. Since *S. aureus* predominantly infects the skin, this begs the question of how *S. aureus* copes with the antimicrobial activity of fatty acids and how they impact the function of bacterial cells.

Virulence factors and regulation

Variety of virulence factors

The virulence capabilities of *S. aureus* have been studied intensely. Of the PubMed articles with "*Staphylococcus aureus*" in the title (more than 123,000), nearly 8% (more than 10,000) contain the word "virulence". *S. aureus* possesses many virulence factors that are important for different aspects of the infection cycle, with many of these factors playing multiple roles for infection. In planktonically growing cells in rich media, the expression of these virulence factors is dependent on the phase of growth. During lag phase and early exponential phase of growth, cell-wall associated molecules and factors important for adhesion to host tissues are expressed. These can include a variety of factors such as clumping factor A [82], fibrinogen and fibronectin-binding

proteins [83], collagen binding protein [84], as well as others. These molecules are often collectively referred to as microbial surface components recognizing adhesive matrix molecules, or MSCRAMMs. The MSCRAMMs are generally important for forming biofilms, which are associated with difficult to treat in-dwelling medical device infections [85-87]

As the planktonic culture enters late exponential phase, *S. aureus* begins to express a variety of secreted proteins. One class of secreted proteins are proteases. These proteases have diverse substrate ranges and serve several functions. For example, the zinc-dependent metalloprotease aureolysin (Aur) targets both host and bacterial proteins. For example, aureolysin has been shown to cleave complement [88]. The serine protease SspA (V8 protease) [89] and cysteine protease SspB are activated by aureolysin. Pro-SspA is processed and activated by aureolysin, which allows for SspA to process and activate pro-SspB to SspB [90]. These and other proteases, such as the serine-like proteases (Spl), are important for targeting host associated molecules [91]. In addition to degrading host factors, these proteins are important for modulating the virulence of *S. aureus.* For example, secreted proteases have been shown to degrade both secreted factors (such as α-hemolysin) and membrane-associated factors (such as FnbA) [92]. Other secreted virulence factors include the DNA-degrading nuclease (Nuc) [93, 94], lipases (Geh and Lip) for degrading host lipid molecules [95, 96], coagulase for converting fibrinogen to fibrin (Coa) [97], among many others. Indeed, the removal of the secreted *S. aureus* protease dramatically stabilizes many secreted proteins [92]. In addition, these proteins enable the bacteria to degrade extracellular proteins for peptide importation [98].

Other classes of secreted virulence factors include proteins involved in evasion of the immune system. The classical example of these types of factors is known as protein A (SpA). SpA is important for interacting with von Willebrand factor and aiding the formation of biofilms [99].

SpA interacts with the Fcγ portion of antibodies which prevents opsonization and eventual phagocytosis of *S. aureus* [100] and this interaction is essential for SpA's role in evading the immune system [101]. The Chemotaxis Inhibitor Protein (CHIPS) interacts with host receptor C5a as well as bacterial-derived formylated peptides, both decreasing the recruitment of immune cells to the bacteria [102, 103]. Staphylococcal Complement Inhibitor (SCIN) is responsible for inhibiting part of the complement cascade [104]. These secreted factors, in addition to the presence of a capsule [97], all give *S. aureus* the chance to evade arms of the immune system and cause a successful infection.

Perhaps the most well characterized virulence factors associated with *S. aureus* are secreted toxins. These toxins damage membranes of different types of host cells in both receptor-mediated and non-receptor mediated mechanism. The hallmark receptor-mediated toxin in *S. aureus* is known as alpha-hemolysin (Hla), which binds to the host receptor ADAM10 commonly found on red blood cells, epithelial cells, and some leukocytes [105]. However, Hla may damage membranes in a non-receptor mediated fashion at high concentrations [105, 106]. *S. aureus* also produces a sphingomyelinase known as β-toxin and is toxic to a variety of different cell types [107-109]. Not all *S. aureus* strains produce β-toxin as it is inactivated by bacteriophage integration in the gene, particularly in human isolates [110, 111]. More recently, *S. aureus* leukocidins have increased in popularity. Commonly located within mobile genetic elements, these are bi-component toxins that target different receptors [112]. These include leukocidins LukDE [113], LukAB (a.k.a. LukGH) [114], Panton-Valentine leukocidin (PVL; LukSF) [13, 115], and γ-hemolysin [116]. The identification of the targets for these leukocidins displays the versatility within the toxin arsenal of *S. aureus* to kill a variety of immune cells. For example, data has been shown that PVL targets the human G-protein coupled receptor C5a [115] and that LukAB targets CD11b and results in the

lysis of human neutrophils [117]. Non-receptor mediated toxins of *S. aureus* are the phenol-soluble modulins (PSMs) and δ-toxin [14]. The PSMs were originally identified in 1999 in *Staphylococcus epidermidis* [118], but were subsequently found to be important drivers of pathogenesis in *S. aureus* [119]. The PSMs are short peptides that are organized into 3 different locations within the *S. aureus* chromosome: PSMα1-4 (20-25 amino acids), PSMβ1-2 (40-44 amino acids), and δ-toxin. Interestingly, δ-toxin is located within the RNAIII gene. These peptides form amphipathic helices meaning they have hydrophobic and hydrophilic amino acid residues, which imbue these molecules with antimicrobial-like properties. While the PSMs target membranes in a non-specific manner, their activity is diminished in the presence of serum [120]. They are very important for killing of neutrophils that have phagocytosed *S. aureus* [121] and biofilm formation and dispersal [122], showcasing the complex role these peptides play during infection.

Regulatory systems of virulence factor production

S. aureus possesses the quorum sensing system named accessory gene regulator, or Agr (Figure 1.4A). The Agr system consists of four genes: membrane-associated peptidase AgrB, the precursor of the autoinducing peptide (AIP) AgrD, and the two-component system AgrC (sensor histidine-kinase) and AgrA (response regulator). These genes are genetically organized in an operon containing divergent promoters P2 and P3. The P2 promoter transcribes RNAII which includes AgrBDCA and is expressed at a basal level [123]. The precursor autoinducing peptide AgrD is processed intracellularly via AgrB, resulting in the secretion of mature AIP [124, 125]. As AIP levels rise during growth (to what is referred to as a "quorum"), AgrC senses AIP and autophosphorylates itself, eventually activating AgrA's DNA binding activity. Activated AgrA then will bind the P3 promoter and drive expression of RNAIII [124]. Phosphorylated AgrA also directly binds the promoter of Phenol-soluble modulins [14], exerting even more control over

virulence factor production. RNAIII post-transcriptionally regulates various virulence factors, most notably *hla* (alpha-hemolysin) via base-pair matching of the RNAIII molecule to the 5`-end of the *hla* RNA molecule [126, 127]. Binding of the RNAIII molecule to the *hla* transcript induces a structural change in the *hla* transcript allowing for the translation of *hla*.

The genome of *S. aureus* contains nine homologous proteins that belong to the SarA family proteins [128] (Figure 1.4B). These proteins are DNA-binding proteins that exert control of virulence factor expression. The most well characterized member of the SarA protein family is SarA. The *sarA* locus contains three separate promoters that drive expression of two different transcripts. The P1 promoter is responsible for expressing the shorter *sarA* transcript (580 base pairs), P2 drives expression of medium *sarA* transcript (840 base pairs), and the P3 promoter expresses the longer *sarA* transcript (1.15 kilo bases) [129]. The P1 and P3 transcripts are predominantly expressed during both log and exponential phases of growth and the P2 transcript is expressed during stationary phase [129]. SarA is capable of directly regulating virulence factor expression via DNA-protein interaction. For example, the promoters for α-hemolysin (*hla*) and protein A (*spa*) are both positively regulated by SarA through conserved SarA binding motifs in the promoter region of the gene [130]. SarA also binds to multiple sites within the *agr* locus, thus regulating virulence of *S. aureus* indirectly through modulation of RNAIII expression [131]. In addition, SarA is well known to control the expression of proteases [132, 133]. SarA also regulates the expression of itself, creating more layers of regulation within this system [134]

Another important way *S. aureus* regulates the expression and production of virulence factors are two-component systems (TCS). The genome of *S. aureus* encodes 16 different TCS, only one of which (WalKR) is essential for viability [135]. In general, TCS consist of a membrane-associated

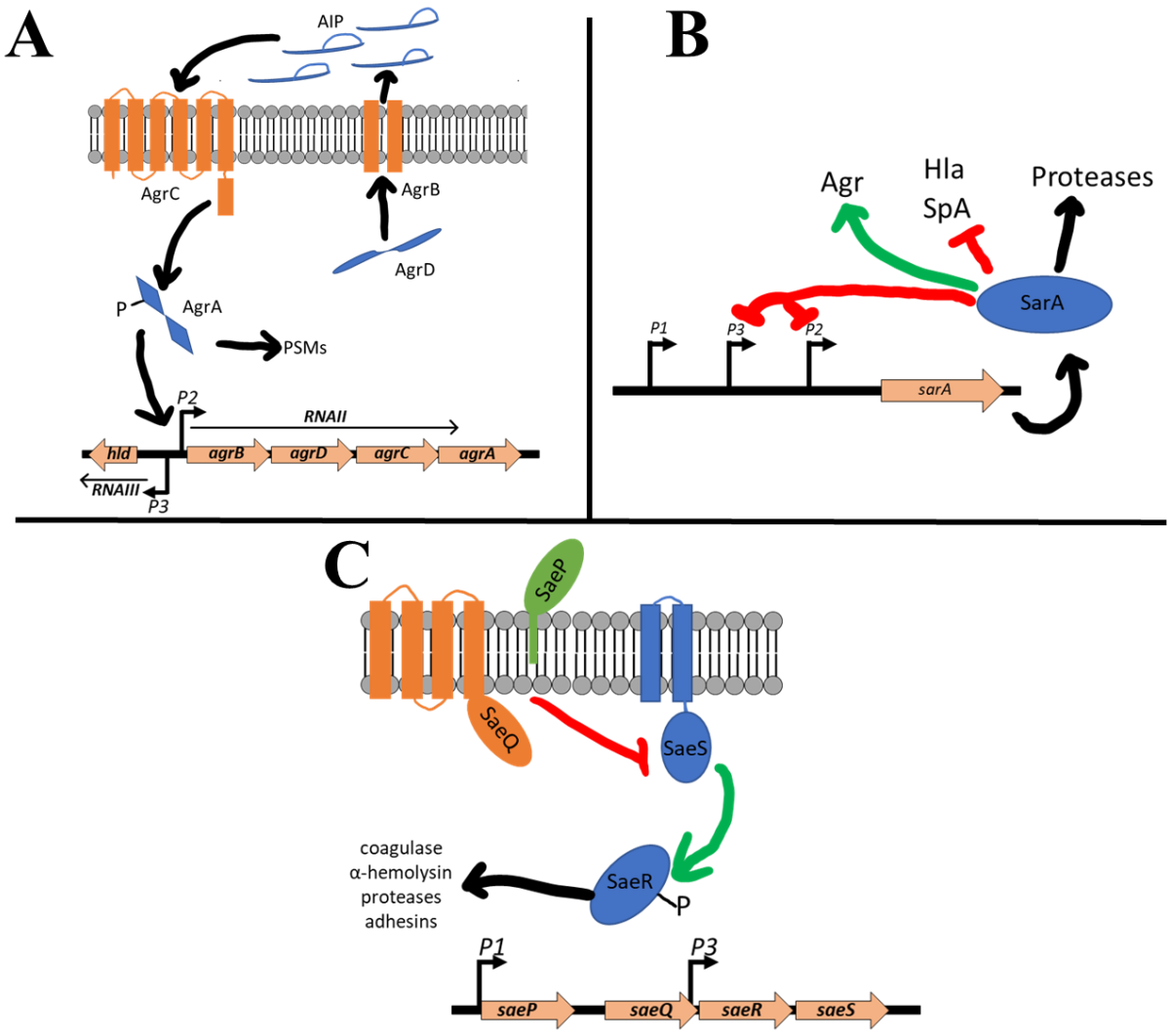
A
AIP
AgrC
AgrB
AgrD
P
AgrA
PSMs
P2
RNAII
hld
agrB
agrD
agrC
agrA
RNAIII
P3
B
Agr
Hla
SpA
Proteases
SarA
P1
P3
P2
sarA
C
SaeP
SaeQ
SaeS
coagulase
α-hemolysin
proteases
adhesins
SaeR
P
P1
P3
saeP
saeQ
saeR
saeS

Figure 1. 4

Figure 1.4. Major virulence regulatory systems in *S. aureus*: **A)** quorum-sensing system Agr, **B)** DNA-binding protein SarA, and **C)** the two-component system SaeRS.

histidine kinase (HK) and cytoplasmic response regulator (RR). When activated by cognate ligand or environmental signal, the HK autophosphorylates at a conserved histidine residue. This phosphoryl group is then transferred to an aspartic acid residue of the RR, activating its DNA-binding activity. Different TCS respond to different stimuli, the identity of which is often not known. The sensor kinase AirS of the AirSR TCS contains an oxygen-responsive iron-sulfur cluster that when oxidized is activated [50]. In turn, the RR AirS becomes phosphorylated and alters transcription of genes accordingly. Other TCS's, such as SrrAB [52, 53] and NreBC [136], also respond to growth in aerobic or anaerobic environments. Responding to cell-wall stress and targeting by antimicrobials is another stimulus shared by several other TCS's in *S. aureus*. WalKR [137, 138], VraSR [139], and GraRS [140, 141] are among the TCS's that respond to membrane damaging agents and help maintain cell wall integrity.

The *S. aureus* exoprotein TCS, known as SaeRS, is a critical regulator of virulence factor expression [142] (Figure 1.4C). SaeRS was first identified by a transposon mutant that had a significant decrease in secreted proteins in *S. aureus* [143]. This TCS is composed of the sensor histidine kinase SaeS and the response regulator SaeR [144]. Despite the TCS name, the auxiliary proteins SaeP, a lipoprotein, and SaeQ, a transmembrane protein, are also involved in the activity of SaeS by activating the phosphatase activity of SaeS *in vitro* [145]. SaePQRS are transcribed as an operon containing two distinct promoters: P3 and P1 [146]. The P3 promoter, which is located within the 3`-end of *saeQ*, is constitutive and allows for basal transcription of *saeR* and *saeS* only. The second promoter, P1, lies upstream of *saePQRS* and contains two SaeR binding-sites. The presence of two SaeR binding-sites allows for this promoter to be induced when levels phosphorylated SaeR are high, representing activated conditions of SaeS. Expression of *saePQRS* from the P1 promoter transcribes *saeP*, *saeQ*, *saeR*, and *saeS*. Thus, expression of the operon from

the P1 promoter serves as a negative feedback mechanism for the Sae via phosphatase activation by SaeP and SaeQ. Primarily acting as an activator of target gene expression, phosphorylated SaeR binds to the promoter regions of various secreted virulence factors [142]. Promoters of target genes fall into two different categories: high and low affinity [147]. High affinity promoters (class II) contain two SaeR binding site. The promoter for α-hemolysin (P_{hla}) is an example of a high affinity promoter that is sensitive to large changes in Sae activity. In contrast, low affinity promoters (class I) contain one SaeR binding sites. The coagulase promoter (P_{coa}) is an example of a low affinity promoter and is sensitive to small fluctuations in phosphorylated SaeR levels.

Exogenous fatty acids, FakA, and virulence regulation.

The fatty acid kinase FakA was initially discover in 2014 using a transposon mutant library screen [66]. Bose and colleagues identified that an insertion into open reading frame (ORF)

SAUSA300_1119 resulted in decreased virulence factor expression [66]. Namely, disruption of this ORF decreased α-hemolysin activity as well as increased production of secreted protease. ORF SAUSA300_1119 was initially named Virulence Factor Regulator B, or VfrB, due to these phenotypes and is co-transcribed with *vfrA* (ORF SAUSA300_1118), of which very little is known. Later in 2014, it was shown that ORF SAUSA300_1119 was a fatty acid kinase responsible for phosphorylating exoFAs for phospholipid synthesis and was renamed FakA for Fatty Acid Kinase A [65]. Two additional proteins were identified to be a part of this system and were found to bind free fatty acids, FakB1 and FakB2 [65]. Despite the identification of FakA, FakB1, and FakB2, how the inactivation of this system negatively impacted virulence was not known.

Expression of α-hemolysin and secreted proteases was known to be regulated via the TCS SaeRS (see preceding section). Given this, Krute and colleagues identified that FakA (or VfrB) positively

regulated the SaeRS TCS and in its absence, resulted in decreased activity of this system [148]. Since FakA utilizes exoFAs, it was shown that the addition of the oleic acid (C18:1 cis) significantly decreased the activity of SaeRS regardless of FakA while myristic acid (C14:0) did not [148]. Subsequent studies identified that, in addition to inactivation of *fakA*, inactivation of both *fakB1* and *fakB2* decreased SaeRS activity [149]. This study also identified that free fatty acids accumulate within a *fakA* mutant of *S. aureus*. The negative impact that free fatty acids have on SaeRS activity was confirmed by expression of the *Neisseria gonorrhea* acyl-ACP synthetase in a *fakA* mutant. This restored SaeRS activity by utilizing the accumulated fatty acids in the *fakA* mutant for phospholipid synthesis. Expression of the *N. gonorrhea* acyl-ACP reduced the pool of free fatty acid pool within the cell, and restored SaeRS activity [149]. To confirm this result, the addition of bovine serum albumin (BSA) to the media restored hemolysin activity in a *fakA* mutant [149].

The following work has assessed how exoFAs and the Fak system in *S. aureus* impacts phospholipid composition and function, central metabolism, and virulence factor regulation. Given the recent discovery of the Fak system and the lack of thorough investigation of how fatty acids impact transcriptional changes in bacteria, this work has helped move the research field forward by identifying previously unknown roles for the Fak system in maintaining metabolic and phospholipid membrane homeostasis. This work has also created a better understanding of how fatty acids impact the activity of SaeRS and virulence production. Together, these data provide a framework for establishing potential mechanisms for fatty acid-dependent changes in bacterial virulence and physiology.

Chapter 2: Exogenous fatty acids remodel *Staphylococcus aureus* lipid composition through fatty acid kinase

This chapter has been previously published as DeMars, Z., Singh, V. K., & Bose, J. L. (©2020). Exogenous Fatty Acids Remodel *Staphylococcus aureus* Lipid Composition through Fatty Acid Kinase. *J Bacteriol*, 202(14), doi:10.1128/JB.00128-20. It is reprinted here in whole with permission.

Introduction

Despite decades of intense research, *Staphylococcus aureus* remains a tremendous cause of infection and morbidity in the human population [2]. Approximately 30% of the population are asymptomatic carriers of *S. aureus* [4]; however, this bacterium can cause infection in numerous anatomical sites, including skin and soft tissues, bones, lungs, hearts, as well as foreign implants such as catheters and prosthetic joints [150]. Originally characterized as a typically hospital-acquired infection, the incidence of infections in the community has increased concern and awareness of this pathogen as community-associated strains have become dominant in the US [9, 151]. Thus, a thorough understanding of how *S. aureus* can establish infection, fend off the immune system, and maintain infection is needed to combat this pathogen.

Phospholipids lie at the interface of the host-pathogen interaction. Membrane associated products, such as lipopolysaccharides, lipoteichoic acids, and lipoproteins are sensed by the germ-line encoded pattern-recognition receptors that induce the activity of numerous host immune cells [74, 75]. In addition to these membrane products, phospholipids themselves can play a role in evading the immune system. For example, lysyl-phosphatidyl glycerol (LPG) has been shown to be important for evading neutrophils and antimicrobial peptides [76, 152]. The composition of the phospholipid membranes of bacteria can also dictate if antimicrobial treatment during infection is successful. Resistance to daptomycin, a lipopeptide antimicrobial, can result from the mutation of cardiolipin synthase (*cls2*) and increased abundance of cardiolipin [77]. Microbial lipids can also serve as antigens for the immune system [78], further emphasizing the role that lipids play during the infection process. More recently, the identification of bacterial extracellular vesicles has also become a topic of interest and could contribute to host-pathogen interactions [79]. These data

clearly suggest that the composition of the phospholipid membrane is a vital component of the host-pathogen interface.

Synthesis of lipids is preceded by the production of fatty acids. *S. aureus* endogenously synthesizes fatty acids via the fatty acid synthesis type II system (FASII) [58]. Due to the differences between fatty acid synthesis enzymes of bacteria from humans, FASII has been the subject for antimicrobial targets [63, 153-155]. Bacteria, including *S. aureus*, can supplement endogenous fatty acid synthesis by utilizing exogenous fatty acids (exoFAs) [65]. These exoFAs are predicted to passively diffuse into the phospholipid membrane. In *S. aureus*, exoFAs are thought to be removed from the membrane by fatty acid-binding proteins FakB1 and FakB2 [65]. Once removed from the membrane, fatty acid kinase, FakA, then phosphorylates the carboxyl head group of the fatty acid creating an acyl-phosphate [65] that can then be used for lipid synthesis. *S. aureus* predominantly synthesizes three classes of phospholipids: phosphatidylglycerol (PG), lysl-phosphatidylglycerol (LPG), and cardiolipin (CL) [69, 76]. One interesting caveat to fatty acid and lipid synthesis in *S. aureus* is the inability of this bacterium to synthesize unsaturated fatty acids [156]. Instead, *S. aureus* utilizes branched-chain fatty acids (BCFAs), derived from the branched-chain amino acids isoleucine, leucine, and valine, to help modulate the membrane in response to environmental stimuli [60, 157]. A large portion of the BCFAs produced by *S. aureus* include odd-numbered iso and anteiso BCFAs, with acyl-chain length of 15 being the most abundant [61, 157].

FakA was first identified as a regulator of virulence due to the decrease in α-hemolysin activity, increased protease activity, and increased dermonecrosis in a murine model of infection [66]. Originally named virulence factor regulator B, VfrB, due to this altered virulence, FakA was eventually identified to be a fatty acid kinase important for phosphorylating exoFAs [65]. Subsequently, the altered virulence factor profile of a *fakA* mutant was identified to be due, in part,

to altered activity of the SaeRS two-component system [149, 158]. The current model for the FakA-dependent alteration of SaeRS signaling is due to the accumulation of fatty acids within the cell [149]. A mechanism for how these accumulated fatty acids within the cell decreases SaeRS signaling is still at large. The absence of FakA affects global metabolism [159] and increases the resistance of *S. aureus* to toxic fatty acids [160, 161].

How the inability to use exoFAs affects the overall membrane lipid composition has not been evaluated. In the current study, we aimed to determine the changes in membrane lipid composition in the absence of FakA. We tested how these overall membrane lipid changes affect the properties of the membrane itself. Lastly, we provide evidence that *S. aureus* grown in the presence of host tissue can use unsaturated fatty acids to supplement phospholipid synthesis, extending our observations from standard laboratory media to include fatty acids found in murine skin. These results increase the importance that the fatty acid utilization system has in the presence of host-derived tissues.

Results

Cellular and extracellular fatty acid profile of fakA mutant. FakA is necessary for *S. aureus* to incorporate exoFAs into acyl chains of membrane lipids. Thus, it would be expected that the absence of FakA would alter the abundance of FAs in the cell. Indeed, a previous study determined that a *fakA* mutant accumulates fatty acids [149]. Our studies are typically performed in TSB and therefore we sought to recapitulate this accumulation of fatty acids at different phases of growth in the *fakA* mutant under our growth conditions and our *S. aureus* strain of choice, AH1263, a derivative of the USA300 strain LAC. Using LC/MS/MS, we quantified the available free fatty acids in TSB and found that 16:0 and 18:0 constitute the most abundant fatty acids (Figure 2.7). Next, we determined how FakA affects fatty acid pools. To this end, the free fatty acid profiles of

cellular and extracellular fatty acids for wild type and *fakA* mutant was determined. This was tested at two-time points representing early (3 hours) and late (6 hours) exponential phase of growth, times that we have previously characterized the metabolic changes in the *fakA* mutant [159]. In agreement with previous research, we observed a significant increase in cellular free fatty acids in the *fakA* mutant compared to wild type (Figure 2.1A) at 6 hours. However, the cellular fatty acid levels were slightly, but significantly, decreased at 3 hours. The identity of the individual fatty acids was also determined, and we observed differences in several fatty acid species between wildtype and *fakA* mutant after 3 hours of growth (Figure 2.8A) and 6 hours of growth (Figure 2.8B). Specifically, we found a significant ($p<0.05$) increase in the proportion of 15:0, 17:0, 19:0, and 20:0 in the *fakA* mutant during late exponential (6 hours) growth phase. We reasoned that an accumulation of fatty acids in the cell could lead to release of fatty acids into the supernatant. We observed an increased abundance of supernatant fatty acids in both strains over time, which was enhanced in the *fakA* mutant (Figure 2.1B). These data demonstrate that the *fakA* mutant accumulates fewer fatty acids during early exponential phase (3 hours) of growth but accumulates more fatty acids during late exponential phase (6 hours) of growth compared to wildtype. It also identifies that the *fakA* mutant possesses altered fatty acid pools compared to the wild-type strain.

Lipid profile for wild type and fakA mutant in TSB. An in-depth analysis of how FakA affects the composition of the lipid membrane of *S. aureus* has not been undertaken. To do this, we performed a comprehensive analysis of the membrane lipids of *fakA* mutant compared to that of wild type when grown in TSB. Lipids were extracted using a modified Bligh and Dryer liquid-liquid lipid extraction protocol [162]. Since lipid ratios are known to vary by growth phase [72, 163], we examined cells during exponential phase (5 hours) and stationary phase (24 hours). As expected,

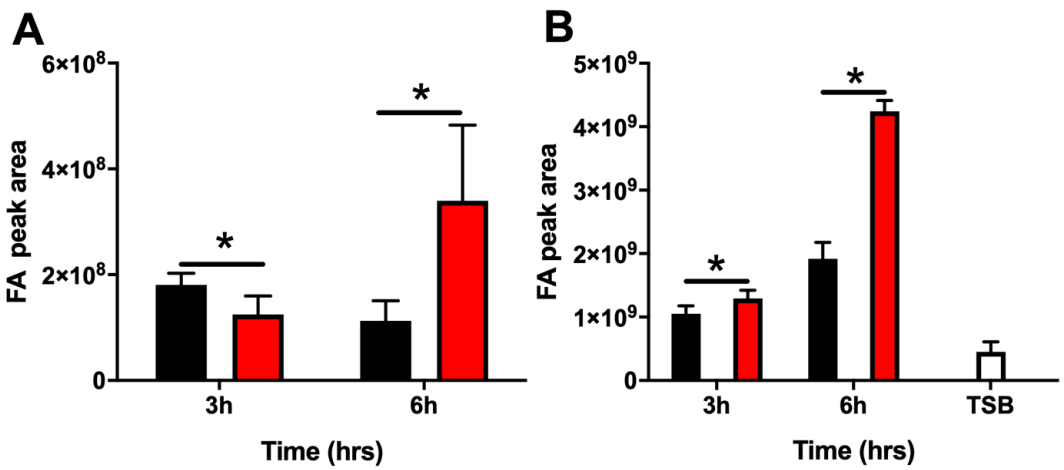
A
6×10^8
4×10^8
2×10^8
0
FA peak area
*
*
3h
6h
Time (hrs)
B
5×10^9
4×10^9
3×10^9
2×10^9
1×10^9
0
FA peak area
*
*
3h
6h
TSB
Time (hrs)

Figure 2. 1

Figure 2.1. Cellular **(A)** and supernatant **(B)** free fatty acids (FA) of wildtype (black) and *fakA* mutant (red) grown for three and six hours in TSB+14mM glucose. Empty bar is free fatty acids from sterile TSB+14mM glucose. Data represents the mean (n=4) with standard deviation, *$p<0.05$ by student t-test.

PG and LPG were the primary lipids in both cells (Figure 2.2A and 2.2B). We observed little difference between the major lipid species between the two strains, with only a modest significant increase in PG and corresponding decrease in CL in the *fakA* mutant during exponential phase of growth (Figure 2.2A). Since LPG and CL are synthesized from PG, the lack of major differences was not unexpected as FakA is important for insertion of exoFAs as phospholipid acyl side chains and not, as far as we know, the activity of the enzymes responsible for lipid species generation. Considering this, we determined the total carbon and saturations of the lipid acyl side chains for PG and LPG in the wildtype and *fakA* mutant. During growth in TSB, lipids containing an unsaturated acyl-chain were near absent at either phase of growth in both strains (Figure 2.2C and 2D). We did identify significant changes in the lipid profiles between the two strains with the *fakA* mutant tending to contain a higher abundance of longer acyl sides chains, predominantly 35:0, than the parent strain.

Since the data in Figure 2.2C and 2.2D represents the total carbon length of both acyl side chains, we performed product ion analysis on pooled samples to determine the most abundant acyl side chain pairings that comprise each lipid (Table 2.2). This analysis revealed that both wildtype and the *fakA* mutant use 15:0 as one acyl sidechain, as expected. The second acyl moiety was the same for each lipid species between the two strains, i.e. 35:0 possessed a 15:0 and 20:0 fatty acid. Thus, despite using the same fatty acids for membrane generation, the mutant possesses a higher percentage of longer acyl-chain containing lipids.

Lipid profile of wild type and fakA mutant in presence of exoFAs. S. aureus is unable to endogenously synthesize unsaturated fatty acids but can incorporate them from the environment through FakA. This allows us to use exogenously added fatty acids to track exoFA utilization and observe where exoFAs are incorporated. Using this approach, we determined the lipid composition

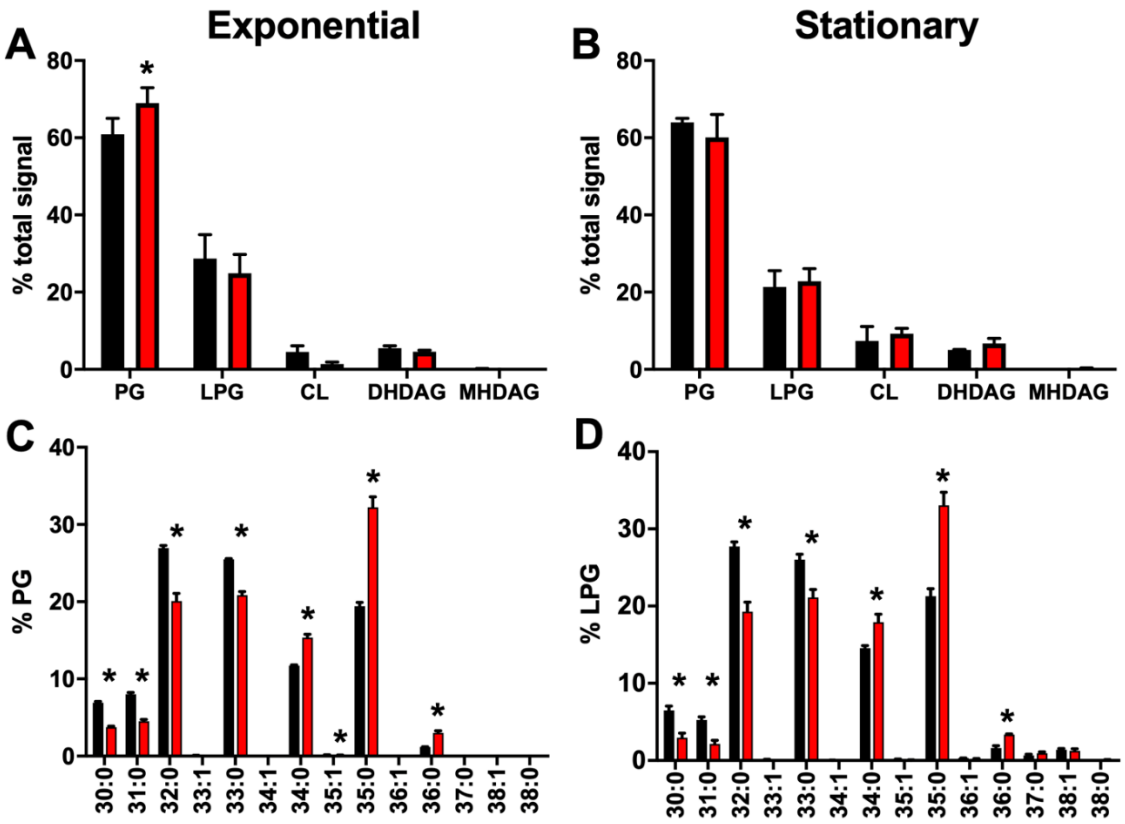
A
Exponential
% total signal
PG
LPG
CL
DHDAG
MHDAG
B
Stationary
C
% PG
D
% LPG
30:0
31:0
32:0
33:1
33:0
34:1
34:0
35:1
35:0
36:1
36:0
37:0
38:1
38:0

Figure 2. 2

Figure 2.2. Lipid analysis for wildtype (black) and *fakA* mutant (red). % total signal for each lipid class was determined at **(A)** exponential and **(B)** stationary phase of growth for phosphatidylglycerol (PG), lysyl-PG (LPG), cardiolipin (CL), dihex-diacylglycerol (DHDAG), and monohex-diacylglycerol (MHDAG). Individual **(C)** PG and **(D)** LPG species from cells in exponential phase were determined and are presented as percent of the total PG or LPG signal. Data represents the mean (n=4) with standard deviation, *$p<0.05$ by student t-test.

of both wildtype and a *fakA* mutant when grown in the presence of oleic acid (18:1), which was chosen due its relatively low toxicity (Figure 2.9) [160]. Previously, we demonstrated that the addition of 0.001% (~31 μM) oleic acid elicits a transcriptional response in *S. aureus* [158]; therefore, we determined the lipid profiles in TSB supplemented with 0.001% oleic acid. We observed little if any incorporation of oleic acid into PG and LPG when grown at this concentration (Figure 2.3A and 2.3C). Indeed, the lipid profile of wildtype and *fakA* mutant grown with added 0.001% oleic acid were indistinguishable from growth in TSB alone (Figure 2.2). In agreement with this, we used Fatty Acid Methyl Ester (FAME) analysis followed by gas chromatography to examine total fatty acid content of the cells and found little oleic acid (18:1) associated with the cells grown in TSB + 0.001% oleic acid (Table 2.3). Thus, while *S. aureus* responds transcriptionally to 0.001% additional oleic acid, this concentration was too low to affect incorporation.

Next, we increased the oleic acid concentration to 0.01% oleic acid (~314μM). At this concentration, the wild-type strain readily used the oleic acid and was observed as the appearance of a single unsaturated fatty acid chain primarily in 32:1, 33:1, 34:1, and 35:1 lipids (Figure 2.3B and 2.3D). We had predicted that oleic acid (18:1) would be found primarily paired with 15:0, the most common fatty acid lipid side chain in *S. aureus*. While we did readily detect 33:1, the most abundant lipid was 35:1 and composed >30% of total lipid species. As expected, there was no unsaturated fatty acid in the lipids isolated from the *fakA* mutant. To confirm that the absence of oleic acid in *fakA* mutant lipids is not due to oleic acid not associating with the cell, we performed FAME followed by gas chromatography analysis on the same extracts used for lipid analysis. Our FAME analysis revealed that in TSB, the wildtype and *fakA* mutant have similar total fatty acids profiles, with increased 20:0 in the *fakA* mutant (Figure 2.4A). When grown with the additional

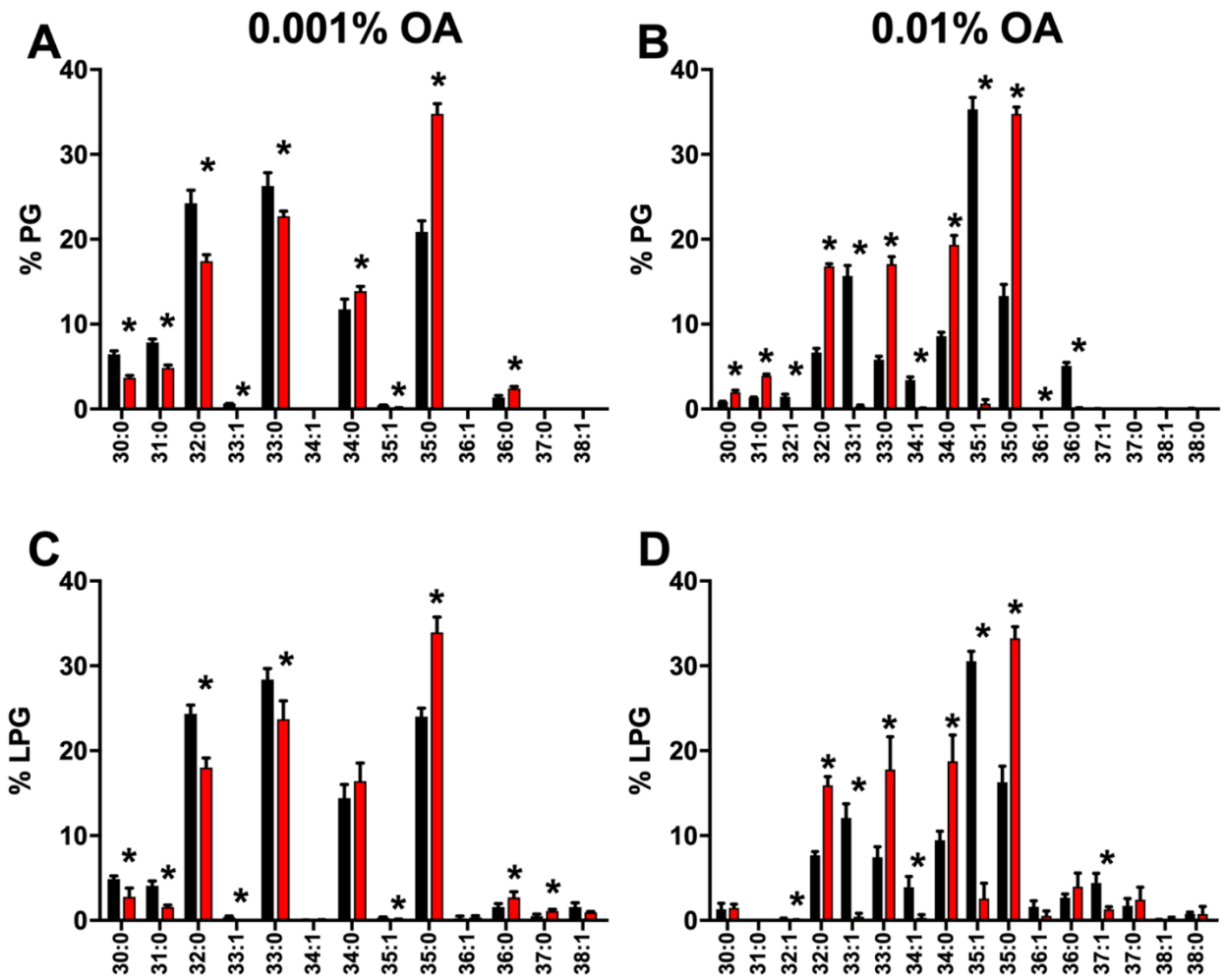
A
0.001% OA
% PG
B
0.01% OA
% PG
C
% LPG
D
% LPG
30:0
31:0
32:0
32:1
33:1
33:0
34:1
34:0
35:1
35:0
36:1
36:0
37:0
37:1
38:1
38:0

Figure 2. 3

Figure 2.3. Lipid profile for wildtype (black) and *fakA* mutant (red) of PG **(A** and **B)** and LPG **(C** and **D)** grown in TSB+0.001% oleic acid **(A** and **C)** or TSB+0.01% oleic acid **(B** and **D)**. Data represent the mean (n=4) with standard deviation, *$p<0.05$ by student t-test.

0.01% oleic acid, this fatty acid was readily detectable from both strains (Figure 2.4B and Table 2.3). FAME identifies all fatty acids, both free and lipid associated. Since oleic acid was identified by FAME but was not found as a component of the *fakA* lipids, we can conclude that oleic acid associates with the cells but cannot be incorporated into the *fakA* mutant. Thus, the lack of oleic acid in mutant membranes is due to a lack of incorporation and not because oleic cannot interact with or enter the cell.

Our lipid profiling indicated that wild-type cells can pair oleic acid with more than one fatty acid to produce a lipid. Moreover, we had expected 33:1 to be the most prevalent lipid species by pairing oleic acid with 15:0. We again used product ion analysis to determine the fatty acid pairing in each lipid (Table 2.2). It was expected that the fatty acid paired with oleic acid would be a saturated fatty acid and that this fatty acid would be equivalent to total lipid carbon length minus the oleic acid. This prediction was true for 32:1 (14:0 and 18:1) and 33:1 (15:0 and 18:1). Considering 18:1 was the added fatty acid, we anticipated 35:1 to be comprised of 17:0 and 18:1 fatty acids. This was not the case as the major 35:1 fatty acid pair consisted of 15:0 and 20:1. The inclusion of 20:1 was also the fatty acid associated in the lower abundant lipid 34:1.

While *S. aureus* membranes comprise both Straight-Chain Fatty Acids (SCFAs) and branched-chain fatty acids (BCFAs), it relies on BCFAs to modulate the rigidity of its lipid membrane [61]. BCFAs in *S. aureus* are comprised of odd numbered iso and anteiso fatty acids and the proportions of BCFAs and SCFAs are highly dependent on the growth environment [60]. We analyzed our FAME data to determine if the absence of *fakA* or the addition of oleic acid impacts BCFA or SCFA preference (Table 2.3). In TSB alone, wildtype and the *fakA* mutant have similar ratios of anteiso/iso fatty acids (~1.5) and BCFA/SCFA (1.65 for wildtype and 1.48 for *fakA* mutant). Not surprising considering our other analysis, when grown in TSB+0.001% oleic acid, the fatty acid

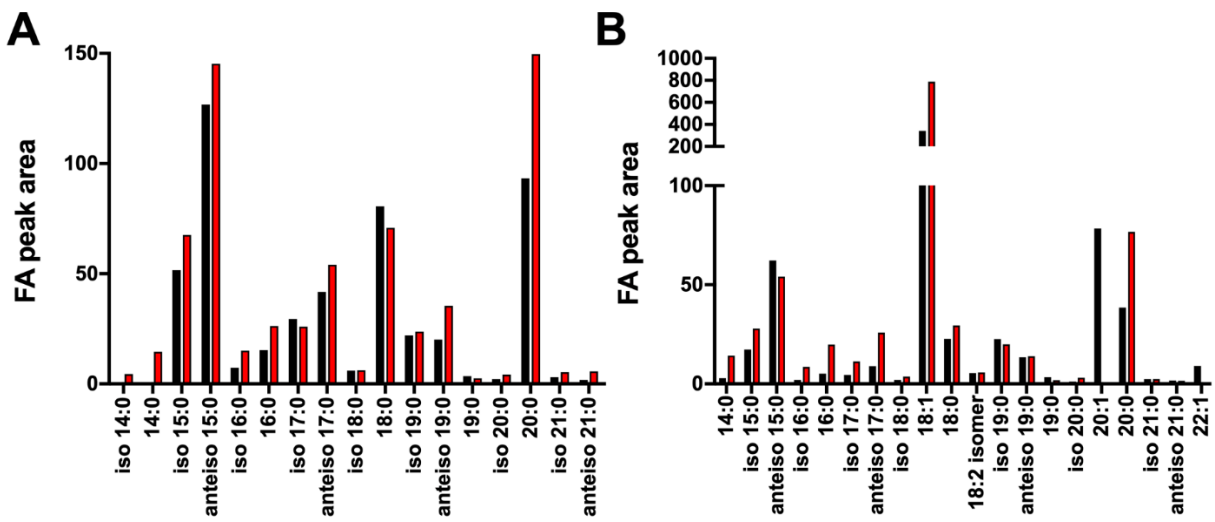
A
FA peak area
150
100
50
0
iso 14:0
14:0
iso 15:0
anteiso 15:0
iso 16:0
16:0
iso 17:0
anteiso 17:0
iso 18:0
18:0
iso 19:0
anteiso 19:0
19:0
iso 20:0
20:0
iso 21:0
anteiso 21:0
B
FA peak area
1000
800
600
400
200
100
50
0
14:0
iso 15:0
anteiso 15:0
iso 16:0
16:0
iso 17:0
anteiso 17:0
iso 18:0
18:1
18:0
18:2 isomer
iso 19:0
anteiso 19:0
19:0
iso 20:0
20:1
20:0
iso 21:0
anteiso 21:0
22:1

Figure 2. 4

Figure 2.4. Fatty acid methyl esterase analysis of lipid extracts from wildtype (black) and *fakA* mutant (red) grown in TSB **(A)** or TSB+0.01% oleic acid **(B)**. Data are from pooled replicates (n=4) from each strain and growth environment.

profile of both wildtype and *fakA* mutant was nearly identical to growth in TSB. By contrast, growth in TSB+0.01% oleic acid resulted in accumulation of oleic acid in both wildtype and *fakA* mutant bacteria. When comparing the BCFA/SCFA ratio under this condition, we observed a dramatic shift, most likely due to the added SCFA oleic acid. For example, wild-type cells grown in TSB contain ~38% SCFA while growth in 0.01% oleic acid led to the cells altering the fatty acid pools to ~78% SCFA. A similar shift (40% to 84%) was also seen in the *fakA* mutant. As noted in previous studies [164], the wild-type *S. aureus* unsaturated fatty acid pool was comprised of both C18:1 and C20:1. This data, along with our lipid and product-ion data, indicates that wild-type *S. aureus* elongates oleic acid (C18:1) to C20:1. This is not observed in the *fakA* mutant, as the majority of oleic acid remained oleic acid. In conclusion, the fatty acid composition of the membrane is dramatically altered in the presence of incorporation-level oleic acid seen in wildtype as the incorporation of oleic acid into PG, LPG and CL.

Membrane function is affected by the inability to utilize exoFAs. The membrane lies at the interface of cellular processes and the external environment. We have now shown that *fakA* influences membrane composition. We previously reported that the *fakA* mutant produces decreased pigment [160], which is associated with membrane fluidity [165-167]. Also, our previous metabolomics study found that the *fakA* mutant has a more reduced cellular environment [159]. The electron transport chain is embedded in the phospholipid membrane, suggesting that fatty acid accumulation and the composition of the membrane may affect respiration. Finally, membrane potential is indicative of metabolic state and membrane function. Therefore, we wanted to determine the role FakA and exoFAs play in membrane fluidity, permeability, membrane potential, and respiratory chain activity.

First, membrane fluidity was determined using the fluorescent probe 1,6-diphenyl-1,3,5-hexatriene (DPH) [61, 165] in wild type and *fakA* mutant grown to exponential phase (5 hours) in TSB with and without incorporation level oleic acid (0.01%). While it did not reach significance (p=0.07), the *fakA* mutant had decreased membrane fluidity compared to wild type (Figure 2.5A). The pigment staphyloxanthin, expressed from the *crt* operon, is known to affect membrane fluidity [168] and *fakA* mutants produce less pigment [168]. To remove this complication, we tested a *crtM* mutant with and without *fakA*. We observed that a *crtM* mutant has more membrane fluidity than its isogenic parents, both in the case of wild type and *fakA*. Interestingly, a *fakA crtM* double mutant has significantly decreased membrane fluidity compared to that of the *crtM* mutant. The addition of 0.01% oleic acid decreased membrane fluidity for both wild type and *fakA* mutant. This was not due to incorporation as part of phospholipids since the wildtype and *fakA* mutants were equivalent. For reasons that are not clear, adding oleic acid to *crtM* mutants had no effect on membrane fluidity (compare *crtM* +/- oleic acid) and, again, we observed lower membrane fluidity in the *fakA crtM* mutant compared to *crtM* alone. Thus, we identified that the absence of FakA affects membrane fluidity and this is not due to the altered pigment levels in the mutant.

We next assessed whether the absence of FakA altered membrane integrity using propidium iodide (P.I.) as an indicator since this stain cannot diffuse into cells unless membranes are compromised. Cells were grown in TSB and membrane integrity was determined when grown in the presence and absence of 0.01% oleic acid. When grown in TSB alone until mid-exponential phase, the wildtype and *fakA* mutant had approximately 3% and 1.1% P.I. positive cells, respectively (Figure 2.5B). However, when cells grown in the presence of 0.01% oleic acid, 16.4% of wildtype cells were P.I. positive compared to that of 2.8% for the *fakA* mutant. Thus, when grown in TSB, the

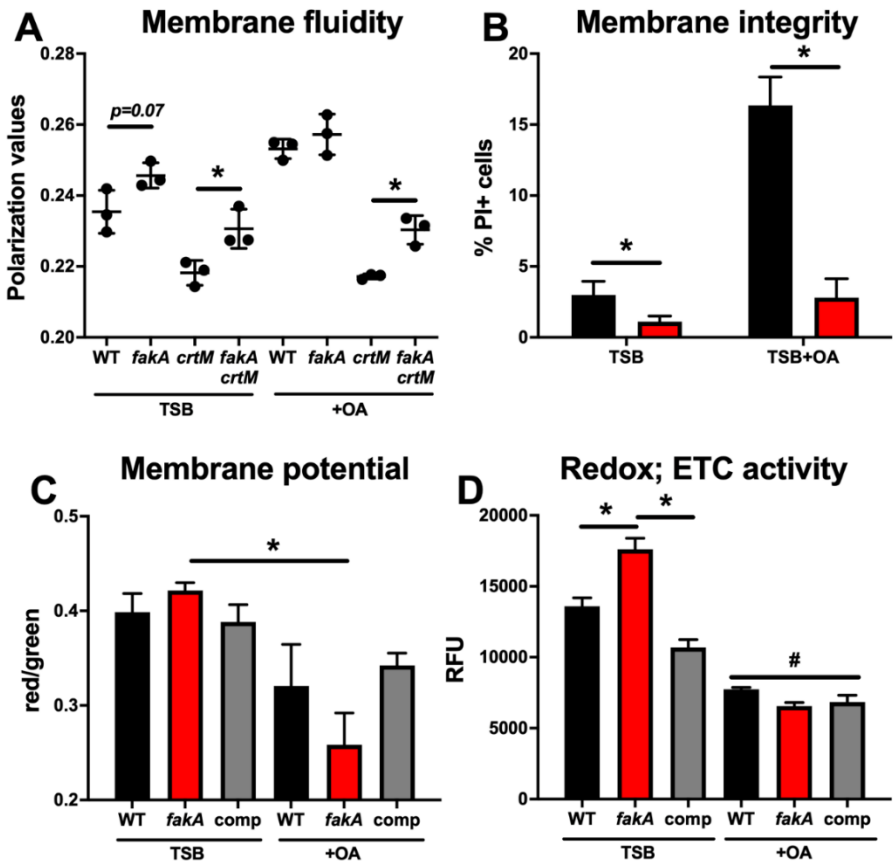
A
Membrane fluidity
Polarization values
0.28
0.26
0.24
0.22
0.20
p=0.07
*
*
WT
fakA
crtM
fakA crtM
WT
fakA
crtM
fakA crtM
TSB
+OA
B
Membrane integrity
% PI+ cells
20
15
10
5
0
*
*
TSB
TSB+OA
C
Membrane potential
red/green
0.5
0.4
0.3
0.2
*
WT
fakA
comp
WT
fakA
comp
TSB
+OA
D
Redox; ETC activity
RFU
20000
15000
10000
5000
0
*
*
#
WT
fakA
comp
WT
fakA
comp
TSB
+OA

Figure 2. 5

Figure 2.5. (A) Membrane fluidity in wildtype, *fakA* mutant, *crtM* mutant, and *fakA crtM* mutants grown in presence (+OA) or absence (TSB) of 0.01% oleic acid. **(B)** Membrane integrity measured using propidium iodide (P.I.) as an indicator for wildtype (black) and *fakA* mutant (red). **(C)** Membrane potential was analyzed using $DiOC(3)_2$ staining of wildtype (black), *fakA* mutant (red), and complemented *fakA* mutant (comp, grey). **(D)** Respiratory activity of wildtype (black), *fakA* mutant (red), and complemented *fakA* mutant (comp, grey) as measured using CTC as an indicator. Data represents the mean (n=3) with SD. *$p<0.05$ by student t-test. "#" indicates that all samples treated with OA were significant from the corresponding strain in TSB alone. Data are representative of at least three independent experiments.

fakA mutant has less permeable membranes whose permeability is less affected by the presence of oleic acid than the wild-type strain.

Membrane potential is important for driving ATP production and transporting ions and metabolites into and out of the cell. We determined the membrane potential ($\Delta\Psi$) of wildtype and *fakA* mutant *S. aureus* using the fluorescent reporter 3,3′-diethyloxacarbocyanine iodide ($DiOC_2(3)$) [169, 170]. Wildtype and *fakA* had similar membrane potentials when grown in TSB alone (Figure 2.5C). When grown in the presence of 0.01% oleic acid, both strains had decreased membrane potentials compared to that when grown in TSB alone, but this was enhanced in the *fakA* mutant with a 40% reduction compared to a 20% reduced potential in wildtype. Thus, under these conditions, oleic acid decreases membrane potential and this may be enhanced in a *fakA* mutant.

Electron transport chain activity was measured using the fluorescent reporter 5-cyano-2,3-ditolyl tetrazolium chloride (CTC) [170]. This reporter is reduced by respiratory dehydrogenases and is thus indicative of cellular respiration. In TSB alone, the *fakA* mutant had significantly more respiratory activity compared to that of wildtype (Figure 2.5D). However, both wildtype and *fakA* mutant display decreased respiratory activity in the presence of incorporation-level oleic acid, which correlates with reduced growth (Figure 2.9). Overall, these studies demonstrate that the *fakA* mutant displays phenotypes that are associated with membrane changes.

Lipid profile is altered when grown in the presence of mouse skin homogenate. The most common infection site of *S. aureus* is the skin, which contains high levels of various fatty acids and lipids [80]. These molecules have antimicrobial properties and limit the growth of certain bacteria. It is unknown if *S. aureus* can utilize fatty acids from mouse skin, though it will harvest fatty acids from other host molecules such as low-density lipoprotein [96]. To gain insight into this, we

determined 1) if *S. aureus* alters its lipids in response to mouse skin, and 2) if *S. aureus* incorporates host fatty acids. To this end, we grew wild-type and *fakA* mutant *S. aureus* in a combination of 75% mouse skin homogenate and 25% TSB. This ratio was chosen based on relatively high bacterial growth (OD_{600} 3.5-4.5) to allow for quality extraction of bacterial lipids. After 24 hours of growth in 75% mouse skin homogenate, cells were isolated, lipids were extracted, and analyzed via LC/MS/MS. To ensure that we did not collect mouse skin lipids without bacterial cells, one sample of 75% mouse skin homogenate and 25% TSB without bacterial cells was treated identically to our bacterial cells we extracted. This sample without bacteria was also analyzed via LC/MS/MS and we found only trace amounts of lipids (Figure 2.10), demonstrating that our data represents lipids isolated from *S. aureus* and not contaminates from the mouse skin. Under this growth condition, we observed equal levels of PG and LPG in the wild-type strain. Unlike in TSB, we saw a pronounced difference in the *fakA* mutant compared to wildtype. In this case, the *fakA* mutant resembled membranes of cells grown in TSB alone with PG being the most abundant, followed by LPG, and CL being the least abundant lipid. The most abundant saturated PG species was 33:0 and 35:0 in wildtype while the *fakA* mutant had a relatively even distribution of 32:0, 34:0, and 35:0. Using the natural unsaturated fatty acids found in mouse skin as a marker of host fatty acid utilizations, we observed considerable incorporation of unsaturated fatty acids as a component of the wild-type cell lipids (Figure 2.6B-D). The unsaturated PG species 33:1, 34:1, 35:1 and 36:1 was all found in *S. aureus* grown in mouse skin homogenate. Similar trends were observed for LPG and CL species. We did not identify lipids containing more than one fatty acid unsaturation. As expected, we did not find unsaturated fatty acids in the lipids of the *fakA* mutant. In conclusion, we show that *S. aureus* can utilize unsaturated fatty acids found in mouse skin homogenate for lipid synthesis.

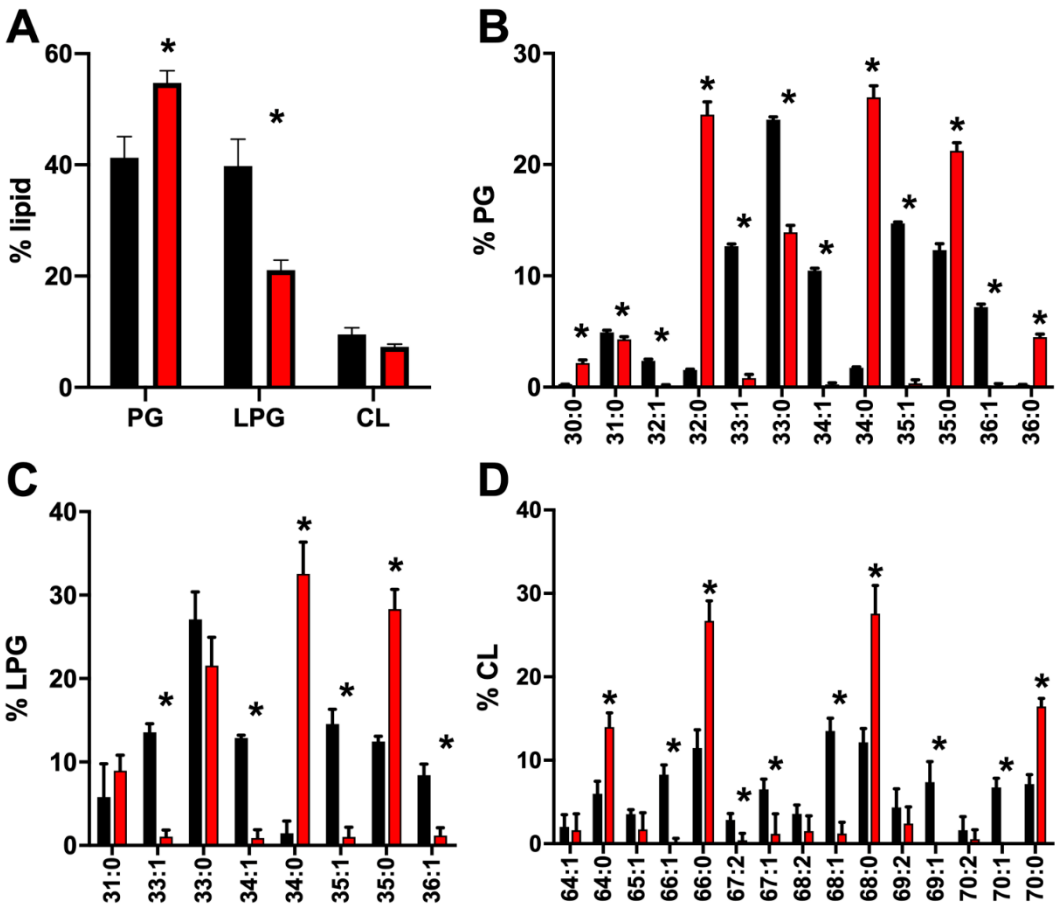
A
% lipid
60
40
20
0
PG
LPG
CL
B
% PG
30
20
10
0
30:0
31:0
32:1
32:0
33:1
33:0
34:1
34:0
35:1
35:0
36:1
36:0
C
% LPG
40
30
20
10
0
31:0
33:1
33:0
34:1
34:0
35:1
35:0
36:1
D
% CL
40
30
20
10
0
64:1
64:0
65:1
66:1
66:0
67:2
67:1
68:2
68:1
68:0
69:2
69:1
70:2
70:1
70:0

Figure 2. 6

Figure 2.6. Lipid profile of wildtype (black) and *fakA* mutant (red) grown in 75% mouse skin homogenate. **(A)** Total percent lipid signal of wildtype and *fakA* mutant by class of lipid. Identification of **(B)** phosphatidylglycerol (PG), **(C)** lysyl-PG (LPG), and **(D)** cardiolipin (CL) represented by the percentage of the total from each class. Data represent the mean (n=4) with standard deviation of representative experiment. *$p<0.05$ by student t-test.

Conclusions

The exoFA utilization system of *S. aureus* has recently emerged as a new metabolic pathway and is made up of at least the fatty acid kinase FakA and the fatty acid binding partner proteins FakB1 and FakB2 [65, 156]. Despite the characterization of this system, how inactivation of this pathway (via deletion of *fakA*) affects the composition of the phospholipid membrane has been unknown. *S. aureus* is routinely cultivated in TSB which is abundant in carbohydrates, protein, and fatty acids, primarily palmitic acid (C16:0) and stearic acid (C18:0). Not surprisingly, based on a previous report, we identified an accumulation of fatty acids in a *fakA* mutant under our growth conditions. However, our studies revealed that this changes over the course of growth and identifies that not only do the *fakA* mutant cells accumulate fatty acids, but that fatty acids are released into the media where they also increase in abundance. It is unknown whether this accumulation of fatty acids in the extracellular growth environment is an intentional process (i.e. release of fatty acids from the cell), due to cell death and turnover, or are actively released by a efflux system that has been proposed [161]. Since only free fatty acids are identified in this experiment, the fatty acids found in the supernatant are likely not part of extracellular membrane vesicles produced by *S. aureus*. The consequence of altered fatty acid metabolism in the *fakA* mutant is not a change in the ratio of primary lipid species, but a reorganization of the fatty acid phospholipid side chains. Moreover, we demonstrate that the addition of excess 18:1 fatty acid leads to its incorporation into wild-type cells, but also a change in the fatty acid pools in both wildtype and *fakA* mutant.

S. aureus is known to produce primarily three phospholipids [76, 171-173]. Phosphatidylglycerol (PG) is the primary phospholipid and is the precursor for the generation of additional phospholipids. Lysl-PG (or LPG) is produced by MprF and while *S. aureus* has two cardiolipin

synthases, cardiolipin is the least abundant species. As expected, our results demonstrated that both wild-type and *fakA* mutant membranes primarily contained PG and LPG. The amount of CL can vary by strain and condition, and we detected only 4.5% of total phospholipids as cardiolipin in our USA300 *S. aureus* strain at either exponential or stationary phase of growth showing that LAC derivatives grown under our conditions produce little CL.

S. aureus generally prefers endogenously produced 15:0 in the sn2 position of the phospholipids and will insert either a second endogenous fatty acid or exoFA in the sn1 position. Our product ion analysis of the wild-type and *fakA* mutant phospholipids most often contained a 15:0 fatty acid. However, the *fakA* mutant paired this 15:0 more frequently with longer chain fatty acids (Figure 2.2) than the parent strain. Phospholipids of lower total carbon abundance (i.e. 30:0, 31:0, 32:0, and 33:0) were more abundant in wildtype compared to that of *fakA* mutant. These phospholipids all contained C15:0 in one sn position, with the other acyl chain being C15:0, C16:0, C17:0, and C18:0 in phospholipids 30:0, 31:0, 32:0 and 33:0, respectively. The most abundant phospholipids observed in wildtype were 32:0 and 33:0. In contrast, the *fakA* mutant tended to have larger fatty acids as part of phospholipids, shifting to 35:0 in both PG and LPG due to the insertion of C20:0 alongside C15:0. This was also reflected in the free fatty acid pools in the *fakA* mutant (Figure 2.8) showing that this mutant possesses and uses a greater abundance of longer fatty acids such as 19:0 and 20:0. However, the presence of exogenous oleic acid altered the normal relationship of use of 15:0 alongside a varying-length second fatty acid. In this case, the wildtype generated lipids with 18:1 oleic acid in combination with not only 15:0, but also commonly 14:0. One observation made from this study, and in agreement with Parsons et al [164] in strain RN4220, is the abundance of fatty acid C20:1 in wild-type *S. aureus*. Since oleic acid (C18:1) was the exoFA added to the media, this demonstrates that *S. aureus* can elongate exoFAs. This was a frequent event since 35:1

composed of 15:0 and 20:1 was the most abundant lipid species identified in wild type when grown in the presence of oleic acid (Table 2.2 and Figure 2.3). Our FAME analysis confirmed that the lack of incorporation of 18:1 into the *fakA* mutant is not due to the inability to associate with the cells and is a result of the inability of the *fakA* mutant to phosphorylate the fatty acid, as expected. The presence of 20:1 has been observed previously and while the exact mechanism behind exoFA elongation has not been elucidated, it has been proposed to occur through FabF, part of the fatty acid biosynthesis pathway [174]. However, our observation that there was no 20:1 fatty acid found in the *fakA* mutant, demonstrates that elongation of exoFAs requires FakA and that only phosphorylated fatty acids can be elongated by *S. aureus*.

In previous studies, we identified that oleic acid can inhibit the Sae two-component system when added exogenously to the media at 0.001% [158]. This was later confirmed by another group [149]. Considering this transcriptional response, we anticipated that this concentration would yield membranes containing oleic acid. However, oleic acid-containing phospholipids were not detected when *S. aureus* was grown in the presence of 0.001% (~31μM) oleic acid. When the concentration of oleic acid was increased ten-fold to 0.01% (~314μM), we observed incorporation of oleic acid into lipids. Thus, there is an apparent concentration-dependent incorporation of exogenous unsaturated fatty acids by *S. aureus*. Moreover, this data revealed that *S. aureus* can sense and respond transcriptionally to levels of fatty acids that are lower than those used for membrane synthesis, further supporting fatty acids as a potent signaling molecule in *S. aureus*.

The membrane is a dynamic structure that dictates multiple functions of the cell. We identified functional changes between wild-type and *fakA* mutant *S. aureus*. In TSB alone, the *fakA* mutant has more rigid membranes regardless of pigment production. Since pigment impacts membrane fluidity and the *fakA* mutant produces less pigment, this could confound membrane fluidity

experiments in this strain. Our data confirms that pigment does impact membrane fluidity (Figure 2.5), but also demonstrates that there is a FakA-dependent component. This could possibly be due to increases in the acyl-chain length of the phospholipids (Figure 2.2C) as longer acyl-chains result in a more rigid membrane. Additionally, a slight decrease in BCFA/SCFA ratios in the *fakA* mutant (Table 2.3) could increase rigidity. To our surprise, addition of 0.01% oleic acid decreased membrane fluidity of both wildtype and *fakA* mutant. While the unsaturated fatty acid linoleic acid (C18:2) has been shown to increase membrane fluidity [175], our data clearly demonstrates that growth in the presence of oleic acid does not result in similar membrane fluidity. There may be two explanations for this possible result. First, this may be due to the difference in structure of the fatty acids. The presence of two unsaturations in linoleic acid may be more disruptive to fluidity compared to that of oleic acid. Secondly, the addition of 0.01% oleic acid dramatically decreases the BCFA/SCFA ratio in both wildtype and *fakA* mutant. To this end, wild-type cells contained 38% and >75% SCFAs when grown in TSB without or with 0.01% oleic acid, respectively. SCFAs, like oleic acid, are known to affect membrane fluidity and our data are consistent with the increased abundance of SCFAs when grown in the presence of oleic acid decreasing membrane fluidity. It appears that oleic acid impacts membrane fluidity without the requirement of being incorporated and this is influenced by the presence of the pigment staphyloxanthin. Notably, previous work suggests that pigment levels are not influenced by fatty acid incorporation [176]. Dissecting this relationship between fatty acid addition, fatty acid utilization, and *S. aureus* pigmentation will be the focus of future studies.

We have established that the *fakA* mutant has altered metabolism [159]. Since the electron transport chain is embedded in the phospholipid membrane, we sought to determine whether the changes in membrane composition in the *fakA* mutant and the presence of 0.01% oleic acid altered

cellular respiration. The *fakA* mutant had more respiratory activity than wildtype in TSB alone (Figure 2.5D). This agrees with our metabolic study showing the *fakA* mutant had an increase in NAD+/NADH and NADP+/NADPH levels at the same phase of growth. Growth in TSB+0.01% oleic acid resulted in decreased respiration in both wildtype and the *fakA* mutant. While the increased respiration of the *fakA* mutant in TSB didn't affect membrane potential, growth in TSB+0.01% oleic acid depolarized both the wildtype and *fakA* mutant; however, the *fakA* mutant was more greatly affected (Figure 2.5C). Previous studies indicated that palmitoleic acid (C16:1), and not oleic acid (C18:1), depolarized membranes [174]. It should be noted that we used approximately three times the concentration of oleic acid as the study mentioned and can likely account for the differences between experiments. Additionally, the study mentioned above was published prior to the identification of FakA and therefore, how incorporation vs free fatty acid exposure could not be tested. Thus, our data indicates that oleic acid will decrease respiration and depolarize membranes at 0.01% (314 µM) regardless of being incorporated into phospholipids. Why the *fakA* mutant has more respiratory activity in TSB is unknown; however, this observation occurs at a point where we identified enhanced growth in the *fakA* mutant during the switch between glucose and acetate/amino acid utilization [159]. Thus, it may be not surprising to see increased respiratory activity during periods of enhanced growth. Why FakA influences metabolism and has not been completely elucidated. This could be due to changes in the membrane that may influence nutrient diffusion or transport. Another possibility is the result of the accumulation of fatty acids, which could have different activities or impact levels based on saturation. A recent study indicated that inactivation of type II NADH dehydrogenases, (Ndh-2s) particularly NdhC, results in fatty acid accumulation and regulation of the SaeRS two-component system [26]. Ndh-2s do not pump ions across the membrane, thus playing an indirect role in

membrane potential. In *E. coli*, Ndh-2s are associated with aerobic respiration while Ndh-1s are associated with anaerobic respiration [177]. Since the *fakA* mutant possesses an aeration-dependent growth enhancement and has increased respiratory activity without a significant increase in membrane potential, we predict that the Ndh-2 are playing a pivotal role in altering metabolism when fatty acids are accumulated within the cell or in the presence of exoFAs. Studies testing how different types of exoFAs affect respiration through Ndh-2s, as well as other members of the respiratory chain, will help us understand the mechanism by which fatty acids are affecting bacterial physiology. It is clear that the inability of *S. aureus* to use fatty acids and/or exposure to exoFAs impacts physiology. This has been seen by us and others as changes in the glucose, acetate, amino acid metabolism, and energy or redox homeostasis that apparently involves at some level NADH dehydrogenases and regulatory proteins such as CcpA, as well as transcriptional response in arginine deiminase and urease [26, 159, 160, 174, 178, 179]. It is also possible that *S. aureus* identifies unsaturated fatty acids as a stress as we previously saw that enhanced resistance to unsaturated fatty acids in a *fakA* mutant requires the alternative sigma factor σ^B [160]. Future studies will be needed to determine the specific mechanism by which fatty acid addition modulate metabolism in *S. aureus* and whether this is a general fatty acid response or is restricted to certain fatty acids types.

We wanted to expand our observations to more closely mimic what the bacteria may encounter during infection. Since *S. aureus* commonly causes infections in the skin, we wanted to determine if *S. aureus* can actively scavenge unsaturated fatty acids for phospholipid synthesis from host tissue. To do this, we homogenized mouse skin and grew wild-type and *fakA* mutant *S. aureus* in 75% mouse skin homogenate supplemented with 25% TSB. While *S. aureus* can grow relatively well in 100% mouse skin homogenate, we added 25% TSB to ensure high bacterial growth. We

confirmed that *S. aureus* can scavenge exoFAs when grown in mouse skin homogenate. We did observe lipidome changes in wild-type *S. aureus* when grown in mouse skin compared to that of TSB+0.01% oleic acid. For example, growth in mouse skin resulted in wild-type *S. aureus* to have relatively similar levels of PG33:0, PG33:1, PG35:0, and PG35:1. This differs from growth in TSB+0.01% oleic acid, where PG35:1 clearly became the most abundant phospholipid. While other studies have found that *S. aureus* can utilize fatty acids from host source, specifically low-density lipoprotein and pig liver homogenate [67, 96], none have used homogenized skin as a medium. Given the propensity of *S. aureus* to commonly infect the skin, our data provides a framework for future studies utilizing skin as a source of fatty acids and how bacterial phospholipid membranes adapt to skin tissue. How *S. aureus* is scavenging fatty acids from mouse skin and whether they are derived from free fatty acids, lipids, or LDL is one component of ongoing studies.

The exoFA utilization pathway of FakB1, FakB2, and FakA is newly described [65, 66]. Despite being necessary for the incorporation of exoFAs into the membrane, a detailed analysis of how this system alters membrane composition has not been performed. Not surprisingly, our results show no change in the PG:LPG:CL ratio by the absence of FakA, but there was a reorganization of the fatty acids side chains, e.g. change in fatty acid length preference, of *S. aureus* phospholipids in the absence of FakA. These studies provide key details on how membrane composition changes in response to exoFAs regardless if they are used for phospholipid synthesis. Furthermore, this work expands our knowledge on how the activity of FakA influences *S. aureus* physiology.

Materials and Methods

Bacterial strains, plasmids, and growth conditions. Bacterial strains and plasmids used in this study are listed in Table 2.1. *S. aureus* was grown in tryptic soy broth (TSB) or tryptic soy agar supplemented with chloramphenicol (10 μg mL^{-1}) or erythromycin (5 μg mL^{-1}) when necessary.

S. aureus cultures were then inoculated at a 1:10 media to flask volume ratio at an initial optical density at 600 nm of 0.1 in TSB and grown at 37^{o}C with shaking at 250 rpm. TSB was supplemented with oleic acid (Alfa Aesar) by adding indicated percent v/v oleic acid to media and vortexed vigorously before aliquoting into flasks.

Fatty acid analysis. Cell pellets and supernatants were flash frozen in liquid nitrogen and stored at -80^{o}C until processed. The cell pellets were washed three times with 1 mL of 40 mM ammonium formate in water. The washed pellets were re-suspended in 50 µL of 5 mM ammonium acetate and homogenized three times for 30 s with a BeadBeater with 15-min rests on ice in between. Protein concentration of the homogenates were measured, and each sample was normalized to 500 µg mL^{-1} and aliquoted at 25 µL for extraction. The supernatants were not normalized and aliquoted at 125 µL for extraction. All samples were extracted by protein precipitation with 1 mL of 80%/20% methanol/water for 20 min at 4°C. The samples were centrifuged at 20,000 x *g* for 10 minutes at 4°C. 1 mL of supernatant was collected and dried down under nitrogen gas at 30°C. The samples were reconstituted at 25 µL of 80:20 acetonitrile/5 mM ammonium acetate in water. Each sample was spiked with 1 µL of fatty acid stable isotope standards.

Analysis of the free fatty acids was performed on a Thermo Q-Exactive Oribtrap mass spectrometer with Dionex UHPLC and autosampler. All samples were analyzed in negative heated electrospray ionization in data dependent MS/MS with a mass resolution of 70,000 in Full MS and 17,500 at *m/z* 200 in data dependent MS/MS. Separation was achieved on an Acquity UPLC HSS T3 2.1 x 150 mm, 1.8 µm column with mobile phase A as 1 mM ammonium acetate and mobile phase B as 0.1% acetic acid in acetonitrile. The flow rate was 500 µL min^{-1} with a column temperature of 30°C. Injection volume was 4 µL. Peak areas were integrated for each analyte and internal standards using Xcalibur.

ESI-MS/MS lipid profiling. An automated electrospray ionization-tandem mass spectrometry approach was used, and data acquisition and analysis and acyl group identification were carried out as described previously [180] with modifications. Each sample was dissolved in 1 mL chloroform and an aliquot of 2 to 39 µL of extract was used.

For analysis of PG, PA, monohexDAG, and dihexDAG, phospholipid and galactolipid internal standards, obtained and quantified as previously described [181], were added in the amounts indicated in Narayanan et al [182] except for: phosphatidylinositol (PI) (16:0/18:0) (0.28 nmol), PI (18:0/18:0) (0.11 nmol), digalactosyldiacylglcyerol (DGDG) (18:0/16:0) (0.44 nmol), DGDG(18:0/18:0) (1.48 nmol), monogalactosyldiacylglycerol (18:0/16:0) (1.67 nmol), MGDG(18:0/18:0) (1.41 nmol), and cardiolipin (CL) (14:0/14:0/14:0/14:0) (0.015 nmol). The sample and internal standard mixture was combined with solvents, such that the ratio of chloroform/methanol/300 mM ammonium acetate in water was 300/665/35, and the final volume was 1.4 mL. Analysis of PG, PA, monohexDAG, and dihexDAG was performed on unfractionated lipid extracts introduced by continuous infusion into the ESI source on a triple quadrupole MS/MS (API 4000, Applied Biosystems, Foster City, CA). Data were collected and analyzed as previously described for analysis of PG, PA, monogalactosyldiacylglycerol (monohexDAG), and digalactosyldiacylglycerol (dihexDAG) [182].

For CL and LPG analysis, phospholipid standards were added one-fifth of the amounts indicated above. CL and LPG were analyzed on a triple quadrupole MS/MS (Xevo TQS, Waters Corp., Milford, MA). Samples were introduced to the Xevo TQS using a Waters 2777 Sample Manager autosampler. Lipid species were detected with the following scans: LPG $[M-H]^-$ in negative ion mode with Precursor 145.0; cardiolipin in negative ion mode with Precursor 153.0. The scan speed was 50 or 100 u per sec^{-1}. The Xevo TQS in negative ion mode has capillary, 2.8 kV, cone voltage,

40 V, source temperature, 150°C, desolvation temperature, 120°C, collision gas, 0.14 mL/min, nebulizer gas flow 7 bar for CL and LPG. Collision energies on the Xevo TQS, with argon in the collision cell, were -75 V for CL, and -35 V for LPG.

Data processing was similar to that previously, including background subtraction, smoothing, integration of spectral peaks, isotopic deconvolution, correction for chemical or instrumental noise, and quantification [183, 184]. Internal standards of the same class were used for PA, PG, and cardiolipin. Lysyl PG was quantified against the PG(40:0) in negative Precursor mode, monohex and dihexDAG were quantified against PG(40:0) in positive NL mode. Finally, the data were corrected for the fraction of the sample analyzed and normalized to signal per CFU to produce data in the units nmol/1e10 CFU.

Product ion analyses were performed on pooled replicates of the treatments on the 4000 QTrap mass spectrometer in enhanced product ion mode. Aliquots of 11 to 14 uL were used. Collision energy was varied as needed for sufficient fragmentation, starting at -45 V. The curtain gas was 10 mL/min, CAD gas was medium, and the electrospray capillary voltage was -4500 V.

Membrane fluidity, integrity, potential, and ETC activity. Membrane fluidity for wildtype and *fakA* mutant strains were carried out as previously described [185]. Membrane integrity was determined using propidium iodide (P.I.) as an indicator. Wildtype and *fakA* mutant bacteria were grown in TSB with or without 0.01% (314 μM) oleic acid for 5 hrs. 1.2 mL of culture spun down and resuspended in 600 μL PBS. The cells were then diluted to an OD_{600} = 0.25 in 500 μL in PBS. As a control, one sample was diluted to OD_{600} = 0.25 in 500 μL 70% ethanol. 1 μL of P.I. (50 mg/mL) was added to the cells and allowed to incubate at room temperature for 15 minutes. P.I. positive cells were determined using flow cytometry.

Membrane potential was determined using the *Bac*Light Bacterial Membrane Potential Kit (Molecular Probes, Invitrogen) [170]. Wildtype and *fakA* mutant bacteria were grown for 5 hrs. Cultures were diluted to an OD_{600} = 0.1 in 1 mL PBS. As a negative control, 10 µL of 500 µM carbonyl cyanide *m*-chlorophenyl hydrazone (CCCP) was added to one sample and vortexed. 10 µL of 3mM $DiOC_2(3)$ was then added to all samples, excluding a no stain control, and vortexed. Samples were then allowed to incubate at room temperature for 30 minutes and analyzed via flow cytometry. The data is presented as the geometric mean ratio of red:green using TexasRed and FITC filters, respectively.

Electron transport chain activity (respiratory activity) was determined using the *Bac*Light RedoxSensor CTC Vitality Kit (Molecular Probes, Invitrogen) [170]. Wildtype and *fakA* mutant bacteria were grown for 5 hrs. Cultures were diluted to and OD_{600} = 0.1 in 650 µL PBS. One sample was diluted in 70% ethanol as a negative control. 65 µL of 50 mM CTC was added to each sample, except for a no stain control. The samples were then incubated in the dark at 37˚C for 30 minutes and analyzed using a Tecan Spark 10M plate reader (Excitation 485+/-20nm and Emission 645+/-40nm).

Generation of mouse skin homogenates. These studies were conducted under an approved protocol by the Institutional Animal Care and Use Committee (IACUC) of the University of Kansas Medical Center. We used mice of the C57BL/6 background. Following sacrifice, mice were shaved and treated with Nair to remove remaining hair. Next, skin was removed and homogenized in PBS using Lysing Matrix H with a FastPrep-24 5G following manufacturer's setting. Homogenates were pooled and sequentially passed through 40 □m and 0.45 □m filters.

Table 2. 1

Strain or plasmid	Relevant characteristics[a]	Reference
AH1263	USA300 CA-MRSA strain LAC without LAC-p03	[86]
JLB2	AH1263 Δ*fakA*	[66]
JLB112	AH1263 *crtM::*NΣ	[160]
JLB129	JLB2 *crtM::*NΣ	[160]
pJB165	*fakA* complement plasmid	[66]

[a] NΣ indicates mutations originating from the Nebraska Transposon Mutant Library

Table 2.1. List of stains used in this study.

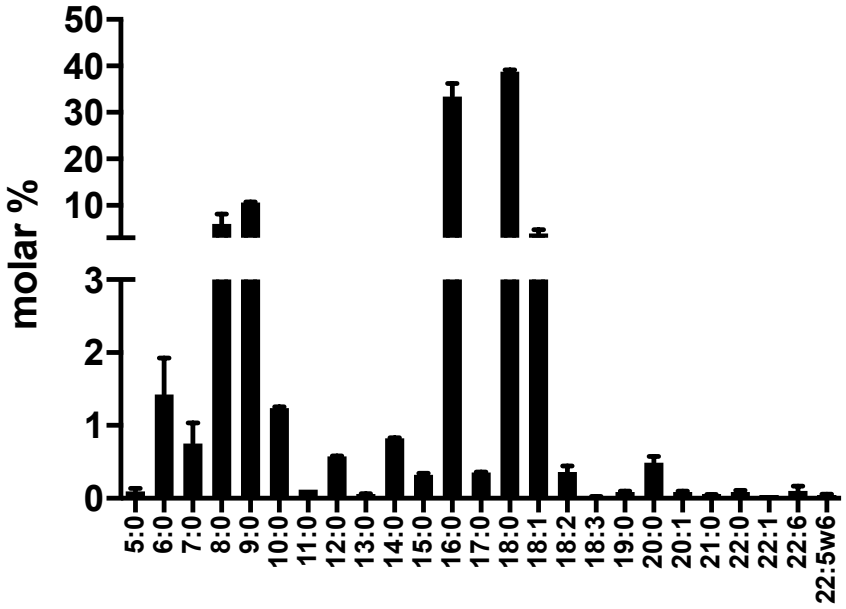
molar %
50
40
30
20
10
3
2
1
0
5:0
6:0
7:0
8:0
9:0
10:0
11:0
12:0
13:0
14:0
15:0
16:0
17:0
18:0
18:1
18:2
18:3
19:0
20:0
20:1
21:0
22:0
22:1
22:6
22:5w6

Figure 2. 7

Figure 2.7. Fatty acid composition of filter-sterilized tryptic soy broth supplemented with 14mM glucose. (Becton Dickinson, Lot #2269294). Data represent the mean (n=2) with standard deviation.

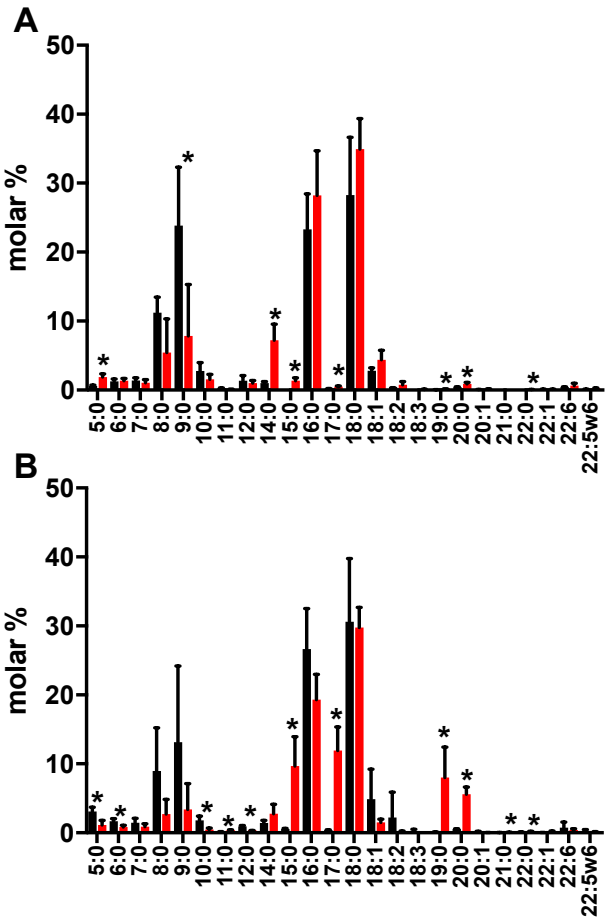
A
B
molar %
50
40
30
20
10
0
5:0
6:0
7:0
8:0
9:0
10:0
11:0
12:0
14:0
15:0
16:0
17:0
18:0
18:1
18:2
18:3
19:0
20:0
20:1
21:0
22:0
22:1
22:6
22:5w6

Figure 2. 8

Figure 2.8. Identification of cellular free fatty acids in wildtype (black) and *fakA* mutant (red) grown for three **(A)** and six hours **(B)** in TSB+14mM glucose. Data are the mean (n=4) with standard deviation. "*" indicates a significant difference ($p<0.05$) between stains by student t-test.

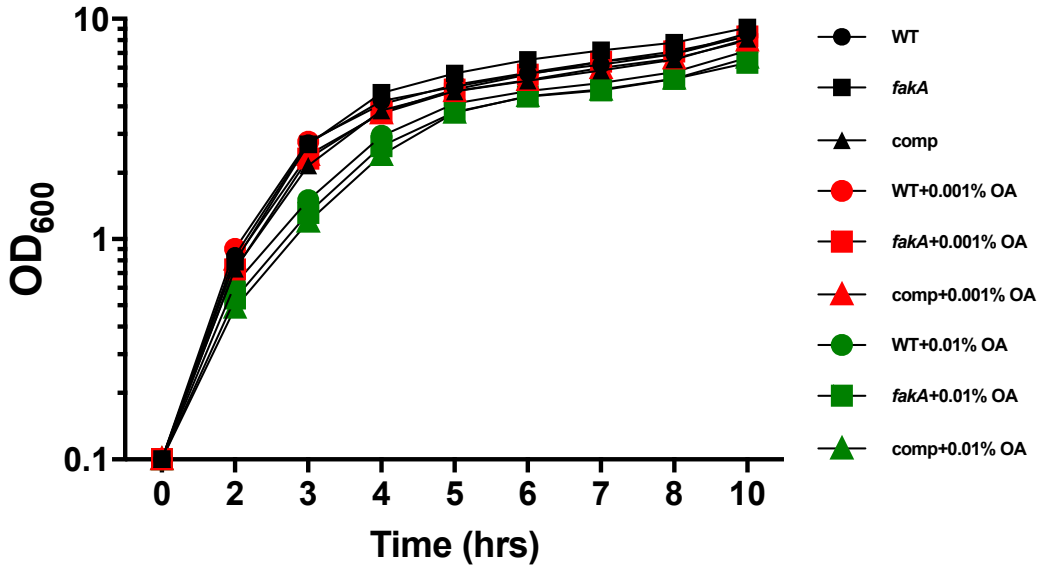
10
1
0.1
OD600
0
2
3
4
5
6
7
8
10
Time (hrs)
WT
fakA
comp
WT+0.001% OA
fakA+0.001% OA
comp+0.001% OA
WT+0.01% OA
fakA+0.01% OA
comp+0.01% OA

Figure 2. 9

Figure 2.9. Growth of wildtype (circles), *fakA* mutant (squares), and *fakA* mutant complement with *fakA* on plasmid pJB165 (triangles) grown in TSB (black symbols), TSB+0.001% oleic acid (red symbols), and TSB+0.01% oleic acid (green symbols). Data represent the mean (n=4) with SD and is representative of three independent experiments. Error bars are present but are smaller than symbols.

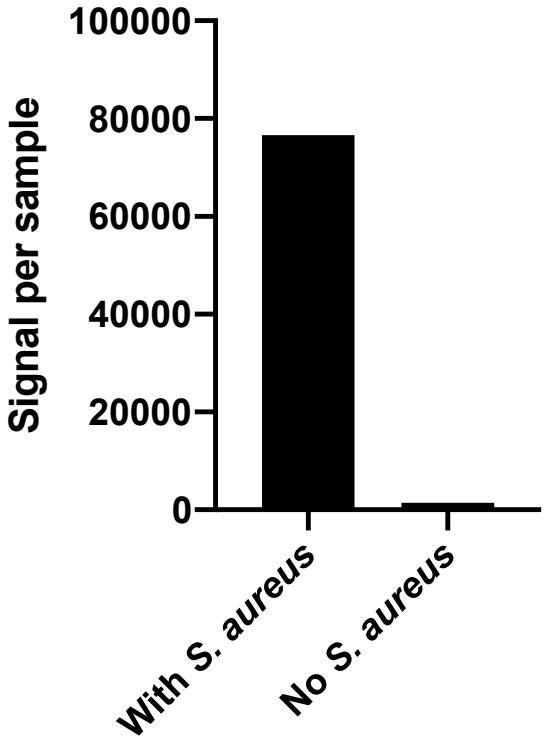
100000
80000
60000
40000
20000
0
Signal per sample
With S. aureus
No S. aureus

Figure 2. 10

Figure 2.10. Lipid quantification from samples of mouse skin homogenate media with *S. aureus* bacteria or parallel sample treated identically but not inoculated with bacteria.

Table 2. 2

		TSB				TSB+0.01% OA		
PG species		**WT**		***fakA***		**WT**		***fakA***
30:0		15:0/15:0		15:0/15:0		15:0/15:0		15:0/15:0
31:0		15:0/16:0		15:0/16:0		15:0/16:0		15:0/16:0
32:1						14:0/18:1		
32:0		15:0/17:0		15:0/17:0		15:0/17:0		15:0/17:0
33:1						15:0/18:1		
33:0		15:0/18:0		15:0/18:0		15:0/18:0		15:0/18:0
34:1						14:0/20:1		
34:0		15:0/19:0		15:0/19:0		15:0/19:0		15:0/19:0
35:1						15:0/20:1		
35:0		15:0/20:0		15:0/20:0		15:0/20:0		15:0/20:0
36:0		15:0/21:0		15:0/21:0		15:0/21:0		15:0/21:0
37:1								
37:0				15:0/22:0		15:0/22:0		17:0/20:0
LPG species								
30:0		15:0/15:0		15:0/20:0		15:0/20:0		
31:0		15:0/16:0		15:0/16:0				
32:0		15:0/17:0		15:0/17:0		15:0/17:0		14:0/18:0
33:1						15:0/18:1		
33:0		15:0/18:0		15:0/18:0		15:0/18:0		
34:0		15:0/19:0		15:0/19:0		15:0/19:0		15:0/19:0
35:0		15:0/20:0		15:0/20:0		15:0/20:0		15:0/20:0
36:0				15:0/21:0				

Table 2.2. Product ion analysis of pooled lipid extracts indicating most abundant acyl-chain composition of phosphatidylglycerol (PG) and lysyl-PG (LPG).

Table 2. 3

	Percentage of each compound					
	TSB		**TSB + 0.001% OA**		**TSB + 0.01% OA**	
	WT	***fakA***	**WT**	***fakA***	**WT**	***fakA***
iso 14:0	0.00	0.67	1.83	1.48	0.00	0.00
14:0	0.00	2.21	0.45	3.10	0.46	1.29
iso 15:0	10.48	10.26	10.85	10.23	2.69	2.52
anteiso 15:0	25.18	22.05	27.17	22.74	9.65	4.88
iso 16:0	1.81	2.29	2.01	2.58	0.32	0.77
16:0	3.01	3.98	2.83	4.63	0.80	1.79
iso 17:0	5.78	3.94	4.53	3.26	0.70	1.02
anteiso 17:0	8.18	8.21	6.54	6.11	1.40	2.33
iso 18:0	1.20	0.95	1.26	1.10	0.31	0.34
18:0	15.79	10.75	14.33	11.28	3.53	2.66
18:1	0.00	0.00	0.20	0.41	52.80	71.11
18:2 isomer	0.00	0.00	0.00	0.00	0.86	0.52
iso 19:0	4.30	3.59	3.66	3.01	3.50	1.80
anteiso 19:0	3.93	5.37	3.38	3.41	2.09	1.26
19:0	0.70	0.40	0.78	0.64	0.52	0.17
iso 20:0	0.42	0.63	0.57	0.79	0.19	0.28
20:0	18.26	22.71	18.14	23.43	5.97	6.92
20:1	0.00	0.00	0.00	0.00	12.14	0.00
iso 21:0	0.60	0.81	0.52	0.62	0.39	0.21
anteiso 21:0	0.36	0.86	0.43	0.50	0.27	0.14
22:0	0.00	0.32	0.20	0.39	0.00	0.00
22:1	0.00	0.00	0.00	0.00	1.41	0.00
% BCFA	62.25	59.64	62.74	55.81	21.51	15.55
% SCFA	37.75	40.36	36.93	43.88	77.63	83.94
BCFA/SCFA ratio	1.65	1.48	1.70	1.27	0.28	0.19
	Percentage of each compound					
	TSB		**TSB + 0.001% OA**		**TSB + 0.01% OA**	

	WT	***fakA***	**WT**	***fakA***	**WT**	***fakA***
% Anteiso	37.66	36.50	37.52	32.75	13.41	8.61
% Iso	24.59	23.14	25.22	23.06	8.10	6.94
Anteiso/iso ratio	1.53	1.58	1.49	1.42	1.66	1.24

Table 2.3. Analysis of FAME data from wildtype and *fakA* mutant grown in TSB with and without 0.001% and 0.01% oleic acid (OA). Data are from pooled replicates (n=4) from each strain and growth environment.

Chapter 3: Redirection of metabolism in response to fatty acid kinase in *Staphylococcus aureus*

This chapter has previously been published as DeMars, Z., & Bose, J. L. (©2018). Redirection of Metabolism in Response to Fatty Acid Kinase in *Staphylococcus aureus*. *J Bacteriol*, 200(19), doi: 10.1128/JB.00345-18. It is reprinted here in whole with permission.

Introduction

The facultative anaerobic Gram-positive bacterium *Staphylococcus aureus* is a common colonizer of the human nares but is also a potent human pathogen. While primarily causing skin infections, *S. aureus* is capable of establishing infection in a multitude of anatomical sites in the human body leading to life-threatening diseases [186]. These different niches have a wide variety of nutrients, necessitating *S. aureus* to have an adaptable metabolism. Perhaps, not surprisingly, virulence factor production and metabolism are linked as *S. aureus* adapts to its environment [32, 187].

S. aureus possesses complete central metabolic pathways, including glycolysis, the pentose phosphate pathway, and the tricarboxylic acid (TCA) cycle. These metabolic pathways, as well as virulence factor production, are under the control of global regulators [32-35]. Carbon catabolite protein A, or CcpA, is a DNA-binding protein and has been shown to regulate multiple branches of metabolism. Importantly, CcpA represses the TCA cycle in the presence of glucose or other glycolytic carbohydrates that generate fructose-1,6-bisphosphate [15, 36-39]. In addition, CcpA controls the expression of genes encoding key enzymes in amino acid metabolism [34, 40, 41]. CodY is a global transcriptional regulator which directly monitors the intracellular concentrations of branch-chained amino acids (BCAAs) as well as levels of cellular GTP [43, 44]. Accordingly, CodY has been shown to regulate BCAA biosynthesis pathways and control a multitude of virulence factors, from repressing toxins to activating microbial surface components recognizing adhesive matrix molecules or MSCRAMMs [33, 45-47]. Deletion of *ccpA* from *Staphylococcus aureus* impacts the transcription of virulence factors, such as the down-regulation of the global effector molecule of the Agr system, *RNAIII* [42]. CodY has also been shown to alter transcription of the *agr* locus and thus virulence factors such as α-hemolysin [33, 48, 49]. More recently, CodY binding motifs were identified upstream of the P1 promoter of the *saePQRS* operon [188],

suggesting a direct role for CodY regulating secreted virulence factors. As a consequence of these two key regulatory proteins, both the availability of carbohydrates and amino acids can induce metabolic changes as well as altering virulence factor production.

The details of carbon flow, particularly from glucose, through central metabolism have been a topic of significant study. In the presence of a preferred carbohydrate, such as glucose, *S. aureus* uses glycolysis to produce pyruvate, which can be converted into multiple metabolites depending on the environment. Under aerobic conditions and in the presence of glucose, the TCA cycle is repressed by CcpA [15] and much of the pyruvate is converted to acetyl-CoA and then acetate, with ATP created by substrate-level phosphorylation by the phosphotransacetylase-acetate kinase (Pta-AckA) pathway [16, 17]. Once glucose and glycolytic intermediates (fructose-1,6-bisphosphate) are depleted from the environment, CcpA repression of the TCA cycle is relieved and acetate is re-assimilated to acetyl-CoA [20] and subsequently processed through the TCA cycle. This switch from acetate production to acetate consumption is known as the "acetate switch" [21], the timing of which is presumably controlled by CcpA both directly and indirectly.

Recently, *fakA* (originally named *vfrB*) was characterized in *Staphylococcus aureus* [66]. This gene encodes a fatty acid kinase which is responsible for phosphorylating exoFAs and incorporating them into the *S. aureus* phospholipid bilayer [65]. FakA has been shown to regulate virulence factor production such as α-hemolysin and several proteases [66], as well as impacting the type VII secretion system [175]. We have shown that FakA mediates at least some of these effects through the activation of the SaeRS two-component system [189]. In addition, FakA influences biofilm formation [190] by an unknown mechanism. Previously, we showed that deletion of the *fakA* gene led to altered growth kinetics [66]. Here, we demonstrate that a *fakA* mutant displays an altered acetate switch as well as an apparent altered amino acid metabolism.

Results

A fakA mutant displays altered growth and acetate kinetics. Previously, we showed that a *fakA* mutant has an extended exponential-phase of growth, resulting in higher growth yield [66], suggesting an altered metabolism in the *fakA* mutant. For a summary of metabolic pathways and changes observed in the *fakA* mutant, see Figure 3.10. To determine the effect that FakA has on the growth of *S. aureus*, wild-type, *fakA* mutant and the *fakA* complemented strains were grown in tryptic soy broth (TSB) supplemented with 14 mM glucose. In agreement with our previous results, we observed enhanced late-exponential phase growth in the *fakA* mutant, which could be restored to wild-type levels when *fakA* was provided on a plasmid (Figure 3.1A). Under aerobic growth in the presence of glucose, *S. aureus* produces acetate as a byproduct which leads to decreased media pH, followed by consumption of acetate and a rise in pH [17, 191, 192]. Interestingly, altered growth kinetics of the *fakA* mutant correlated with an increased culture pH (Figure 3.1B), consistent with decreased production or enhanced utilization of acetate in the *fakA* mutant. Growing the *fakA* mutant under decreased flask:media ratios resulted in no significant growth advantage compared to the wild-type strain (Figure 3.11A). Furthermore, the growth advantage observed in the *fakA* mutant was diminished during the exponential phase of growth when grown in TSB lacking glucose, with growth returning to wild-type levels (Figure 3.11B). To determine if the growth advantage was due to altered acidification of the media, wildtype, the *fakA* mutant, and the complement strain were grown in TSB buffered to a pH of 7.2 with 50 mM MOPS (Figure 3.11C). All strains grew similar to unbuffered media, indicating this growth phenotype is the result of media pH changes. Taken together, this data suggests that FakA alters bacterial growth at exponential phase of growth in a glucose and oxygen-dependent manner, indicative of changes in the acetate switch.

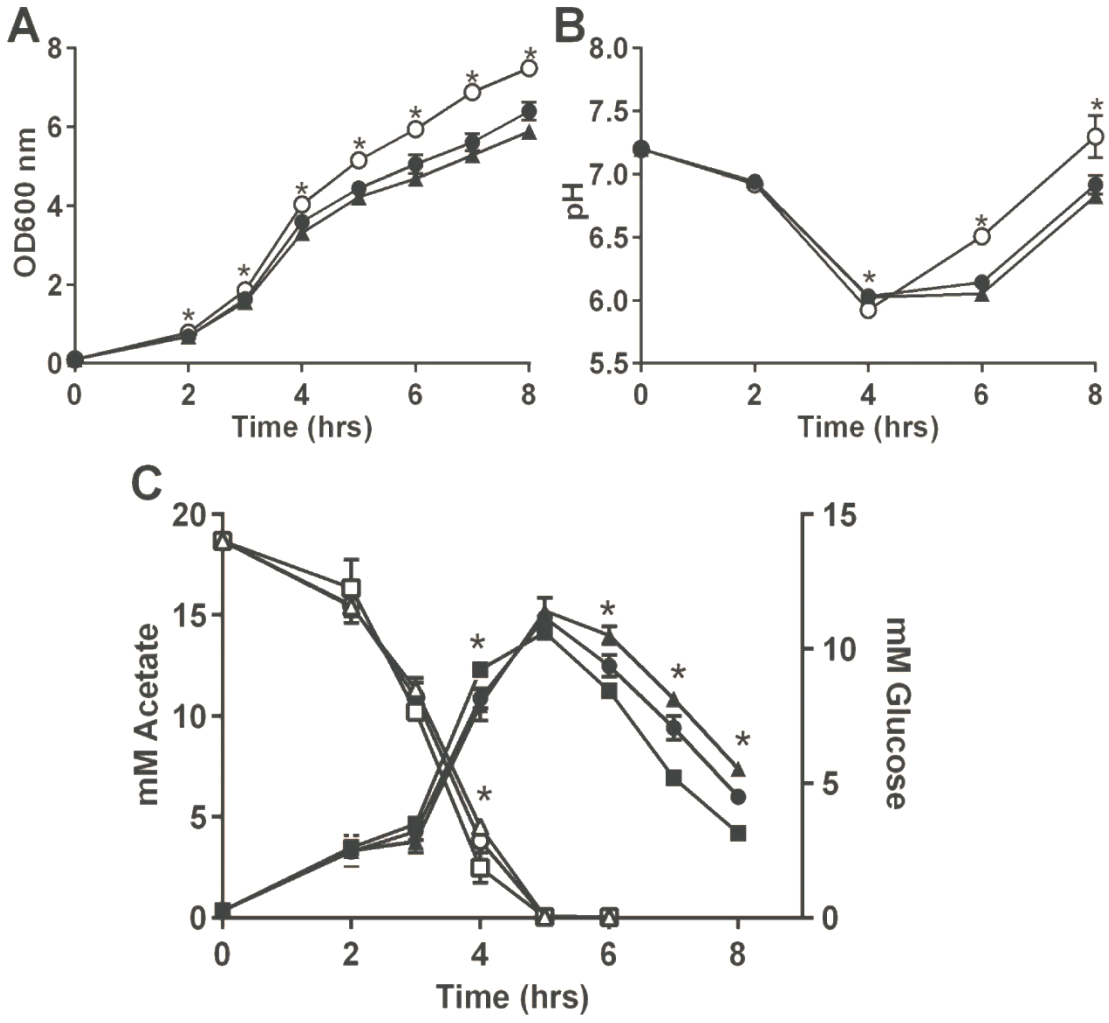
A
OD600 nm
Time (hrs)
B
pH
Time (hrs)
C
mM Acetate
mM Glucose
Time (hrs)

Figure 3. 1

Figure 3.1. (A) Growth of wild-type (closed circle), *fakA* mutant (open circle), and *fakA* complement (closed triangle) strains in TSB + 14 mM glucose at a 1:10 media to flask ratio. **(B)** pH of culture from panel A. Data is the average (n=3) with standard deviation of a representative experiment. All points have error bars and may be smaller than symbols. **(C)** Extracellular acetate (closed symbols) and glucose (open symbols) was determined for wild-type (circles), *fakA* mutant (squares) and complement strains (triangles). Data are the average (n=6) with standard deviation. *denotes significance ($p<0.05$) using t-test compared to wildtype.

Altered acetate production and the timing of the growth divergence between the wild-type and *fakA* mutant strains correlates with previous studies showing the switch from glucose to acetate utilization in *S. aureus* [191, 192]. To directly examine whether glucose to acetate conversion and subsequent acetate consumption is altered in the *fakA* mutant, both acetate and glucose concentrations were determined (Figure 3.1C). In agreement with previous work [192], glucose was consumed in early exponential phase with a corresponding increase in acetate levels until glucose was depleted. The *fakA* mutant consumed more glucose by hour four which corresponded with a slight increase in acetate production and to the start of the growth divergence. During enhanced growth of the *fakA* mutant, decreased levels of acetate were present in the media, correlating to the increased pH observed in Figure 3.1B. The changes in glucose and acetate utilization were both restored when *fakA* was provided on a plasmid. Together, these results demonstrate that glucose and acetate metabolism is different in the *fakA* mutant, the timing of which suggests an altered acetate switch.

Altered growth of the fakA mutant is dependent on AckA. Along with the observation of altered acetate levels in the *fakA* mutant compared to the wildtype, we predicted that the altered growth of a *fakA* mutant would involve the Pta-AckA and AcsA pathways that are the primary mechanism to produce [192] and consume acetate [20], respectively. Not surprisingly, the *ackA* and *fakA ackA* mutant strains grew poorly compared to both wildtype and the *fakA* mutant (Figure 3.2A). This agrees with previous studies that highlight the importance of the production of energy from the Pta-AckA pathway in *S. aureus* [41, 191, 193]. However, the growth (Figure 3.2A) was similar in the *fakA ackA* mutant compared to the *ackA* mutant, indicating that the enhanced growth of the *fakA* mutant during exponential phase of growth is reliant on AckA. The *fakA ackA* mutant did have modest increased growth compared to the *ackA* mutant at several time points. First, a slight

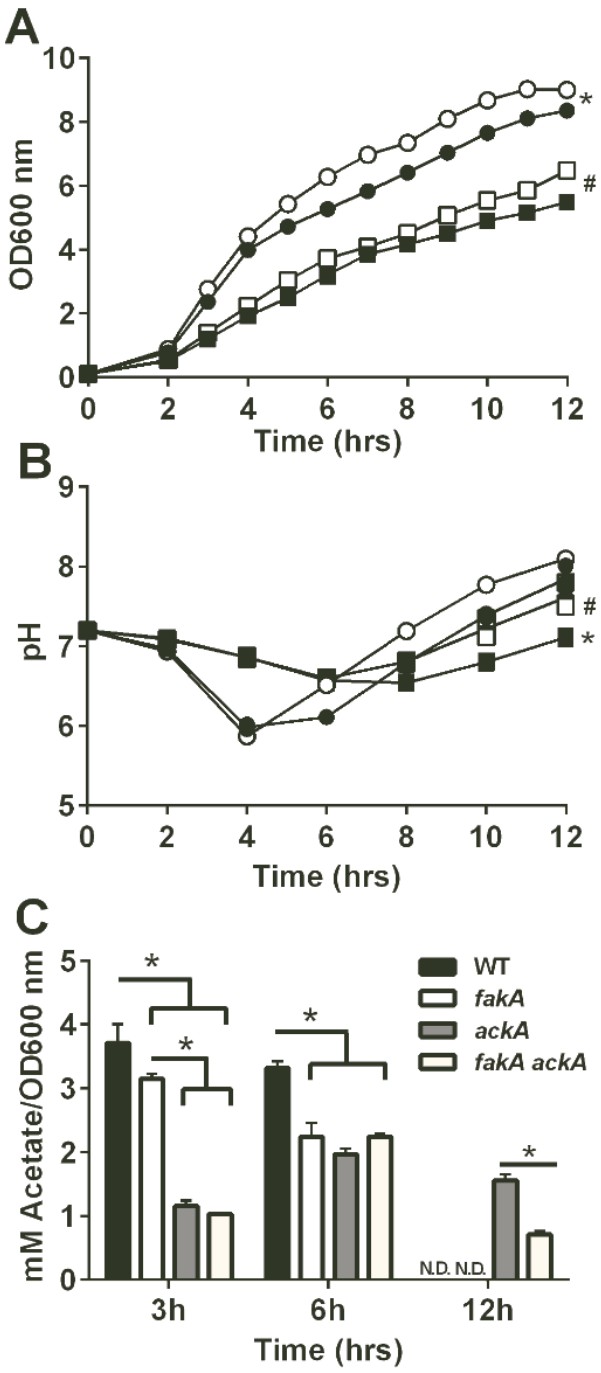
A
OD600 nm
Time (hrs)
B
pH
Time (hrs)
C
mM Acetate/OD600 nm
WT
fakA
ackA
fakA ackA
N.D. N.D.
3h
6h
12h
Time (hrs)

Figure 3. 2

Figure 3.2. (A) Growth of wildtype (closed circle), *fakA* mutant (open circles), *ackA* mutant (closed square), and *fakA ackA* mutant (open square). *denotes a significant difference ($p<0.05$) for all points after 2 hr for WT vs *fakA* while # indicates significance for hours 4, 5, and 9-12 for *ackA* vs *fakA ackA*. **(B)** pH of culture media from panel A. * denotes significant difference ($p<0.05$) for all points after 2 hr for WT vs *ackA* while # identifies differences ($p<0.05$) for all points after 2 hours except 6 hrs for *ackA* vs *fakA ackA*. **(C)** Quantification of acetate in the culture media at indicated time points. *denote significant differences ($p<0.05$). "N.D." denotes none detected. For all panels, data are the average (n=3) with standard deviation of a representative experiment. All points have error bars and may be smaller than symbols.

enhanced growth was observed at four and five hours of growth, similar as seen with the *fakA* mutant compared to wildtype in the absence of glucose (Figure 3.11B), as well as at the latest time points examined. As seen in a previous report [192], the *ackA* mutants did produce some acetate (Figure 3.2C). There was no difference in acetate between the *ackA* and *fakA ackA* mutant at either three or six hours of growth although the *fakA ackA* mutant consumed more acetate by 12 hrs. This could be responsible for the increased growth observed in the *fakA ackA* mutant compared to the *ackA* mutant (Figure 3.2). Current models suggest AcsA as the means to assimilate acetate for redirection into the TCA cycle [17, 20], though experimental confirmation is lacking. Surprisingly, *acsA* and *fakA acsA* mutants resembled the wildtype and the *fakA* mutant, respectively, during most of growth (Figure 3.12). AcsA had a modest effect in both strains after 8 hours, well past the point of glucose exhaustion from the media. Interestingly, the *acsA* mutant depleted approximately 75% of produced acetate (Figure 3.12, compare *ascA* at 3 and 12 hrs). Much like the parent strains, the *fakA acsA* mutant had less acetate in the media compared to the *acsA* mutant. These data demonstrate a role for acetate produced via AckA in the enhanced growth of the *fakA* mutant, but in contrast to most models, the majority of acetate is being depleted via another mechanism rather than the AcsA pathway.

The fakA mutant has altered central metabolites while maintaining acetyl-CoA levels. Alterations in carbon flow through the acetate metabolism would likely change additional metabolic processes. To assess other metabolic changes in the *fakA* mutant**,** we used LC/MS/MS to quantify key metabolic intermediates at three or six hours of growth. Pyruvate levels were below the limit of detection (~1 nM mg^{-1} protein) for both the wild-type and *fakA* mutant strains at either time point (data not shown). Acetyl-CoA was readily detected and there was no significant difference between the strains (Figure 3.3A), demonstrating that despite differences in growth kinetics and

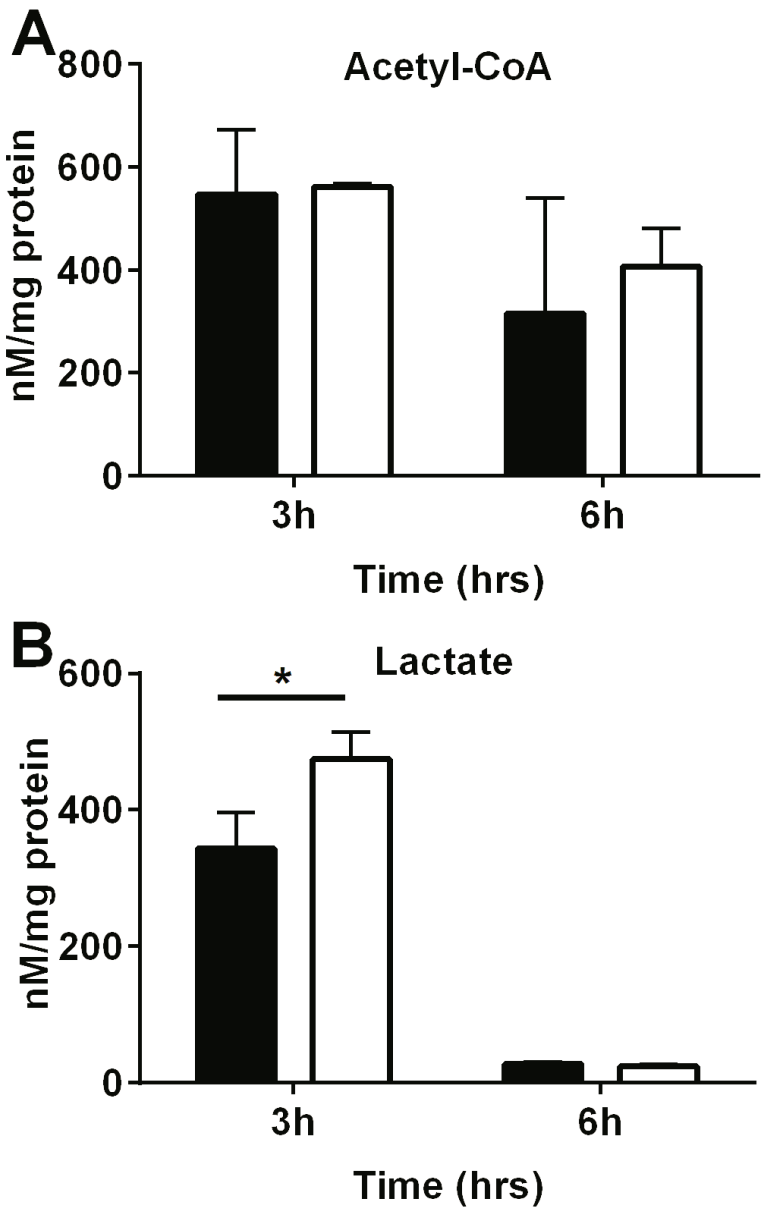
A
Acetyl-CoA
800
600
400
200
0
nM/mg protein
3h
6h
Time (hrs)
B
Lactate
*
600
400
200
0
nM/mg protein
3h
6h
Time (hrs)

Figure 3. 3

Figure 3.3. Quantification of intracellular levels of acetyl-CoA **(A)** and lactate **(B)** after three and six hours of growth for wildtype (black bars) and *fakA* mutant (white bars). Data are the average (n=4) with standard deviation and normalized to protein concentration. *denote significant differences ($p<0.05$) compared to wildtype based on t-test.

altered acetate metabolism, acetyl-CoA levels are maintained. Since acetate levels, but not acetyl-CoA were altered in the *fakA* mutant, we suspected that carbon was being shuttled to alternative metabolites**.** We found that the *fakA* mutant had a 38.3% increase in intracellular lactate compared to wildtype at three hours of growth, but no difference at six hours (Figure 3.3B). Although not statistically significant, we also identified increased lactate in the supernatants of the *fakA* mutant compared to the wild-type strain (Table 3.2). However, lactate production was not a major contributing factor to growth as the growth and pH of *ldh1*, *fakA ldh1, ldh2* and *fakA ldh2* mutants showed no significant differences (Figure 3.13). In addition, mutation of *alsS*, which produces acetoin from pyruvate, did not alter growth of wildtype or the *fakA* mutant (Figure 3.13).

Since FakA is necessary for exoFA use, we tested whether the endogenous fatty acid synthesis system was altered. This is also one direction which acetyl-CoA is diverted. We found no difference between the wild-type and *fakA* mutant strains in malonyl-CoA (Figure 3.4A), the intermediate that feeds into fatty acid biosynthesis. We also determined the transcription levels for *fabH,* which encodes a key enzyme in fatty acid synthesis [59, 194]. In agreement with unaltered malonyl-CoA, *fabH* expression was not significantly changed in the absence of *fakA* (Figure 3.4B), indicating that the absence of *fakA* does not affect the endogenous fatty acid synthesis pathway.

One major fate for acetyl-CoA is the TCA cycle. Indeed, when glucose is exhausted from the environment, acetate is converted to acetyl-CoA for use in the TCA cycle. Therefore, we examined the concentration of several key TCA cycle intermediates**.** Succinate, fumarate and malate levels were not significantly different between wildtype and the *fakA* mutant after three or six hours of growth (Table 3.2). Compared to wildtype, the *fakA* mutant had decreased intracellular citrate and α-ketoglutarate early in growth, but significantly increased levels during the enhanced growth (six hours). For the full list of quantified organic acids, see Table 3.2.

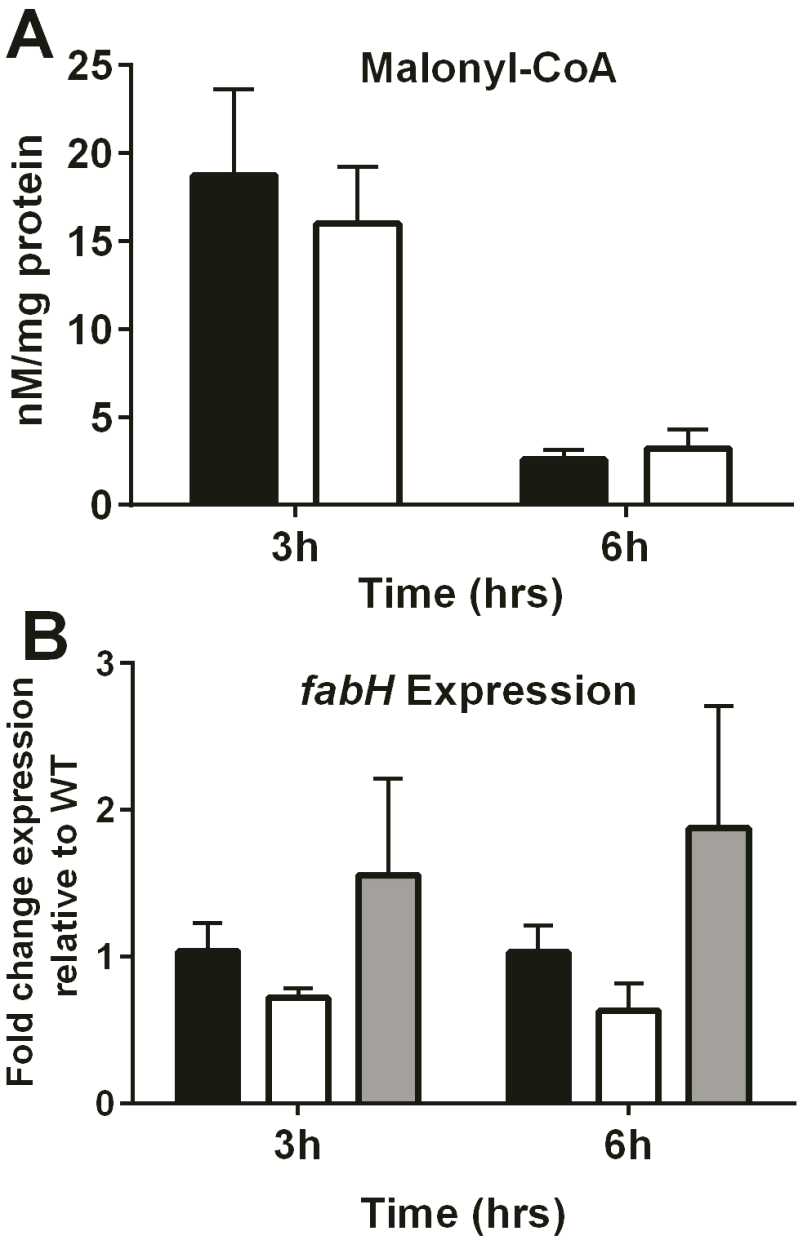
A
Malonyl-CoA
nM/mg protein
25
20
15
10
5
0
3h
6h
Time (hrs)
B
fabH Expression
Fold change expression relative to WT
3
2
1
0
3h
6h
Time (hrs)

Figure 3. 4

Figure 3.4. (A) Quantification of intracellular levels of malonyl-CoA after three and six hours of growth for wildtype (black bars) and *fakA* mutant (white bars). Data are the average (n=4) with standard deviation and normalized to protein concentration. *$p<0.05$. **(B)** fabH transcript levels at three and six hours of growth in wildtype (black bars), *fakA* mutant (white bars), and *fakA* complement (grey bars). Data are the average (n=3) fold-change relative to wildtype with standard error of the mean.

The fakA mutant has a modified redox state. During growth utilizing glucose, wild-type cells make most of their ATP through substrate phosphorylation via acetate production. Generation of ATP then shifts to the TCA cycle and electron transport chain following glucose exhaustion. Given that acetyl-CoA levels were unaltered in the *fakA* mutant compared to wildtype, we examined the redox and energy state of the cells using LC/MS/MS. After three hours of growth, the *fakA* mutant displayed a significant decrease in the NAD^+/NADH ratio compared to wildtype (Figure 3.5A) that transitioned to a significantly increased ratio during the enhanced growth (six hours) (Figure 3.5A). While no difference was observed for $NADP^+$/NADPH at three hours of growth, this ratio was increased in the *fakA* mutant compared to wildtype (Figure 3.5B) at six hours and this is attributed to increased $NADP^+$ at this time. Interestingly, at six hours of growth, the *fakA* mutant had increased levels of both ADP and ATP, yet the ADP/ATP (Table 3.3) ratio was similar to that of the parent strain (Figure 3.5C). Additionally, AMP levels were significantly increased in the *fakA* mutant (Table 3.3). We also used the ATP, ADP, and AMP results to calculate the adenylate energy charge (AEC) as described by Atkinson et al [195]. Using this analysis, the *fakA* mutant was found to have a decreased AEC at both time points examined (Figure 3.5D). Together, these data indicate that the *fakA* mutant has a more oxidized cellular environment than the wild-type strain during the enhanced growth and has an overall decreased cellular energy status. For a full list of quantified nucleotides, see Table 3.3.

FakA modulates amino acid metabolism. Recently, Halsey et al [41] reported that different amino acids play unique roles for bacterial growth in the absence of glucose. For example, the amino acids glutamate, glutamine, proline, arginine, asparagine, and aspartate were shown to provide the organism with TCA cycle intermediates like α-ketoglutarate and oxaloacetate. The amino acids alanine, glycine, and threonine are converted to pyruvate and acetate via the Pta-AckA pathway

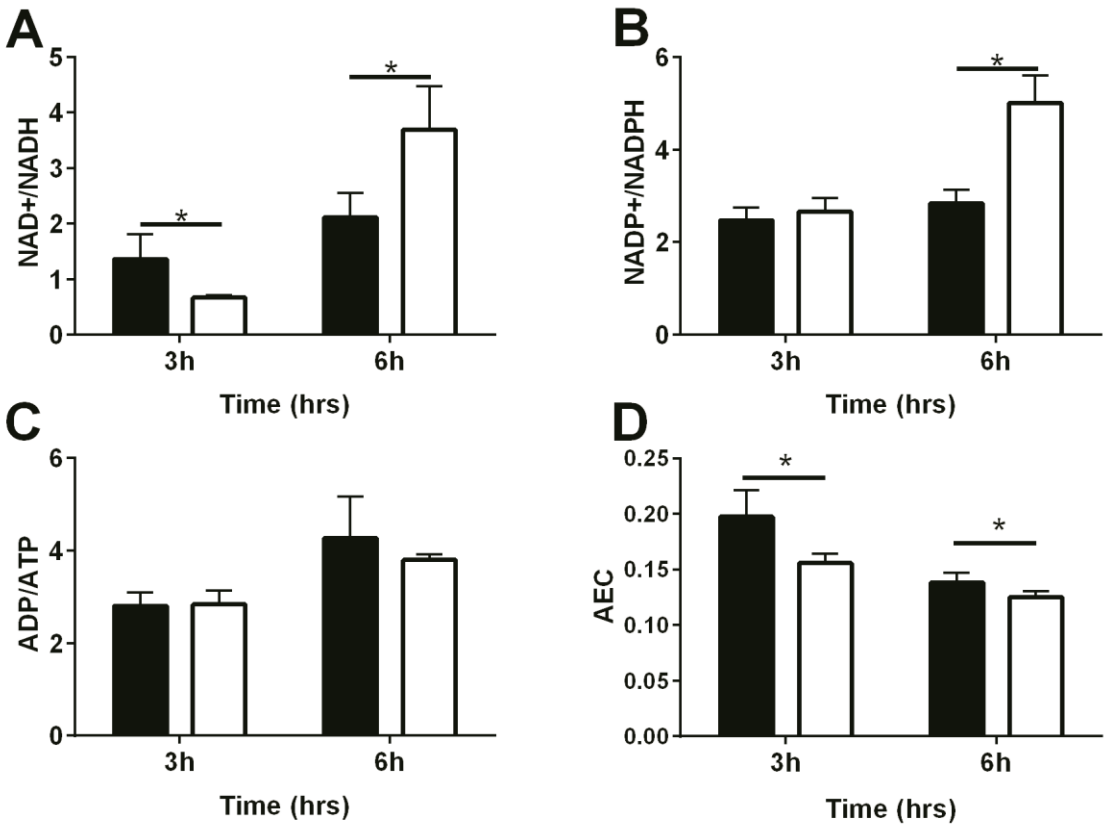
A
NAD+/NADH
5
4
3
2
1
0
*
*
3h
6h
Time (hrs)
B
NADP+/NADPH
6
4
2
0
*
3h
6h
Time (hrs)
C
ADP/ATP
6
4
2
0
3h
6h
Time (hrs)
D
AEC
0.25
0.20
0.15
0.10
0.05
0.00
*
*
3h
6h
Time (hrs)

Figure 3.5

Figure 3.5. Cellular ratio of NAD+/NADH **(A)**, NADP+/NADPH **(B)**, ADP/ATP **(C)**, and **(D)** adenylate energy charge (AEC) determined by LC/MS/MS after three and six hours of growth for wildtype (black bars) and *fakA* mutant (white bars). Data are the average ratio (n=4) with standard deviation after normalization to protein concentration. *denote significant differences ($p<0.05$) compared to wildtype based on t-test.

[41]. We sought to determine the amino acid profiles of both wild-type and the *fakA* mutant strains as they may reflect the altered metabolism observed in the mutant strain. When analyzing cellular amino acids at either three or six hours of growth, we identified significant changes in 15 out of 22 amino acids tested at one or both time points, demonstrating significant changes to amino acid metabolism in the *fakA* mutant (Figure 3.6).

Amino acids that can be converted to pyruvate were less abundant in *fakA* mutant cells. Specifically, threonine, glycine, and alanine were all at reduced levels at six hours in the *fakA* mutant (Figure 3.6). These same amino acids were consumed from the media at a greater rate when the starting levels in the media were compared to the supernatants. We also observed significant changes in amino acids that are involved in the urea cycle. Intracellular arginine, histidine, proline, and glutamate (Figure 3.6) were all increased in the *fakA* mutant after three hours of growth compared to wildtype. At six hours, arginine levels were similar in the wildtype and the *fakA* mutant, while histidine was lower. At this same time, proline and glutamate were increased in the mutant.

Two non-proteinogenic amino acids were also examined. Citrulline and ornithine are amino acids involved in the urea cycle, which is a key pathway in amino acid catabolism and allows available carbon to enter the TCA cycle via α-ketoglutarate. After three and six hours of growth, citrulline and ornithine were significantly increased in the *fakA* mutant compared to wildtype (Figure 3.6), suggesting altered urea cycle activity. Therefore, we hypothesized that urease activity would be impacted. The urea cycle connects glutamate and amino acids producing glutamate to the TCA cycle and is subjected to carbon catabolite regulation independently of the presence of glucose [15, 40]. Urease activity was determined after three and six hours of growth. The activity of urease was increased in the *fakA* mutant compared to wildtype at both time points (Figure 3.7A). This is likely

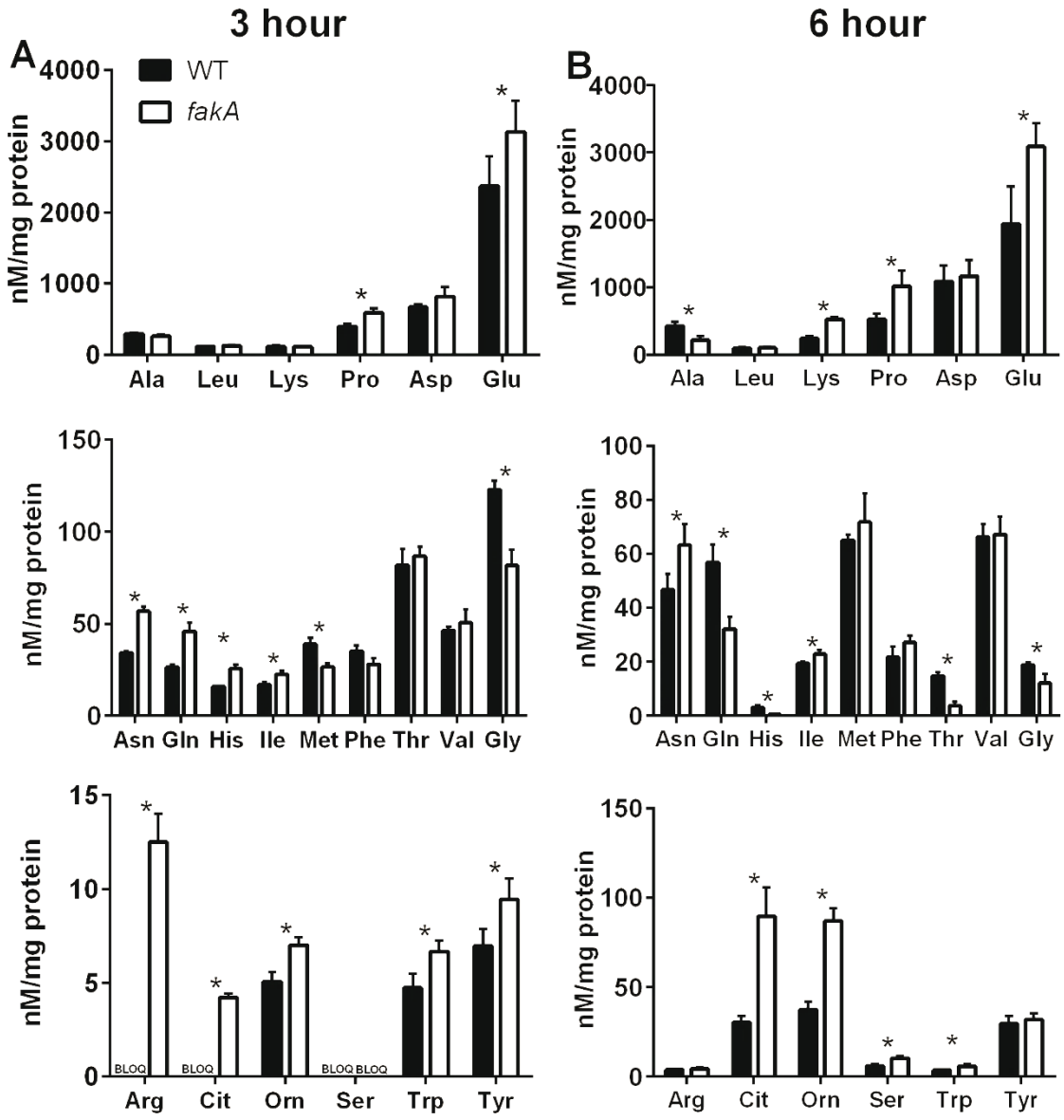
3 hour
6 hour
A
B
WT
fakA
nM/mg protein
4000
3000
2000
1000
0
Ala
Leu
Lys
Pro
Asp
Glu
150
100
50
Asn
Gln
His
Ile
Met
Phe
Thr
Val
Gly
80
60
40
20
15
10
5
BLOQ
Arg
Cit
Orn
Ser
Trp
Tyr

Figure 3.6

Figure 3.6. Quantification of intracellular amino acids from wildtype (black bars) and *fakA* mutant (white bars) grown for three **(A)** or six hours **(B)**. Concentrations were normalized to protein concentration. Data are the average (n=4) with standard deviation from a representative experiment. *denote significant differences ($p<0.05$) compared to wildtype based on t-test. BLOQ indicates concentrations below the limit of quantification.

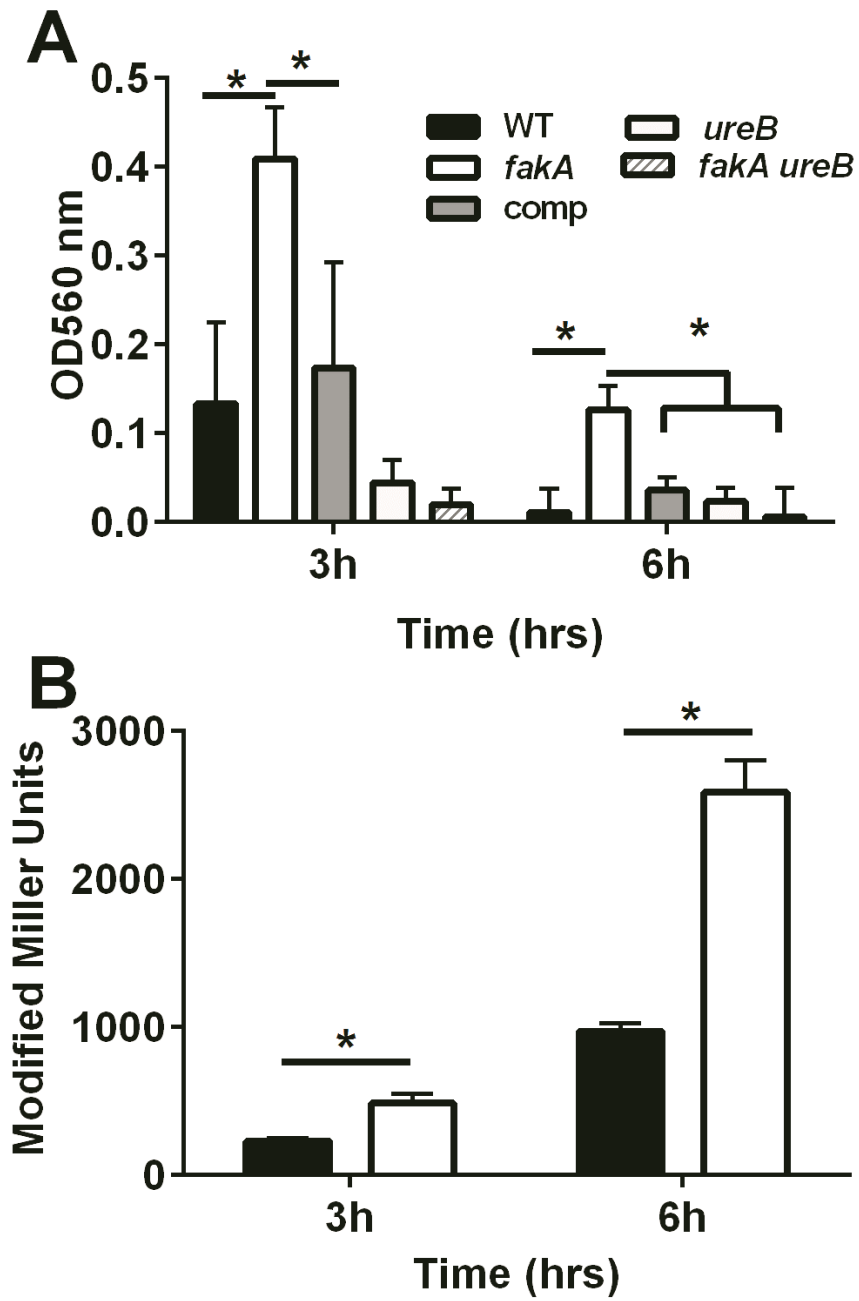
A
0.5
0.4
0.3
0.2
0.1
0.0
OD560 nm
*
*
*
*
WT
fakA
comp
ureB
fakA ureB
3h
6h
Time (hrs)
B
3000
2000
1000
0
Modified Miller Units
*
*
3h
6h
Time (hrs)

Figure 3.7

Figure 3.7. (A) Urease activity was determined via absorbance at 560 nm for indicated strains grown for three or six hours. **(B)** β-galactosidase activity from a P_{ure}-*lacZ* reporter measured in wildtype (black bars) and *fakA* mutant (white bars) grown for three or six hours. All data is the average (n=3) with standard deviation of a representative experiment. *denote significant differences ($p<0.05$) based on t-test.

due to increased urease levels since in the *fakA* mutant we observed increased expression of a β-galactosidase-based reporter of the urease promoter (Figure 3.7B). Despite this increase in urease activity, inactivation of urease in both wildtype and *fakA* mutant strains did not alter growth in our conditions (data not shown).

Global regulators CcpA and CodY alter growth of the fakA mutant. The altered growth of the *fakA* mutant is observed as glucose is depleted from the media. Since CcpA carries out its regulation in a glucose dependent manner, we reasoned that CcpA may have a role in the *fakA* mutant's altered growth. Therefore, growth was monitored in the absence of *ccpA*. The *ccpA* and *fakA ccpA* mutants grew similarly to the *fakA* mutant, and better than the wild-type strain after glucose depletion from the media (Figure 3.8A). One indicator of CcpA activity is expression of *gltA*, which is repressed by CcpA [15]. To assess potential alterations in CcpA activity, *gltA* mRNA levels were assessed after three and six hours of growth. Interestingly, transcription of *gltA* was increased two-fold in the *fakA* mutant compared to wildtype while glucose was present but decreased upon glucose exhaustion (6 hours), similar to a *ccpA* mutant (Figure 3.8B). This result indicates CcpA activity may be altered in the *fakA* mutant.

We observed differences in amino acid metabolism (Table 3.4) and guanine-based nucleotides (Table 3.3), both of which alter CodY activity. In addition, amino acids are abundant in TSB and it was possible that enhanced growth may be due, in part, to amino acid utilization. Due to the role of CodY in regulating amino acid metabolism, we hypothesized that it may affect growth of the *fakA* mutant. Indeed, inactivation of *codY* in the *fakA* mutant diminished the growth of the *fakA* mutant to near wild-type levels while the single *codY* mutant displayed no altered growth (Figure 3.8C). CodY is known to repress expression of *ilvD* [196]; therefore we used this transcript as an indicator of CodY activity. *ilvD* expression was not significantly altered in the *fakA* mutant

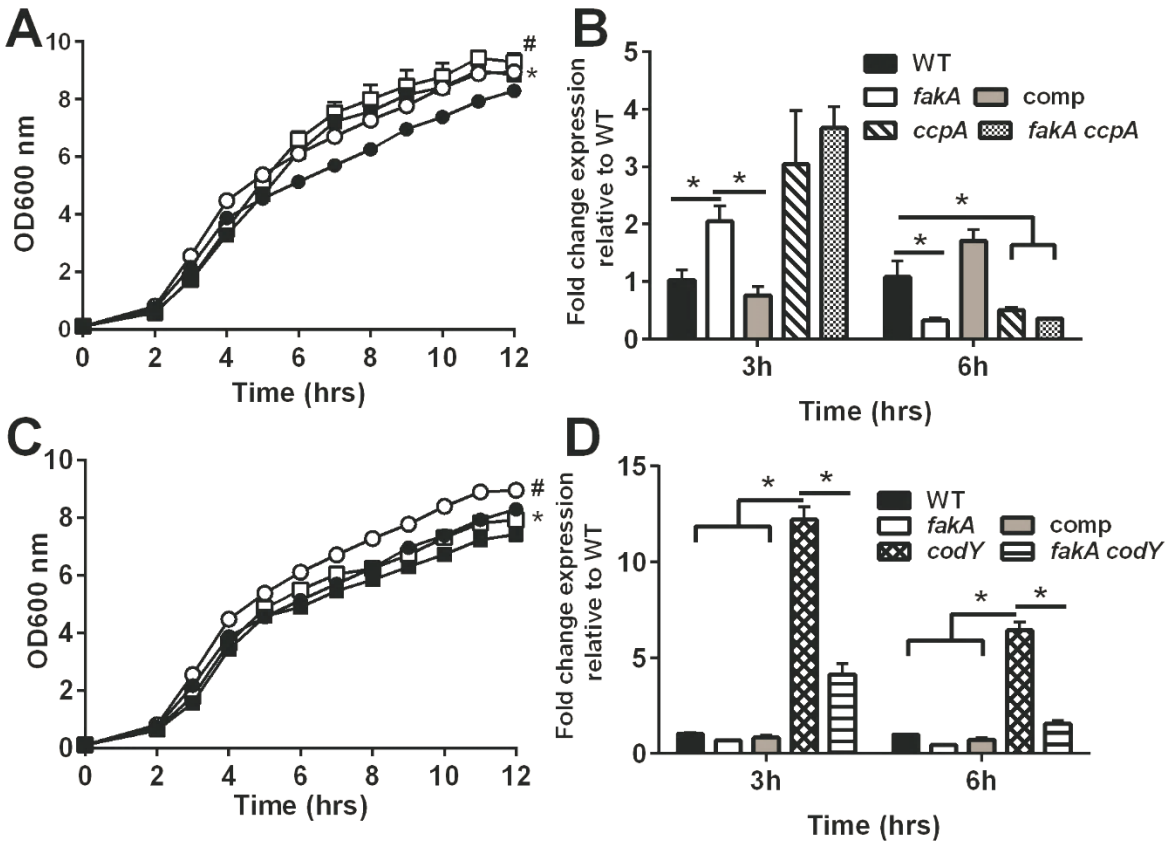
A
OD600 nm
Time (hrs)
#
*
B
Fold change expression relative to WT
WT
fakA
comp
ccpA
fakA ccpA
3h
6h
Time (hrs)
C
OD600 nm
Time (hrs)
#
*
D
Fold change expression relative to WT
WT
fakA
comp
codY
fakA codY
3h
6h
Time (hrs)

Figure 3.8

Figure 3.8. (A) Growth of wildtype (closed circle), *fakA* mutant (open circle), *ccpA* mutant (closed square), and *fakA ccpA* mutant (open square). All data is the average (n=3) with standard deviation of a representative experiment. * indicates significant difference ($p<0.05$) between WT vs *ccpA* mutant for all time points except 5 hrs and # shows significant difference between *fakA* vs *fakA ccpA* mutant only at hours 2-4 and 11. **(B)** Transcript levels of gltA determined via qRT-PCR after three or six hours of growth. Data are the average (n=3) fold-change relative to wildtype (wildtype=1) with standard error of the mean. *denote significant differences ($p<0.05$) based on t-test. **(C)** Growth of wildtype (closed circle), *fakA* mutant (open circle), *codY* mutant (closed square), and *fakA codY* mutant (open square). Data are the average (n=3) with standard deviation of a representative experiment. *indicates significance ($p<0.05$) between WT and *codY* mutant only at hrs 2, 3, 9, 10, and 12, while # identifies difference between *fakA* vs *fakA codY* mutant at all time points. **(D)** Transcript levels of *ilvD* determined via qRT-PCR at three or six hours of growth. Data is the average (n=3) fold-change relative to wildtype (wildtype=1) with standard error of the mean. *denote significant differences ($p<0.05$) based on t-test.

compared to wildtype after three hours (Figure 3.8D). Surprisingly, *ilvD* expression was reduced in the absence of *codY* and *fakA* together compared to the *codY* mutant alone.

GudB is necessary for growth post-glucose consumption. Glutamate dehydrogenase, encoded by *gudB*, produces α-ketoglutarate from glutamate, linking the urea cycle amino acids to central metabolism [41]. Since we observed altered urease activity and amino acids levels associated with the urea cycle in the *fakA* mutant, we hypothesized that directing carbon from these pathways into central metabolism would be important for the growth of the *fakA* mutant. This is also suggested by the increased α-ketoglutarate observed in the *fakA* mutant (Table 3.2). Indeed, mutation of *gudB* hindered growth of both wild-type and the *fakA* mutant strains (Figure 3.9A). Likewise, the pH of the media was not different between the *gudB* and *fakA gudB* mutants (Figure 3.9B). This highlights the importance of the production of α-ketoglutarate via glutamate and amino acids that can be converted to glutamate as an important provider of carbon in complex media upon glucose-consumption and is necessary for growth of both wild-type and the *fakA* mutant.

Conclusions

While FakA is involved in the utilization of exoFAs, we provide data that the function of FakA extends into maintaining metabolic homeostasis (Figure 3.10). In the absence of FakA, we observed an altered acetate switch, redox state, and changes in key metabolites as well as intracellular amino acid pools when grown in complex laboratory media, providing a metabolic snapshot of the metabolic state of the cell during growth. The apparent shift in global metabolism observed in the *fakA* mutant results in an increased NAD^+/NADH ratio inside the cell. We also provide evidence supporting FakA-dependent activity of CcpA as shown through altered transcription of *gltA* observed in the *fakA* mutant. It should be noted that we have recently reported

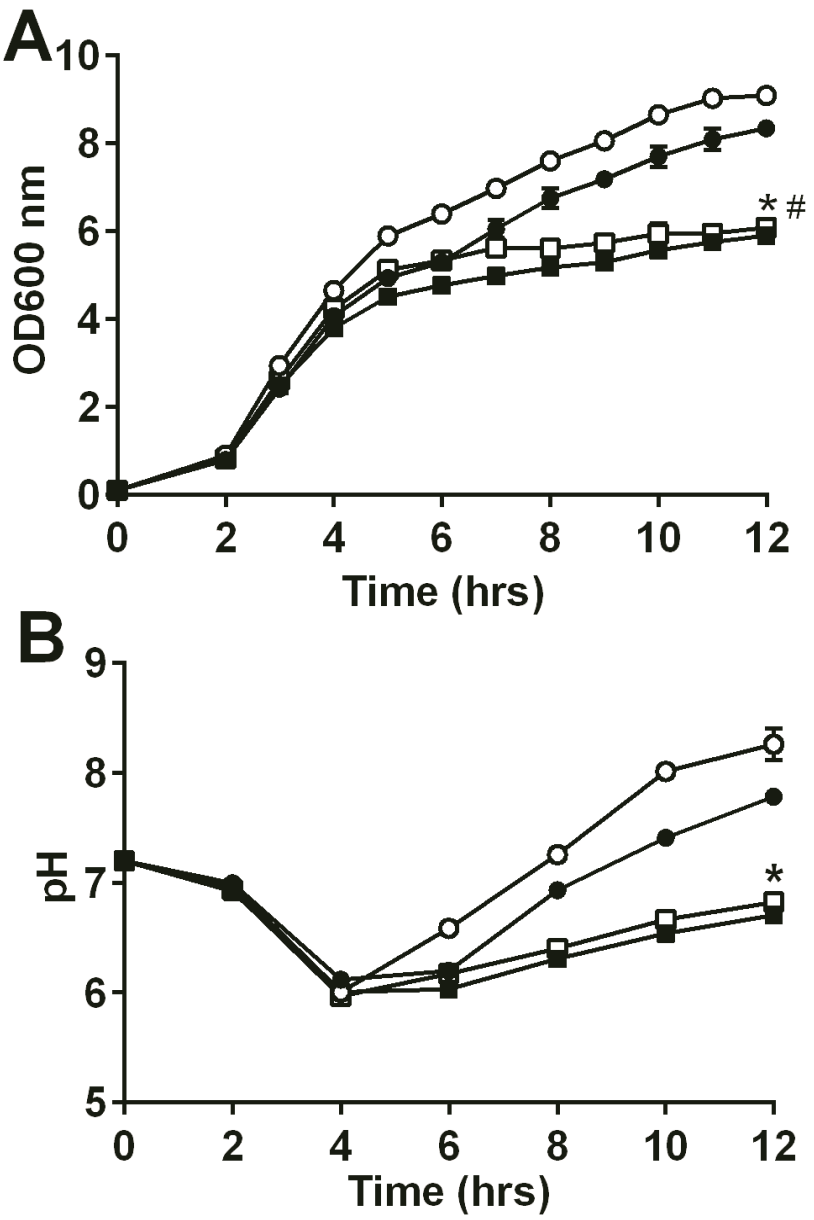
A
OD600 nm
10
8
6
4
2
0
0
2
4
6
8
10
12
Time (hrs)
*
#
B
pH
9
8
7
6
5
0
2
4
6
8
10
12
Time (hrs)
*

Figure 3.9

Figure 3.9. (A) Growth of wild-type (closed circle), *fakA* mutant (open circle), *gudB* mutant (closed square), and *fakA gudB* mutant (open square). *denotes a significant difference ($p<0.05$) for wild-type v.s. *gudB* mutant at all points after 4 hrs and # identifies difference for *fakA* mutant v.s. *fakA gudB* mutant for all time points after 2 hrs. **(B)** pH of culture media from panel A. Data are the average (n=3) with standard deviation of a representative experiment. *denotes a significant difference ($p<0.05$) at all points for gudB mutant vs parent strains using a t-test. All points have error bars and may be smaller than symbols.

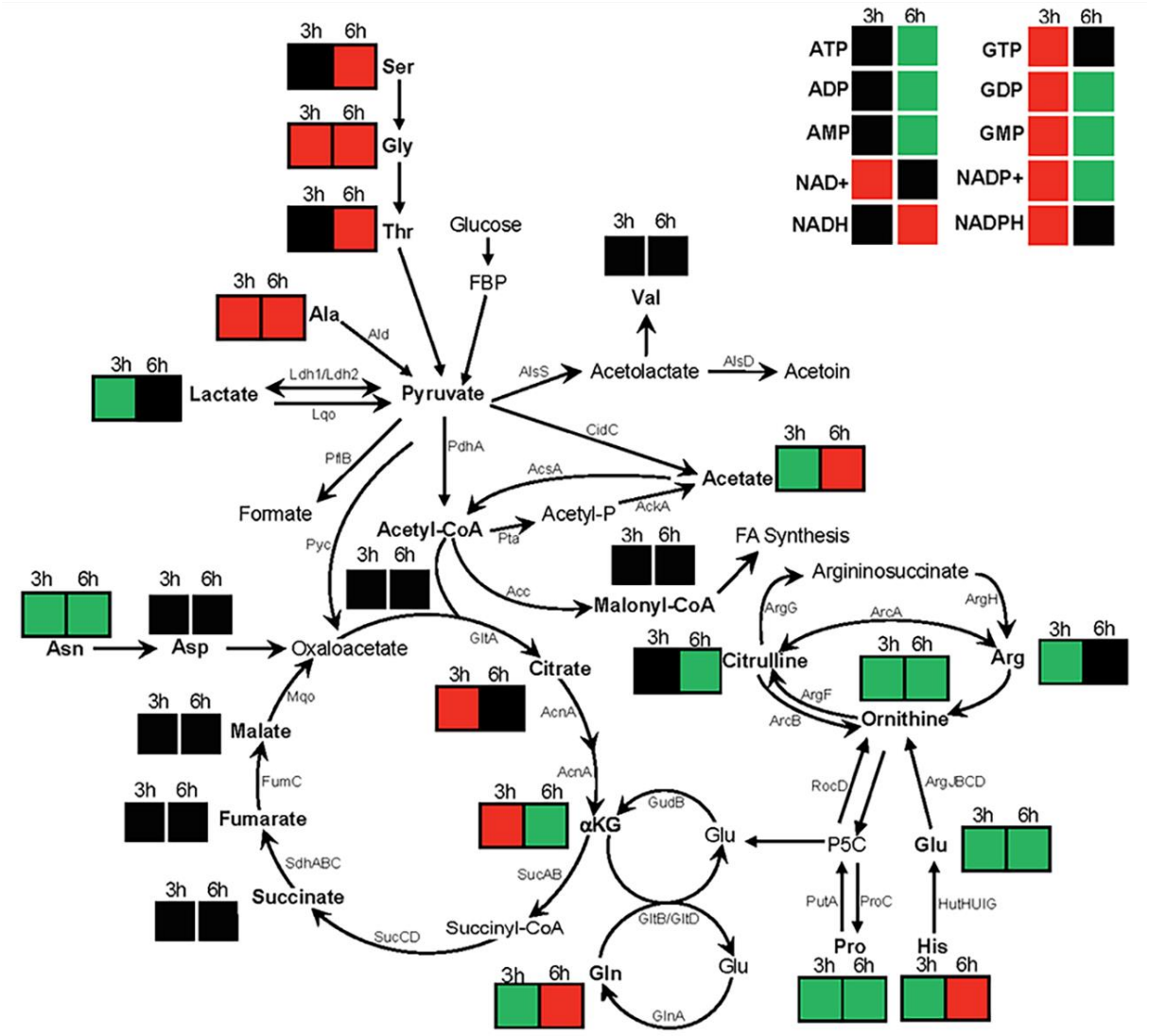
3h 6h
ATP
ADP
AMP
NAD+
NADH
GTP
GDP
GMP
NADP+
NADPH
Ser
Gly
Thr
Glucose
FBP
Val
Ala
Ald
Lactate
Ldh1/Ldh2
Lqo
Pyruvate
AlsS
Acetolactate
AlsD
Acetoin
CidC
Acetate
PflB
PdhA
AcsA
AckA
Formate
Acetyl-CoA
Acetyl-P
Pta
Pyc
FA Synthesis
Acc
Malonyl-CoA
Argininosuccinate
ArgG
ArcA
ArgH
Arg
Asn
Asp
Oxaloacetate
GltA
Citrate
Citrulline
ArgF
ArcB
Ornithine
Mqo
Malate
AcnA
FumC
Fumarate
αKG
GudB
Glu
RocD
ArgJBCD
P5C
SdhABC
SucAB
Succinate
Succinyl-CoA
SucCD
GltB/GltD
PutA
ProC
HutHUIG
Pro
His
Gln
GlnA

Figure 3.10

Figure 3.10. Relative change in intracellular concentrations of metabolites and their location in metabolism. Colors indicate either an increase (green box), decrease (red box), and no significant change (black box) at three or six hours in the *fakA* mutant compared to wildtype.

that FakA is an activator of the SaeRS two-component system [189] while another group demonstrated that CodY binds to the *sae* P1 promoter [197]. Thus, it was reasonable to postulate that Sae would be important for the growth phenotype observed in the *fakA* mutant. However, in our previous study we did not note a growth difference between the *fakA* mutant and the *fakA sae* combination mutant. We re-examined this under the growth conditions here and again observed no contribution of *sae* to the enhanced growth of the *fakA* mutant (data not shown), demonstrating that ability of FakA to effect multiple cellular networks.

The details of glucose/acetate metabolism have been well described for *S. aureus* with acetate re-assimilated post-glucose consumption. Acetate is primarily generated by the Pta-AckA pathway and acetate consumption is thought to be mediated by AscA, which converts acetate to acetyl-CoA. In support of this, both wildtype and the *fakA* mutant generated acetate until glucose exhaustion, at which point acetate was consumed with the mutant depleting acetate at a higher rate (Figure 3.1). Both strains depleted acetate by 12 hours (Figure 3.2C). As expected, we observed diminished levels of acetate in the *ackA* mutants, indicating the Pta-AckA pathway as being the predominate pathway for acetate production in both strains. Contrary to the model, we observed the depletion of approximately 75% of the acetate produced in the absence of *acsA* (Figure 3.12). Similar to wildtype versus the *fakA* mutant, the deletion of *fakA* in the *acsA* mutant led to increased acetate consumption. While these data don't directly measure acetate conversion to acetyl-CoA, clearly removal of acetate from the media requires enzymes beyond AscA. Together, these data provide evidence for an enzyme capable of compensating for the lack of AcsA. The identity of this enzyme is unknown; however, there is a putative AMP-binding enzyme (SAUSA300_2542, EC: 6.2.1.1) that may be redundant to that of *acsA*. In addition, there is evidence in *E. coli* that AckA can work in reverse [17, 20, 198] but the kinetics are not favorable at the concentrations produced

by *S. aureus*. Also, acetate levels did not decrease in the *ackA* mutant (Figure 3.2C), suggesting that this is not the case. The identification of the enzyme responsible for acetate consumption in *S. aureus* or if AckA can act to consume acetate awaits further investigation.

Acetate is often thought to be a primary source of carbon for *S. aureus* post-glucose depletion, yet even strains that don't completely use acetate grow well. Another abundant nutrient source in TSB is peptides and amino acids, some of which can be shuttled into the TCA cycle due to GudB; therefore, the result that mutation of *gudB* alters growth post-glucose consumption is not surprising. Halsey et al [41] recently showed that in chemically-defined media, amino acids that can be converted to glutamate are an important source of carbon [41]. This seems to be the case in complex media such as TSB as well. Indeed, the *gudB* and *fakA gudB* mutants entered stationary phase once glucose was consumed demonstrating the importance of amino acids for *S. aureus* growth post-glucose consumption. This result highlights the importance of shuttling amino acids into the TCA cycle for growth of *S. aureus* despite an alternate energy source such as acetate. Furthermore, we hypothesize that the activity of glutamate dehydrogenase and the concomitant production of ammonia is necessary for the increased pH observed during growth of wild-type and *fakA* strains, respectively.

We provide data suggesting a *fakA*-mediated effect on CcpA activity by using the expression of *gltA* (citrate synthase) as readout of CcpA activity. While *gltA* has been used a marker for CcpA activity, the expression of this gene is dependent on more than just CcpA. Thus, one limitation for this experiment is that *fakA* alters *gltA* through other means. Furthermore, CcpA is activated by Hpr kinase, which is in turn activated by fructose-1,6-bisphosphate (FBP) [37]. While we show that CcpA activity is affected by the lack of *fakA,* we did not measure levels of FBP in the *fakA* mutant. Thus, a change in steady-state FBP levels in *fakA* could be responsible for the altered

CcpA activity suggested. Furthermore, Hpr is linked to the glucose PTS system and changes in transport could affect Hpr, and subsequently CcpA, activity [37]. More directed studies at the activity of CcpA in the context of FakA are needed to further characterize this relationship.

While regulation of *ilvD* is complex, it is used as an indicator mRNA for CodY activity. As expected, inactivation of *codY* increased transcription of *ilvD*, whereas no difference was observed in the *fakA* mutant alone. However, we observed decreased *ilvD* transcription in the *fakA codY* mutant compared to the *codY* mutant (Figure 3.8D), indicating that in the absence of the repressor CodY an additional activator is necessary for *ilvD* expression. Moreover, this proposed activator has reduced activity in the absence of FakA and *ilvD* expression cannot be fully induced. The gene products *gcp* and *yeaZ* have been shown to repress *ilv-leu* transcription; however, the mechanism has not been identified [199, 200]. Since these proteins repress *ilvD* expression, it is unlikely that they are the proteins by which FakA acts in the absence of CodY. It is possible that the decrease in *ilvD* expression in the *fakA codY* mutant compared to the *codY* mutant is not transcriptional and are the result of early transcription termination or mRNA stability. Recently, a report identified an attenuator peptide and termination loop structure in the 5' UTR of *ilvD* that is dependent on amino acid levels [197]. The change in the concentration of amino acids could have effects on regulatory factors such as this attenuator peptide. However, the identification of the regulatory factor uncovered by our data remains to be elucidated.

Fatty acid biosynthesis begins with the conversion of acetyl-CoA to malonyl-CoA, which is then eventually converted to phospholipids for membrane incorporation [59]. Due to its role in utilizing exoFAs, it was possible that fatty acid biosynthesis would be upregulated in the absence of *fakA*. We observed no difference in either intracellular malonyl-CoA levels or in the transcription of fatty acid biosynthesis genes indicating that in complex media, the absence of *fakA* does not result

in increased *de novo* fatty acid biosynthesis. This was not surprising since it has been shown that exposure of *S. aureus* to a fatty acid-rich environment does not alter expression of the fatty acid biosynthesis pathway [62] and that exoFAs do not alter cellular malonyl-CoA levels [201]. In support of this, our data demonstrates that the ability to use environment fatty acids does not influence the endogenous synthesis pathway.

In this study, we have demonstrated a rewiring of *S. aureus* metabolism in response to the presence or absence of the fatty acid kinase. This alteration of metabolism involves changes in central metabolism as well as pathways for amino acid utilization. Furthermore, these results when combined with work previously done in our lab and by other groups demonstrates an important link between fatty acid metabolism, central metabolism, and virulence factor regulation.

Materials and Methods

Bacterial strains, plasmids, and growth conditions. The bacterial strains and plasmids used in this study are presented in Table 3.1. *Escherichia coli* strains were grown in lysogeny broth (LB) or on LB agar (15% w/v) supplemented with ampicillin (100 µg mL^{-1}) for antibiotic selection when necessary. *S. aureus* was grown in TSB supplemented with chloramphenicol (10 µg mL^{-1}) or erythromycin (5 µg mL^{-1}) when necessary. For analyzing bacterial growth, *S. aureus* overnight cultures were initially inoculated to an optical density at 600 nm of 0.1 in TSB without dextrose supplemented with 14 mM glucose and filter-sterilized. Unless otherwise stated, cultures were incubated at 37°C with shaking at 250 rpm in a flask-to-media ratio of 10:1. Growth was measured using optical density 600 nm readings or by assessing the number of CFU mL^{-1} on TSB with 15% (w/v) agar.

Measurement of glucose and acetate concentrations in the culture medium. Aliquots of bacterial cultures (1.0 mL) were pelleted at 21,130 x g for 5 minutes. Supernatants were decanted and stored at -20°C until analysis was performed. Acetate and glucose was quantified using kits purchased from R-Biopharm (Washington, MO) according to manufacturer's protocol.

Measurement of urease activity. Urease activity was determined according to Onal Okyay et al [202] with minor adjustments. Briefly, overnight cultures were inoculated to an optical density 600 nm of 0.5 in Stuart's Broth [203]. The suspensions were incubated at 37°C with shaking at 250 rpm for 24 hours. Following incubation, the suspensions were centrifuged at 3,160 x g for 10 minutes and the supernatants were removed and scanned. Optical density scans ranging from 400 nm to 600 nm were performed at time of inoculation and after three, six, and 24 hours of growth using a Tecan Spark 10M plate reader (Tecan Group Ltd, Mannedorf, Switzerland). Optical density values at wavelength 560 nm as a measure of urease activity were compared using a media blank.

Production of S. aureus mutants. S. aureus transposon mutants are listed in Table 1 and were obtained from BEI Resources or Dr. Paul Fey. Bacteriophage φ11 were propagated on mutants containing the desired transposon by combining 5 mL of TSB with 5 mL Phage Buffer (in 500 mL water: 6.47 g glycerol-2-phosphate, disodium salt, 0.06 g $MgSO_4$, 2.4 g NaCl, 0.5 g gelatin), 100 µL φ11 (~$1x10^{10}$ bacteriophage), and 100 µL of overnight donor strain, mixed by inversion, and incubated statically at room temperature overnight. The resulting φ11 bacteriophage was then filter-sterilized using a 0.45 µm filter syringe and stored at 4°C until use. Transductions were performed as described previously [204]. Genotypes were confirmed in transductants via PCR.

Analysis of β-galactosidase activity. To construct pZD3, primers Purease-F2 (*aatgaattc*GATGATGCTACCTACAATAGCCGCTA) and Purease-R2 (*ggacgtcgac*CCAATTTCATATTAGATACAATTTACAAAATT) were used to amplify the promoter region of *ureA* from the AH1263 chromosome. The resulting PCR fragment was digested with EcoR1 and Sal1 and ligated into the same sites of pJB185 to produce pZD3. β-galactosidase activity was determined as previously described [189]. Briefly, one mL of bacterial culture was collected after three or six hours of growth. Cells were pelleted, resuspended in 1.2 mL Z-buffer (60 mM Na_2HPO_4, 40 mM NaH_2PO_4, 10 mM KCl, 1 mM $MgSO_4$, and 3.4 mL β-mercaptoethanol) and lysed using a FastPrep-24 5G homogenizer (MP Biomedicals), according to the manufacturer's recommended settings for *S. aureus* cells. β-galactosidase activity was determined by adding 140 µL of *ortho*-nitrophenyl-β-galactosidase (ONPG) (4 mg mL^{-1} [wt/vol]) to 700 µL of cell lysates and allowing reaction to turn slightly yellow at (absorbance at 420 nm less than 1.0) at 37°C. The reaction was stopped with 200 µL of 1 M sodium bicarbonate and then absorbance was measured at 420 nm. The β-galactosidase activity was determined based on protein concentration using a Bradford assay with Bio-Rad protein concentration reagent and reported as modified Miller units.

Reverse transcription-quantitative real-time PCR. RNA was extracted using an RNeasy minikit (Qiagen) after three and six hours of growth in TSB + 14 mM glucose. The isolated RNA was treated with DNA-free kit (Ambion) to remove DNA contamination. RNA samples was quantified using a NanoDrop One (ThermoFisher Scientific) instrument. RNA was standardized to 500 ng and used for cDNA synthesis using QuantiTect reverse transcription kit (Qiagen). cDNA was diluted 1:10 and used as template DNA for quantitative PCR using FastStart essential DNA Green Master Mix in a LightCycler 96 system (Roche). Data was calculated and analyzed according to

Livak et al [205]. Data is the average of biological triplicates each ran as technical duplicates. Primers CNK61 (GATATGCCATTTCCAACTGTCG) and CNK63 (GCTGCAAGTTGATCCATAGAGG) were used to amplify *fabH*, RT-*ilvD*-F (GGACCAGGTATGCCTGAAAT) and RT-*ilvD*-R (GGGGAAATATGACCAACTGC) were used to amplify *ilvD*, RT-*gltA*-F (TGGAAAAACGTATGGCAGAA) and RT-*gltA*-R (CCATCCTGCAGAACGACTTA) were used to amplify *gltA*. Data was standardized to *sigA* (*rpoD*) using primes RT-*sigA*-F (AACTGAATCCAAGTGATCTTAGTG) and RT-*sigA*-R (TCATCACCTTGTTCAATACGTTTG) as this has been shown to be a good calibrator previously [206, 207] and we typically observe less than one C_T difference between strains.

Cell collection and metabolite sample preparation for metabolite analysis. All glassware was triple washed with HPLC-grade water, then three times with HPLC-grade acetone, and, finally, three times more with water. Overnight cultures of AH1263 and JLB2 were diluted to an OD_{600nm} of 0.1 in TSB with 14 mM glucose at a 1:10 media to flask ratio and incubated at 37^{o}C with shaking at 250 rpm. Four biological replicates were examined. Samples were removed at three or six hours post-inoculation and centrifuged to pellet the cells. After centrifugation, supernatants were separated into 1 ml aliquots and frozen by submersion in liquid nitrogen. The cell pellets were washed in cold PBS, aliquoted, re-centrifuged and had PBS removed with immediate submersion in liquid nitrogen. All samples were stored at -80^{o}C until analyzed. For cell pellets, an additional tube was used for cell quantification and protein content determination using a Bradford assay with Bio-Rad protein concentration reagent. Samples were processed using LC/MS/MS as previously described [208]. The adenylate energy charge was calculated as (ATP + 0.5 ADP) / (AMP + ATP + ADP) as previously described [195]. Data were analyzed using a paired student t-test where $P<0.05$ was considered statistically significant.

Statistical analyses. All statistical analyses were performed using Prism, version 6 (GraphPad). Statistical significance was determined using unpaired t-test with the Holm-Sidak method for multiple comparisons where $p<0.05$ was considered statistically significant unless otherwise stated. As stated above, mass spectrometry statistics were analyzed by the SECIM Core using with a t-test in Microsoft Excel and re-validated using Prism.

Table 3.1

Strain, Plasmid or oligonucleotide	Relevant characteristics[a]	Source or reference
Strain		
RN4220	Highly transformable *S. aureus*	[209]
AH1263	USA300 CA-MRSA strain LAC without LAC-p03	[86]
JLB2	AH1263 Δ*fakA*	[66]
JLB113	AH1263 *ccpA::tetL*	[40]
JLB114	AH1263 Δ*fakA ccpA*::*tetL*	This study
JLB127	AH1263 *ackA*::NΣ	This study
JLB128	AH1263 Δ*fakA ackA::*NΣ	This study
JLB132	AH1263 *ureB*::NΣ	This study
JLB133	AH1263 Δ*fakA ureB*::NΣ	This study
JLB158	AH1263 *gudB*::NΣ	This study
JLB159	AH1263 Δ*fakA gudB*::NΣ	This study
NE385	Source of *acsA*::NΣ	[210]
NE1397	Source of *alsS*::NΣ	[210]
NE1642	Source of *ureB*::NΣ	[210]
KB8007	JE2- Δ*ackA::ermB;* Em^r	[192]
JLB165	AH1263 *codY*::NΣ	This study
JLB166	AH1263 Δ*fakA codY::*NΣ	This study
NE1518	Source of *gudB::*NΣ	[210]
NE1555	Source of *codY::*NΣ	[210]

Strain, Plasmid or oligonucleotide	**Relevant characteristics[a]**	**Source or reference**
NE1670	Source of *ccpA::*NΣ	[210]
NE1923	Source of *ldh1::*NΣ	[210]
NE1816	Source of *ldh2::*NΣ	[210]
JLB115	AH1263 *saeR::*NΣ	[189]
JLB116	AH1263 Δ*fakA saeR::*NΣ	[189]
JLB115	AH1263 *acsA::*NΣ	This study
JLB116	AH1263 Δ*fakA acsA::*NΣ	This study
JLB188	AH1263 *ldh1::*NΣ	This study
JLB189	AH1263 Δ*fakA ldh1::*NΣ	This study
JLB196	AH1263 *ldh2::*NΣ	This study
JLB197	AH1263 Δ*fakA ldh2::*NΣ	This study
JLB135	AH1263 *alsS::*NΣ	This study
JLB136	AH1263 Δ*fakA alsS::*NΣ	This study
Plasmids		
pJB185	Promoterless codon-optimized *lacZ:*Amp/Cm^r	[189]
pJB165	*fakA* complement	[66]
pZD3	P_{ure}-*lacZ* reporter	This study

Oligonucleotides[b]

RT_ilvD_F	GGACCAGGTATGCCTGAAAT	This study
RT_ilvD_R	GGGGAAATATGACCAACTGC	This study
RT_gltA_F	TGGAAAAACGTATGGCAGAA	This study
RT_gltA_R	CCATCCTGCAGAACGACTTA	This study
RT-sigA-F	AACTGAATCCAAGTGATCTTAGTG	[211]
RT-sigA-R	TCATCACCTTGTTCAATACGTTTG	[211]
Purease-F2	*aatgaattc*GATGATGCTACCTACAATAGCCGCTA	This study
Purease-R2	*ggacgtcgac*CCAATTTCATATTAGATACAATTTACAAAATT	This study
CNK61	GATATGCCATTTCCAACTGTCG	This study
CNK63	GCTGCAAGTTGATCCATAGAGG	This study

[a] Antibiotic resistance abbreviations used: *ampR*, ampicillin resistance; *ermR*, erythromycin resistance; tetL, tetracycline resistance; *Cm*^{r}, chloramphenicol resistance.

[b] Oligonucleotides sequences are provided in the 5'-3' orientation. Lowercase italics indicates non-homologous sequences added for cloning purposes.

Table 3.1. Strains, plasmids, and oligonucleotides used in this study.

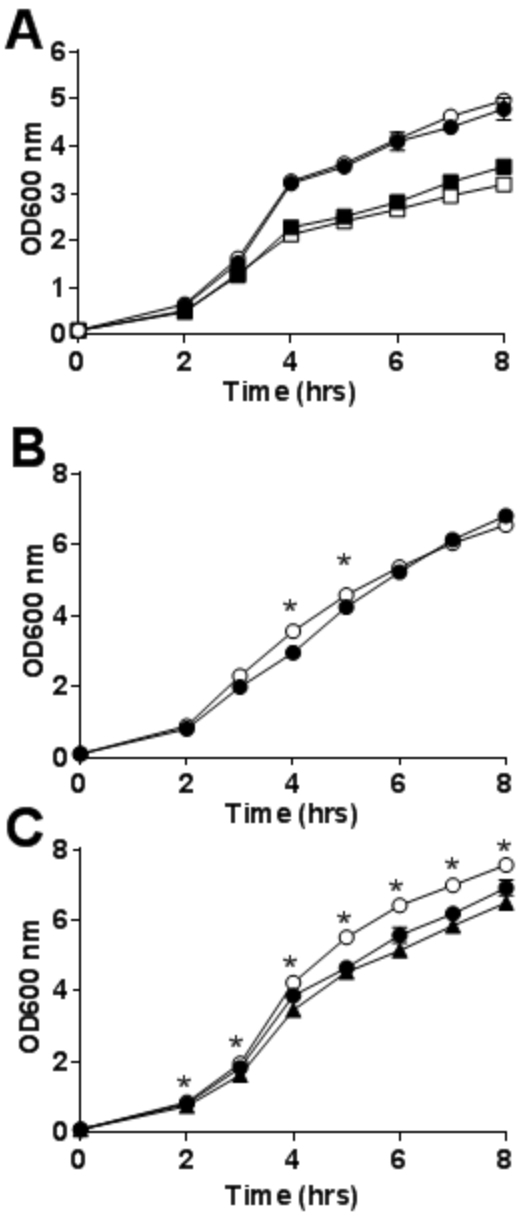

Figure 3.11

Figure 3.11. (A) Growth of wildtype (closed symbols) and *fakA* mutant (open symbols) in TSB + 14 mM glucose with 1:3.3 media to flask ratio (circles) and 1:1.66 flask to media ratio (squares). **(B)** Growth of wildtype (closed circle) and *fakA* mutant (open circle) in TSB without glucose. **(C)** Growth of wildtype (closed circle), *fakA* mutant (empty circle) and *fakA* complement (filled triangle) grown in TSB buffered with 50 mM MOPS. Data are the average (n=3) with standard deviation of a representative experiment. All points have error bars and may be smaller than symbols. *denote significant difference ($p<0.05$) from wildtype using a t-test.

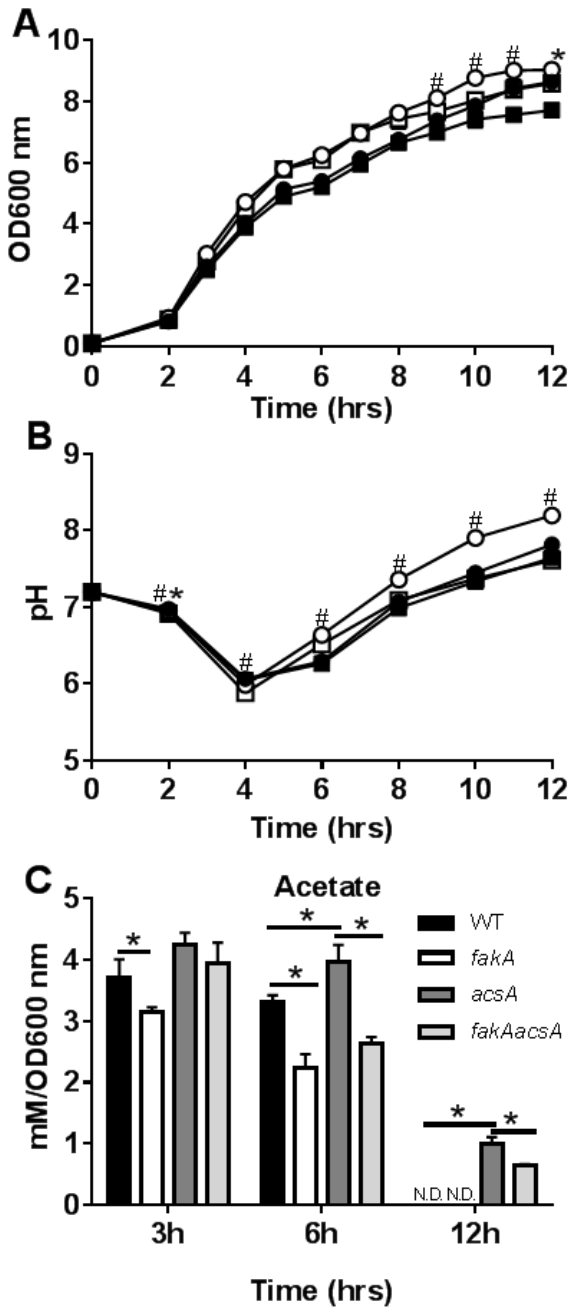
A
OD600 nm
Time (hrs)
B
pH
Time (hrs)
C
Acetate
mM/OD600 nm
WT
fakA
acsA
fakAacsA
N.D. N.D.
3h
6h
12h
Time (hrs)

Figure 3.12

Figure 3.12. (A) Growth of wildtype (closed circle), *fakA* mutant (open circle), *acsA* mutant (closed square), and *fakA acsA* mutant (open square) **(B)** pH of culture from panel A. **(C)** Quantification of acetate in the culture media at indicated time points. Data are the average (n=3) with standard deviation of a representative experiment. For panels A and B, *denotes significant difference ($p<0.05$) using a t-test for wildtype v.s. *acsA* mutant and "#" for *fakA* mutant v.s. *fakA acsA* mutant. For panel C, *indicates significant differences ($p<0.05$) as indicated. ND indicates "not detected".

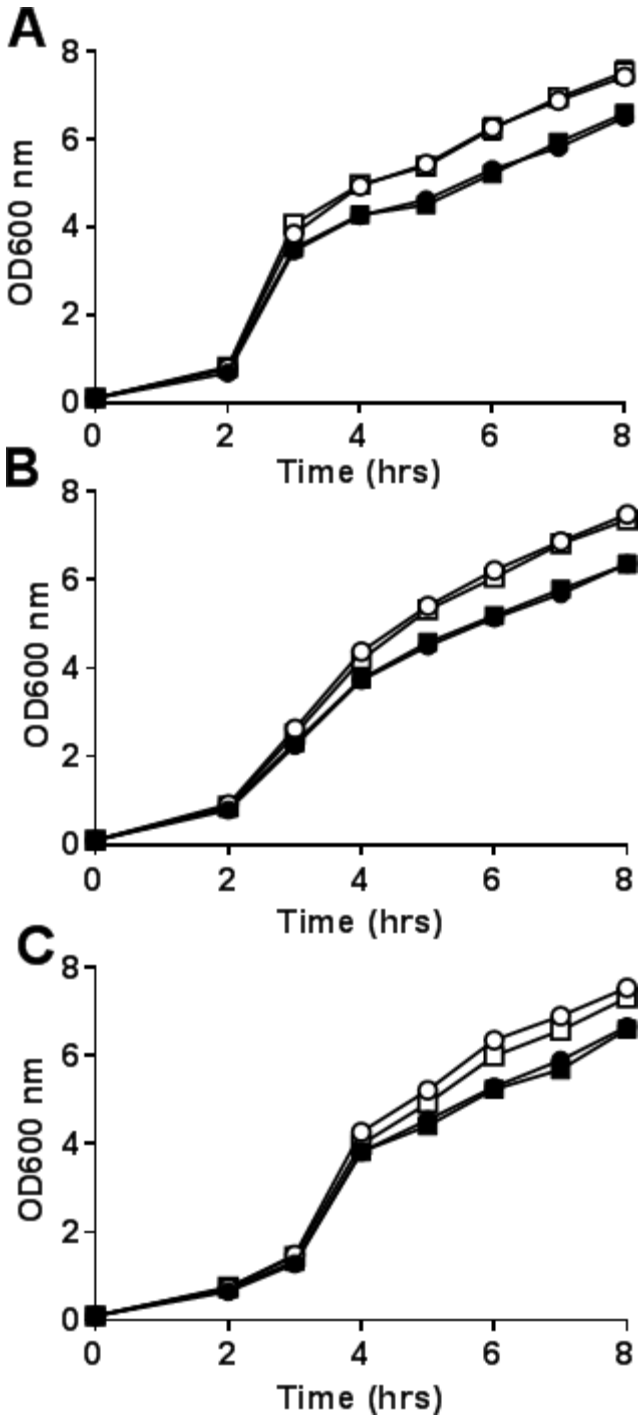

FIgure 3.13

Figure 3.13. (A) Growth of wildtype (closed circles), *fakA* mutant (open circles), *ldh1* mutant (closed squares), and *fakA ldh1* mutant (open squares). (B) Growth of wildtype (closed circles), *fakA* mutant (open circles), *ldh2* mutant (closed squares), and *fakA ldh2* mutant (open squares) (C) Growth of wildtype (closed circles), *fakA* mutant (open circles), *alsS* mutant (closed squares), and *fakA alsS* mutant (open squares).

Table 3.2

Organic Acid[a]	Media	Strain	Cells[b]			
			3h	P-value	6h	P-value
α-ketoglutarate	3.22	WT	1.62	0.029	0.45	0.011
		Δ*fakA*	1.19		0.66	
β-hydroxybutyrate	80.70	WT	2.42	0.037	4.12	0.061
		Δ*fakA*	1.72		3.16	
acetyl-CoA	n.d.[c]	WT	546.77	0.830	314.84	0.540
		Δ*fakA*	560.95		406.66	
citrate	16.00	WT	1.71	0.053	0.85	0.032
		Δ*fakA*	1.42		1.47	
fumarate	6.56	WT	BLOQ		0.37	0.456
		Δ*fakA*	BLOQ		0.35	
lactate	77.30	WT	343.36	0.014	27.54	0.278
		Δ*fakA*	474.73		24.86	
malate	702.44	WT	1.15		BLOQ	
		Δ*fakA*	BLOQ		0.42	
malonyl-CoA	n.d.[c]	WT	18.74	0.408	2.60	0.345
		Δ*fakA*	15.99		3.22	
Succinate	80.67	WT	58.22	0.388	191.81	0.142
		Δ*fakA*	48.18		247.46	

[a]Quantification of selected organic acids by LC/MS/MS of sterile media before inoculation or cells after threeand six hours of growth in TSB + 14 mM glucose.

[b]values are in nM per mg protein. Statistically-significant differences are marked by underline. BLOQ indicatesbelow limit of quantification.

[C]not determined.

Table 3.2. Quantification of organic acids.

Table 3.3

Nucleotide[a]	3 hrs				6 hrs			
	WT[b]	Δ*fakA*[b]	% change[c]	P-value	WT[b]	Δ*fakA*[b]	% change[c]	P-value
NAM	1.42	3.88			1.13	1.18		
NMN	0.38	0.12	-68.6	0.001	0.20	0.21		
NAD	46.84	28.18	-39.8	0.005	40.99	52.39		
NADP	2.86	2.04			1.96	3.13	60.1	0.002
AMP	70.26	71.47			32.67	59.03	80.7	0.004
ADP	18.25	17.20			7.97	12.20	53.0	0.017
ADPR	11.97	18.55	55.0	0.005	5.57	2.55	-54.2	0.011
ATP	6.52	6.09			1.92	3.22	67.2	0.015
GMP	14.58	10.27	-29.5	0.007	9.40	18.57	97.5	0.005
GDP	15.39	10.44	-32.1	0.001	6.34	9.89	56.1	0.013
GTP	3.61	2.19	-39.2	0.002	1.32	1.67		
CMP	7.55	6.18	-18.1	0.015	6.46	12.79	97.9	0.006
CDP	1.66	1.03	-37.9	0.032	1.07	1.78	66.6	0.018
CTP	0.87	0.47	-45.2	0.001	0.30	0.47	56.1	0.029
UMP	15.80	19.20	21.5	0.014	8.46	20.08	137.3	0.009
UDP	18.36	19.73			8.57	13.73	60.2	0.009
TMP	5.17	5.37			2.92	14.77	406.6	0.021
TDP	3.57	4.91	37.3	0.002	1.43	4.64	224.9	0.004
TTP	0.80	0.85			0.21	0.76	253.4	0.002
IMP	10.58	8.22	-22.4	0.033	1.38	4.95	258.3	0.005
IDP	0.36	0.16	-57.2	0.003	0.04	0.03		
ITP	0.54	0.23	-58.0	0.008	0.06	0.05		
NADH	36.50	42.00			19.60	14.32	-26.9	0.007
NADPH	1.16	0.77	-33.6	0.021	0.69	0.63		
NAD/NADH	1.37	0.67	-51.0	0.020	2.12	3.70	74.2	0.013
NADP/NADPH	2.47	2.66			2.84	5.01	76.3	0.001

[a]Quantified using LC/MS/MS from cells collected after three or six hours of growth in TSB + 14 mM glucose.

[b]Shown as nM per mg protein, except for NAD/NADH and NADP/NADPH (shown as ratio).

[c]Change in mutant from wild-type (WT) strain, red box denotes a decrease in mutant while green identifies anincrease in mutant. Only those with significant differences ($p < 0.05$) are shown.

Table 3.3. Quantification of cellular nucleotides.

Table 3.4

Amino acid	Media[a]	Strain	Supernatant[b]			
			3h	P-value	6h	P-value
Alanine	2692.08	WT	594.03	0.256	382.43	0.002
		Δ*fakA*	988.13		72.20	
Arginine	1616.45	WT	901.83	0.528	916.62	0.547
		Δ*fakA*	1114.91		604.18	
Asparagine	870.91	WT	39.85	0.036	22.43	0.313
		Δ*fakA*	75.96		19.39	
Aspartate	602.03	WT	162.84	0.567	193.21	0.007
		Δ*fakA*	198.94		3.66	
Citruline	20.01	WT	19.46	0.428	26.68	0.283
		Δ*fakA*	12.39		19.50	
Glutamate	2387.40	WT	489.98	0.265	257.68	0.085
		Δ*fakA*	842.71		19.87	
Glutamine	542.46	WT	BLOQ		BLOQ	
		Δ*fakA*	2.47		BLOQ	
Glycine	758.59	WT	111.32	0.729	25.32	0.369
		Δ*fakA*	87.15		7.65	
Hisitidine	567.36	WT	246.92	0.253	218.62	0.591
		Δ*fakA*	344.32		143.46	
Isoleucine	1539.47	WT	575.56	0.167	433.75	0.901
		Δ*fakA*	895.23		403.93	
Leucine	7071.18	WT	2870.56	0.329	2322.54	0.576
		Δ*fakA*	3832.42		1672.32	
Lysine	6442.79	WT	1662.38	0.352	1381.47	0.531
		Δ*fakA*	2189.76		923.10	
Ornithine	51.92	WT	30.25	0.151	43.70	0.569
		Δ*fakA*	23.79		49.01	
Methionine	1318.28	WT	443.97	0.659	385.42	0.383
		Δ*fakA*	679.39		261.61	
Phenylalanine	1910.52	WT	1004.86	0.744	1012.08	0.494
		Δ*fakA*	1122.32		673.73	
Proline	398.74	WT	183.10	0.446	193.10	0.670
		Δ*fakA*	248.13		232.58	
Serine	1544.93	WT	56.55	0.005	15.82	0.174
		Δ*fakA*	171.51		4.17	
Threonine	1453.77	WT	119.45	0.049	26.46	0.365
		Δ*fakA*	473.13		0.97	
Tryptophan	551.52	WT	248.25	0.617	253.99	0.681
		Δ*fakA*	293.05		196.59	
Tyrosine	563.59	WT	207.77	0.218	213.68	0.724
		Δ*fakA*	317.66		167.61	
Valine	2717.28	WT	1184.58	0.430	1104.39	0.742
		Δ*fakA*	1545.04		883.73	

[a]μM concentration of sterile media determined by LC/MS/MS.

[b]μM concentration determined by LC/MS/MS and normalized to relative optical density. Statistically-significantdifferences are marked with an underline. BLOQ indicates below limit of quantification.

Table 3.4. Quantification of extracellular amino acids.

Chapter 4: The sensor kinase SaeS senses fatty acids at the membrane.

Introduction

According to the Centers of Disease Control and Prevention (CDC), approximately 2.8 million people in the U.S. are infected by antibiotic-resistant bacteria each year. It is estimated that antibiotic-resistant *Staphylococcus aureus* (*S. aureus*) accounted for over 300,000 hospitalizations and over 10,000 deaths in 2017, indicating that *S. aureus* is a key contributor to the burden of antibiotic-resistant infections (CDC). *S. aureus* is a Gram-positive bacterium that asymptomatically colonizes 20-30% of the population, predominately in the anterior nares and the skin [2]. Despite being asymptomatic, *S. aureus* can establish infections in nearly every anatomical site but most commonly causes infections in the skin [10, 212]. This bacterium is responsible for most of the skin and soft-tissue infections observed in the clinic [11] and was estimated to cost the U.S. healthcare system $1.7 billion in 2017 (CDC). With the large burden that *S. aureus* places on the healthcare system, an emphasis on understanding what makes *S. aureus* such a successful pathogen and designing novel therapeutics that target it is needed.

Well-timed regulation of the virulence arsenal of *S. aureus* and being able to sense and respond to external stimuli are essential for the success of pathogenic bacteria. These organism encounter and need to respond to a variety of stimuli, both inside and outside the host. These signals can include changes in osmolarity, temperature, the presence or absence of oxygen, pH and host-associated factors. Some of these signals are sensed by Two-Component Systems (TCS) which allow bacteria to sense the stimulus and adjust expression of target genes accordingly [213, 214]. TCS's generally consist of a membrane bound histidine-kinase (HK) and a cytoplasmic response regulator (RR). Activating stimuli causes autophosphorylation of the HK at a conserved histidine residue. The phosphoryl group is transferred to an aspartic acid residue of the RR. The phosphorylated RR then binds specific DNA sites and alters the transcription of target genes. *S. aureus* possesses 16

different TCS that respond to varying growth conditions and stimuli and employ different mechanisms to transduce their response to change transcription [135]. Responding to cell-wall stress and targeting by antimicrobials is a stimulus shared by several TCS's in *S. aureus*, particularly intramembrane HKs. WalKR [137, 138], the only essential TCS in *S. aureus* [135], VraSR [139], and GraRS [140, 141] and SaeRS are among the TCS's that respond to membrane damaging agents and help maintain cell wall integrity.

SaeRS, which stands for the *S. aureus* Exoprotein regulator, is a critical regulator of virulence factor expression [142]. SaeRS was first identified by a transposon mutant that had a significant decrease in secreted proteins in *S. aureus* [143]. This TCS is composed of the sensor histidine kinase SaeS and the response regulator SaeR [144]. Despite the TCS name, two auxiliary proteins SaeP, a lipoprotein, and SaeQ, a transmembrane protein, are also involved in the activity of SaeS by activating the phosphatase activity of SaeS [145]. *saePQRS* are transcribed as an operon containing two distinct promoters: P3 and P1 [146]. The P3 promoter, which is located within the 3`-end of *saeQ*, is constitutive and allows for basal transcription of *saeR* and *saeS*. The second promoter lies upstream of *saePQRS* and contains two SaeR binding-sites. The presence of two SaeR binding-sites allows for this promoter to be induced when levels of phosphorylated SaeR are high, representing activated conditions of SaeS. Expression of *saePQRS* from the P1 promoter transcribes *saeP*, *saeQ*, *saeR*, and *saeS*. Thus, expression of the operon from the P1 promoter serves as a negative feedback mechanism for the Sae operon via phosphatase activitation of SaeS by SaeP and SaeQ. Primarily acting as an activator of target gene expression, phosphorylated SaeR also binds to the promoter regions of various secreted virulence factors [142]. Promoters of target genes fall into two different categories: high and low affinity [147]. High affinity promoters (class II) contain one SaeR binding site. The promoter for α-hemolysin (P_{hla}) is an example of a high

affinity promoter that is sensitive to large changes in Sae activity. In contrast, low affinity promoters (class I) contain two SaeR binding sites. The coagulase promoter (P_{coa}) is an example of a low affinity promoter and is sensitive to small fluctuations in phosphorylated SaeR levels. Low affinity promoters need more phosphorylated SaeR to become activated and are activated when the kinase activity of SaeS is increased compared to basal levels.

The genome of *S. aureus* encodes four different intramembrane sensor kinases. SaeS, along with GraS [215], VraS [216], and BraS [217], are referred to as intramembrane sensor kinases due to the absence of an extracellular ligand binding domain and possess small extracellular loops. SaeS is comprised of two transmembrane domains connected by an extracytoplasmic linker peptide (ELP) of 9 amino acids in length. HAMP and histidine kinase domains are adjacent to the second transmembrane domain and reside on the cytoplasmic side of the phospholipid membrane. Despite no extracellular ligand binding domain, SaeS becomes activated in the presence of host-associated factors. The most well characterized activating molecule is human neutrophil peptide 1, or HNP-1 [218]. While no direct interaction between SaeS and HNP-1 has been shown, the amino acid sequence of the ELP is essential for HNP-1 to activate SaeS [219]. The *saeS* gene in various *S. aureus* strains naturally contains point mutations. Strains Mu50, MW2, and USA600 contain two mutations located within the histidine kinase domain of SaeS (N227S and E268K), however they result in no change in SaeS activity [94]. The Newman strain of *S. aureus* possesses a single substitution mutation in the first transmembrane domain of *saeS* [220]. The substitution (L18P) renders SaeS constitutively active in this strain [147]. One interesting observation made from Newman SaeS is that treatment with sodium dodecyl sulfate (SDS) increases SaeS activity in strain Newman while such treatment decreases USA300 SaeS activity [221]. Creating chimeric SaeS by

swapping the N-terminal transmembrane domains of GraS with SaeS rendered SaeS in an activated state, not needing HNP-1 treatment to become induced [219].

Inactivation of the SaeRS TCS has been shown to be induced by acidic pH and growth in the presence of high salt concentrations [218]. Free fatty acids have also been known to alter bacterial virulence factor production via SaeRS [149]. First, growth of *S. aureus* in the presence of sapienic acid was shown to decrease the expression of targets of SaeRS by proteomic analysis [178]. Specifically, unsaturated fatty acids such as oleic acid and linoleic acid are more potent inhbitors of SaeRS than their saturated counterparts. Fatty acids were then implicated in decreasing SaeRS activity via the discovery and characterization of the exogenous fatty acid kinase FakA [65] (originally named VfrB [66]). These studies showed that deleting *fakA* decreased hemolysis of rabbit blood by α-hemolysin (*hla*), expression of secreted proteases, and coagulase expression [66, 148]. These phenotypes in the *fakA* mutant were later attributed to the accumulation of exoFAs within the cell [149].

While no direct mechanism for the inactivation of SaeRS by fatty acids exists, there is an apparent relationship among respiratory activity, redox balance, SaeRS activity, and growth in the presence of fatty acids. Strains deleted of the respiratory dehydrogenases *ndhF* and *ndhC* were shown to accumulate free fatty acids and inhibit SaeRS activity [26]. The authors in that study suggest that altered NAD+/NADH ratios impacts fatty acid metabolism and causes accumulation of cellular fatty acids, negatively impacting SaeRS activity [26]. SaeRS also plays a role in biofilm formation by positively regulating fibronectin-binding protein A (FnBPA) expression and murein hydrolase AtlA activity [87], showing that growth environment and respiratory balance impact SaeRS-dependent virulence processes.

Here, we assessed how different fatty acids (acyl-chain length, number, and orientation of saturations) impact SaeRS activity. We also tested whether the negative impact fatty acids have on SaeRS activity correlates with alterations in respiratory activity. To determine whether the native transmembrane domains of SaeS were important for the systems sensitivity to fatty acids, we utilized *S. aureus* strains expressing chimeric GraS/SaeS proteins and determined SaeRS activity. Since the substitution mutation (P18L) in Newman dictates the response of SaeRS to different stimuli, we swapped the USA300 and Newman mutations and determined how it affected the response of SaeRS to fatty acids.

Results

Effect of different fatty acids and on SaeRS activity. Fatty acids have been shown to negatively impact SaeRS activity. These studies have centered around the unsaturated fatty acids, oleic acid (C18:1 *cis*) [148] and sapienic acid (C16:1, 1ω10 *cis*) [178]. Additionally, saturated free fatty acid accumulation in a fatty acid kinase (*fakA*) mutant decreases SaeRS activity, possibly due to accumulating free fatty acids [149, 222] To expand on this, we aimed to test how fatty acids of different length, number of desaturations, and orientation of the desaturations impact SaeRS activity.

To determine how effective different fatty acids were in decreasing SaeRS activity, we first performed growth curves with different concentrations of fatty acids. This was done to find a concentration for each fatty acid which does not greatly hinder growth (Figure 4.8). The fatty acids were then added to USA300 cultures grown in TSB, and at mid-exponential phase (six hours), P_{coa}-*lacZ* activity was determined as a readout of SaeRS activity (Figure 4.1). Previous work from our lab shows that myristic acid (C14:0) was not significantly inhibitory at 109 μM

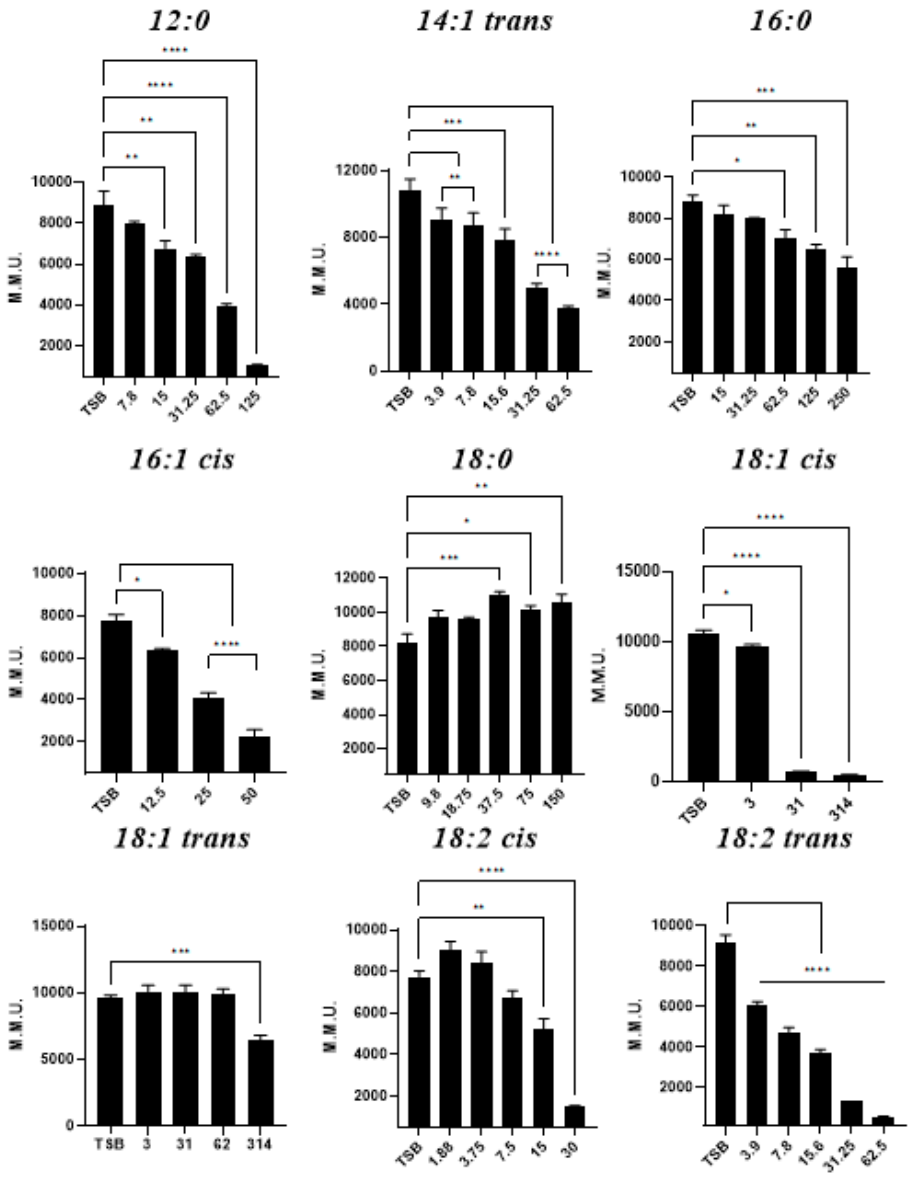
12:0
14:1 trans
16:0
16:1 cis
18:0
18:1 cis
18:1 trans
18:2 cis
18:2 trans
M.M.U.
TSB
7.8
15
31.25
62.5
125
3.9
250
12.5
25
50
9.8
18.75
37.5
75
150
3
31
314
62
1.88
3.75
7.5
15
30

Figure 4.1

Figure 4.1. P_{coa}-lacZ activity of exponential phase (six hours) S. aureus strain AH1263 grown in TSB supplemented with the indicated fatty acids (μM) represented as Modified Miller Units (M.M.U.) Fatty acids are as follows: 12:0- lauric acid, 14:1 trans- myristelaidic acid, 16:1 cis- palmitoleic acid, 18:1 cis- oleic acid, 18:2 cis- linoleic acid, 16:0- palmitic acid, 18:0- stearic acid, 18:1 trans- elaidic acid, and 18:2 trans- linoelaidic acid. Data are representative of multiple experiments and was analyzed via Ordinary one-way ANOVA (Prism). *$p<0.05$, **$p<0.01$, ***$p<0.005$, and ****$p<0.0001$.

[148]. Similar results were observed for the saturated fatty acids palmitic acid (C16:0) and stearic acid (C18:0); palmitic acid was inhibitory to SaeRS activity at a concentration of 62.5 μM whereas stearic acid increased SaeRS activity at concentrations up to 150 μM. However, the shorter chain lauric acid (C12:0) was significantly inhibitory to SaeRS activity at levels as low as 15 μM. Growth of *S. aureus* is more sensitive to unsaturated fatty acids compared to saturated fatty acids [160]. Similarly, SaeRS activity is more sensitive to saturated fatty acids as compared to unsaturated fatty acids such as oleic acid (C18:1 *cis*) being more active against SaeRS compared to stearic acid (C18:0). We wanted to test how the orientation of the double bond found in unsaturated fatty acids impacts SaeRS activity. Unsaturated fatty acids can be in the *cis* or *trans* conformation, with *cis* fatty acids being more bent than *trans* fatty acids. Myrsitelaidic acid (C14:1 trans) was inhibitory to SaeRS activity at much lower levels than myristic acid (C14:0) [148], inhibiting at concentrations as low as 3.9 μM. Likewise, the presence of single *cis*-orientated desaturations in palmitoleic acid (16:1 *cis*) and oleic acid (C18:1 *cis*) were inhibitory to SaeRS activity at concentrations as low as 12.5 μM and 4.9 μM, respectively. Elaidic acid (C18:1 *trans*) was slightly inhibitory to SaeRS activity at concentrations of 314 μM, however, it was not inhibitory at concentrations of 62.5μM and lower. Linoleic acid (C18:2 *cis*) and linoelaidic acid (C18:2 *trans*) are both comprised of two desaturations in differnt orientations. Linoelaidic acid was significantly inhibitory for SaeRS at levels as low as 3.9 μM while linoleic acid was inhibitory at 15 μM. Our data indicate oleic acid (C18:1 *cis*) and linoelaidic acid (C18:2 *trans*) were especially good at decreasing SaeRS activity and that the orientation of the double bond plays an important role for SaeRS sensitivity only in the context of mono-unsaturated fatty acids.

Fatty acid impact on respiratory activity. A study in the 1970's identified fatty acid type and concentration-dependent effects on respiratory activity and metabolite up take in bacteria: lower

concentrations of fatty acids increased respiration and higher concentrations depleted respiration [223].Previous data from our lab and others indicates that oleic acid decreases respiratory activity [174, 222]. Our data above suggests that fatty acids with different structures differentially impact SaeRS activity. Respiration and redox balance have also been implicated as a possible stimulus for altering SaeRS activity [26, 87]. We assessed how fatty acid isoforms, oleic acid and elaidic acid, as well as linoleic acid and linoelaidic acid, impact respiratory activity using the fluorescent reporter CTC [170].

When cells were grown in the presence of oleic acid (C18:1 *cis*), only the concentration of 314μM significantly impacted respiratory activity compared to that of TSB alone (Figure 4.2A), as previously demonstrated [222]. In contrast, growth in the presence of elaidic acid (C18:1 *trans*) did not reduce respiratory activity even at concentrations up to 314 μM, a concentration that decreased SaeRS activity. Growth in the presence of 31 μM elaidic acid (C18:1 *trans*) increased respiratory activity compared to growth in TSB alone. The same experimental design was used to test linoleic (C18:2 *cis*) and linoelaidic (C18:2 *trans*) acid's effect on respiration. Our initial hypothesis was that these fatty acids would mirror that of oleic acid and decrease respiration due to the presence of two double bonds. Like other reports [223], growth with 30 μM linoleic acid significantly decreased respiration (Figure 4.2B). Linoelaidic acid did not significantly impact respiration at 62.5 μM, even though this concentration decreased SaeRS activity. These data suggest that, while altered respiration may influence SaeRS activity, fatty acids can affect SaeRS in a respiration-independent manner.

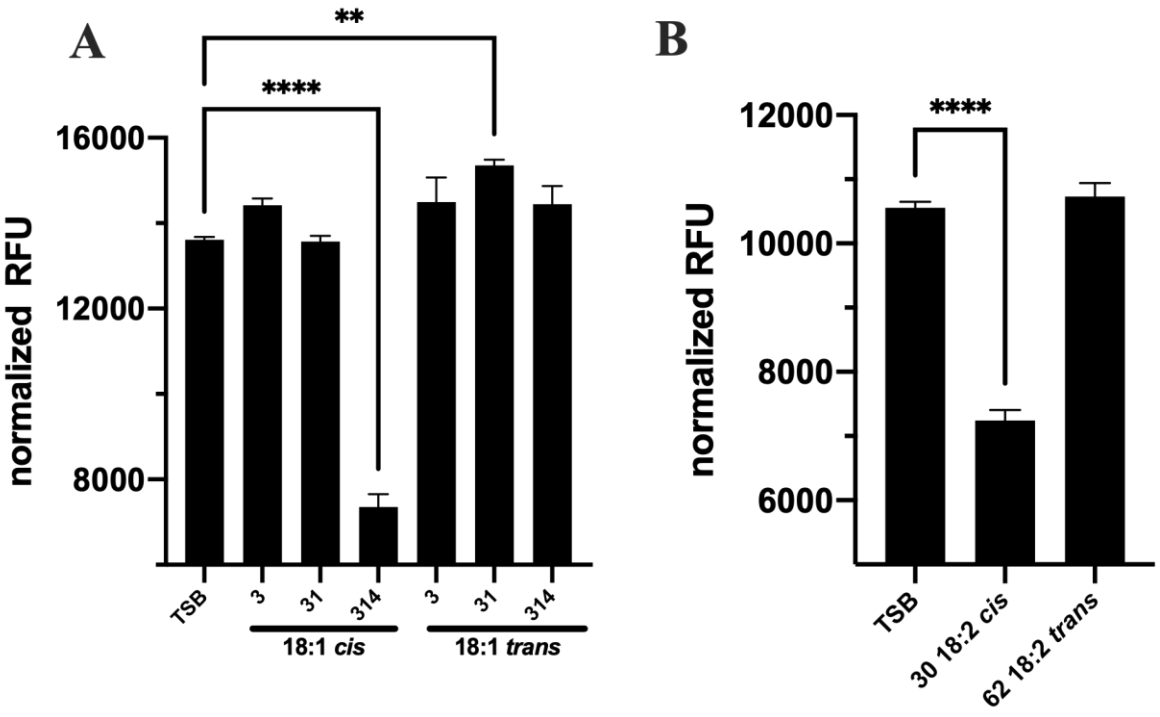
A
**
****
16000
12000
8000
normalized RFU
TSB
3
31
314
3
31
314
18:1 cis
18:1 trans
B
****
12000
10000
8000
6000
normalized RFU
TSB
30 18:2 cis
62 18:2 trans

Figure 4.2

Figure 4.2. Respiratory analysis using CTC for wild-type *S. aureus* grown to exponential phase (six hours) in TSB supplemented with fatty acid (μM) **A)** oleic acid (C18:1 *cis*) and elaidic acid (C18:1 *trans*) and **B**) linoleic acid (C18:2 *cis*) and linoelaidic acid (C18:2 *trans*). Data are presented as relative fluorescent units (RFU) normalized to OD600 and is representative of multiple experiments. Data were analyzed via Ordinary one-way ANOVA (Prism). **$p<0.01$, ***$p<0.005$, and ****$p<0.0001$.

SaeP and SaeQ are not required for fatty acid reduction of SaeRS activity. To avoid over-activation, sensor kinase's typically have phosphatase enzymatic activity. SaeS is bi-functional and has both kinase (activation) and phosphatase activity (inactivation) [145]. The ability of SaeS to switch from a kinase to a phosphatase has been shown to be dependent on the accessory proteins SaeP and SaeQ [145]. These genes are expressed from the P1 promoter, which is only expressed when P~SaeR levels are sufficiently high, representing an induced state of SaeS. This serves as negative-feedback regulation step that prevents over production and mis-timed production of SaeRS-dependent virulence factors. Since fatty acids decrease the activity of SaeRS, these two accessory proteins could potentially provide a mechanism for this. We first monitored expression from the P3 promoter of the Sae operon in the presence of absence of oleic acid (C18:1 *cis*) using P_{P3}-*lacZ* reporter (Figure 4.3A). Expression from this promoter was unchanged when grown in the presence of oleic acid (C18:1 *cis*). This indicates that basal expression of *saeRS* is not affected by oleic acid (C18:1 *cis*), suggesting that basal activity of SaeRS is also not affected. Since the P1 promoter is sensitive to SaeRS activity and high levels of P~SaeR, it was replaced with $P_{xyl/tetO}$ to account for possible changes in expression of *saeP* and *saeQ*. Oleic acid (C18:1 *cis*) decreased P_{coa}-*lacZ* activity even with this non-native promoter (Figure 4.3B), demonstrating that fatty acids are not impacting expression of the *sae* operon. Next, in-frame deletion mutations of both *saeP* and *saeQ* were created and P_{coa}-*lacZ* activity was monitored in the presence and absence of oleic acid (C18:1 *cis*). The response of P_{coa}-*lacZ* to oleic acid (C18:1 *cis*) was not impacted by the absence of either *saeP* or *saeQ* (Figure 4.3C), ruling out a potential role for SaeP and SaeQ in the sensitivity of SaeS to fatty acid treatment.

USA300 allele of SaeS is sensitive to fatty acids. Different alleles of SaeS are present within different strains of *S. aureus*. Compared to our wild-type LAC strain USA300, strain Newman

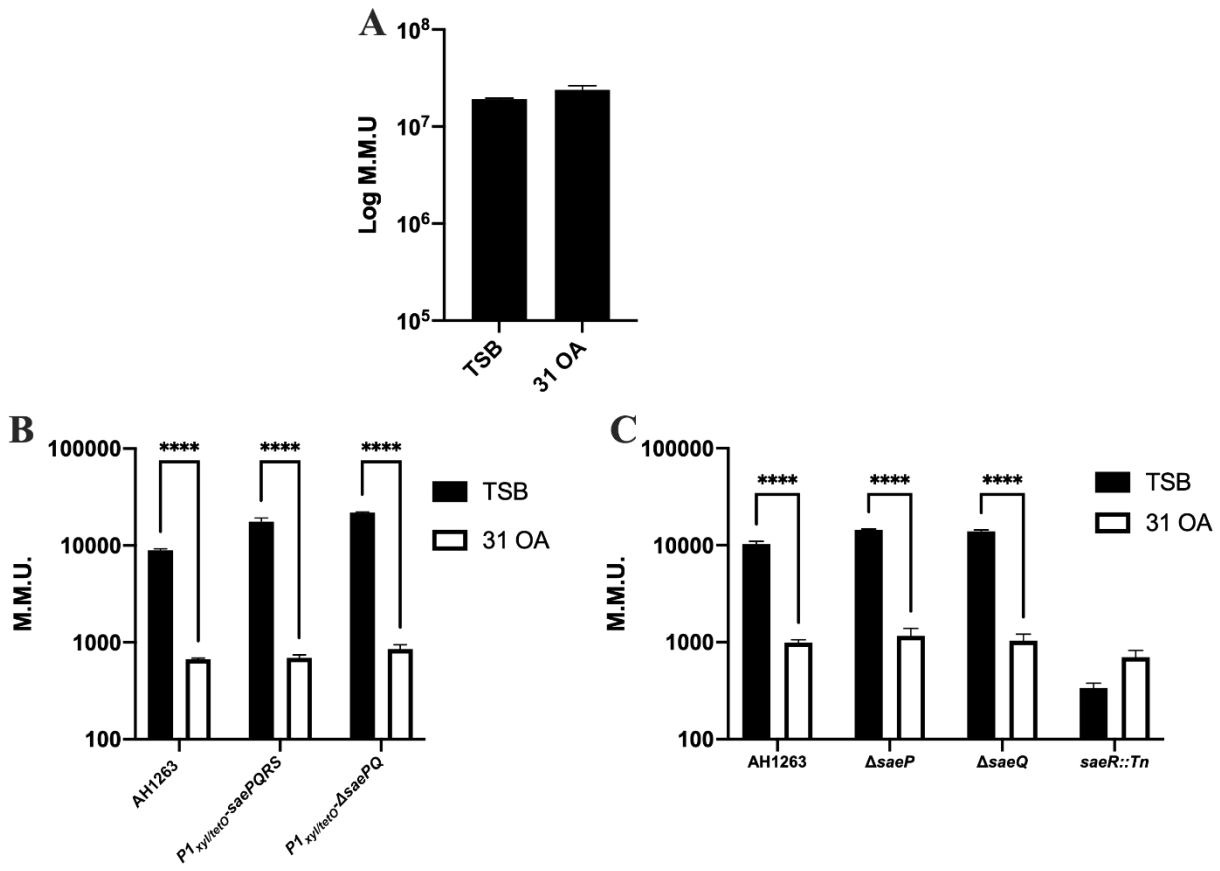
A
Log M.M.U
10^8
10^7
10^6
10^5
TSB
31 OA
B
M.M.U.
100000
10000
1000
100
****
****
****
TSB
31 OA
AH1263
P1xyl/tetO-saePQRS
P1xyl/tetO-ΔsaePQ
C
M.M.U.
100000
10000
1000
100
****
****
****
TSB
31 OA
AH1263
ΔsaeP
ΔsaeQ
saeR::Tn

Figure 4.3

Figure 4.3. SaeP and SaeQ do not impact SaeRS sensitivity to fatty acid treatment. **A)** P_{P3}-*lacZ* activity of *S. aureus* strain AH1263 grown in TSB to exponential phase (six hours) with and without oleic acid (μM). Data is represented as Modified Miller Units (M.M.U.). **B)** P_{coa}-*lacZ* activity of *S. aureus* AH1263, AH1263 with non-native P1 promoter of SaeRS, and AH1263 non-native P1 promoter Δ*saePQ* grown to exponential phase (six hours) in TSB with and without oleic acid (μM). Data is represented as Modified Miller Units (M.M.U.). **C)** P_{coa}-*lacZ* activity of *S. aureus* AH1263, Δ*saeP*, Δ*saeP*,and *saeR*::Tn grown in TSB to exponential phase (six hours) with and without oleic acid (μM). Data is represented as Modified Miller Units (M.M.U.). All data are representative of multiple experiments. Data was analyzed via Ordinary one-way ANOVA (Prism). ****$p<0.0001$.

possesses a substitution mutation (P18L) within the second transmembrane domain of SaeS. These two alleles of SaeS respond differently to specific stimuli. Whereas strain Newman does not respond to HNP-1, strain USA300 is activated by it. We wanted to test whether activation of SaeRS via HNP-1 in strain USA300 would still be impacted by the presence of fatty acid (Figure 4.9). Addition of low and high concentrations of HNP-1 (0.5μg/mL and 5.0μg/mL, respectively) significantly induced SaeRS activity compared to TSB alone. Growth in the presence of low levels of HNP-1 did not overcome inhibition of SaeRS via oleic acid. The presence of high levels of HNP-1 was able to overcome inhibition via oleic acid, however, oleic acid did significantly decrease SaeRS activity when compared to high levels of HNP-1 alone. Our data suggest that activation of HNP-1 can overcome inactivation via oleic in a concentration dependent manner.

Previous work has shown the substitution mutation in strain Newman causes SaeS to be activated by SDS, while SaeS activity in LAC strains (such as USA300) was decreased [221]. Since both SDS and fatty acids alter membrane stability, we hypothesized that both SDS and free fatty acids would stimulate SaeRS in a similar manner. To test this, we used strains with the Newman substitution mutation in the USA300 background and the USA300 substitution mutation (P18L) into the Newman background. These strains were then used to test how the substitution impacts SaeS response to fatty acid treatment. SaeR target promoters are classified into two classes. Class I are sensitive to large decreases and class II promoters sensitive to small decreases in P~SaeR levels. First, expression of the class II promoter *hla* (α-hemolysin) was determined in the absence and presence of oleic acid (C18:1 *cis*). Growth in the presence of oleic acid (C18:1 *cis*) did not impact activity of the alpha-hemolysin promoter in AH1263, AH1263 $SaeS^{L18P}$, Newman, and Newman $SaeS^{P18L}$ (Figure 4.4A). Next, the activity of the class I promoter *coa* (coagulase) was determined in the presence of oleic acid (C18:1 *cis*) (Figure 4.4B). As expected, oleic acid (C18:1

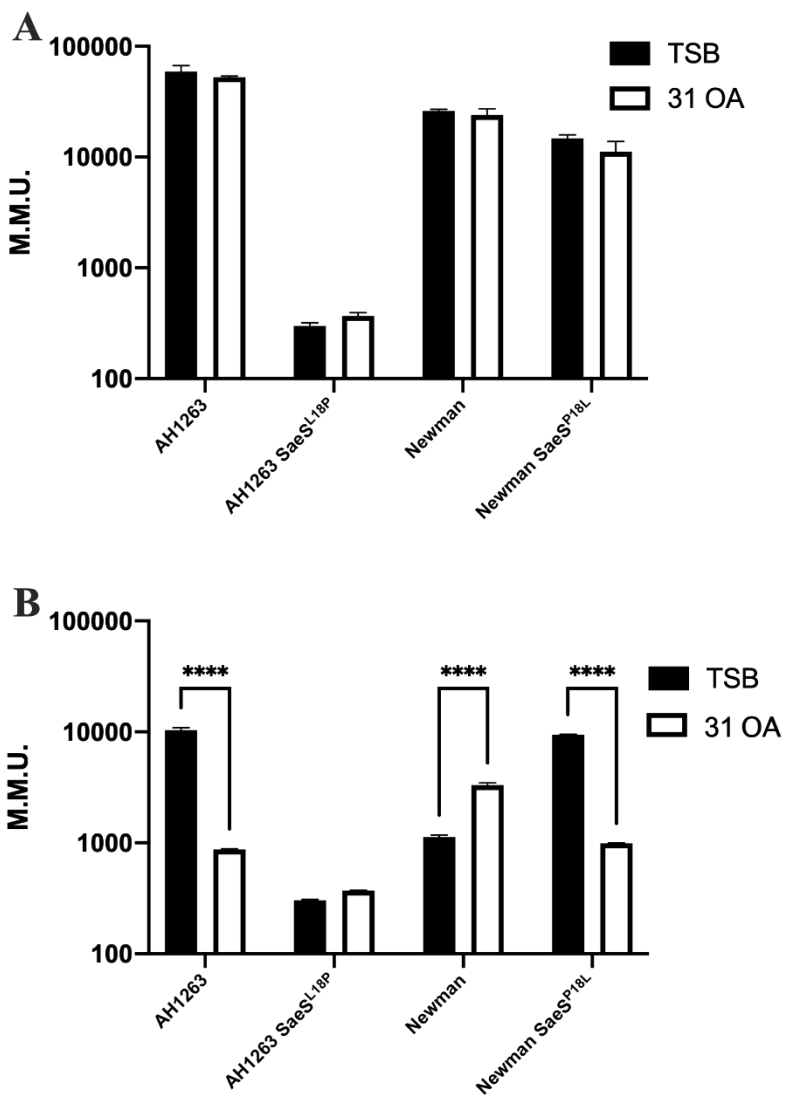
A
100000
10000
1000
100
M.M.U.
TSB
31 OA
AH1263
AH1263 SaeS L18P
Newman
Newman SaeS P18L
B
100000
10000
1000
100
M.M.U.
****
****
****
TSB
31 OA
AH1263
AH1263 SaeS L18P
Newman
Newman SaeS P18L

Figure 4.4

Figure 4.4. USA300 allele of SaeS (P18L) is negatively impacted by fatty acid. P_{hla} *–lacZ* **(A)** and P_{coa}*-lacZ* **(B)** activity of wild-type AH1263, AH1263 $SaeS^{L18P}$, wild-type Newman, and Newman $SaeS^{P18L}$ grown to exponential phase (six hours) in TSB supplemented with fatty acid (μM). Data are representative of multiple experiments (n=3). Data were analyzed via Ordinary one-way ANOVA (Prism). ****p<0.0001.

cis) significantly decreased coagulase promoter activity in strain AH1263. Expression of both alpha-hemolysin and coagulase in strain AH1263 SaeS^{L18P} was generally decreased compared to wild type AH1263. Despite that, coagulase promoter activity was not significantly decreased in the presence of oleic acid in this strain. Growth in fatty acid significantly increased coagulase promoter activity in strain Newman. In contrast, coagulase promoter activity in strain Newman SaeS^{P18L} was sensitive to growth in the presence of fatty acid and decreased when compared to growth in TSB. These data highlight the importance that the Newman substitution within the first transmembrane domain of SaeS plays in responding to exogenous stimuli.

With the connection between redox balance and SaeRS activity, we hypothesized that cysteine residues in SaeS would be sensitive to these changes. To test this, we compared *S. aureus* strains expressing both wild type SaeS and SaeS containing substitution mutations (Cys to Ser) at amino acid 50 and 56 in the second transmembrane domain of the protein. (SaeS^{C50S,C56S}). We found that expression of SaeS^{C50S,C56S} did not activate SaeRS while expression of wild type SaeS did (Figure 4.10). Since these cysteine-serine substitutions inactivate SaeS, we were unable to test their role in fatty acid sensitivity of SaeS.

Replacement of N-terminal domain of SaeS with GraS desensitizes SaeS to fatty acids. There are only four intramembrane HKs encoded in the *S. aureus* genome and they generally respond to membrane-targeting molecules. Previous work by Liu et al created chromosomally integrated GraS/SaeS chimera expression vectors [219] (Figure 4.5). The GraS-TM/SaeS construct replaced the native SaeS transmembrane domains with the GraS transmembrane domains, leaving the native extracytoplasmic linker peptide of SaeS intact. The GraS-ND/SaeS construct replaced the entire N-terminal domain of SaeS with GraS N-terminal domain, including both transmembrane domains and the extracytoplasmic linker peptide. We also utilized the SaeS cytoplasmic only construct

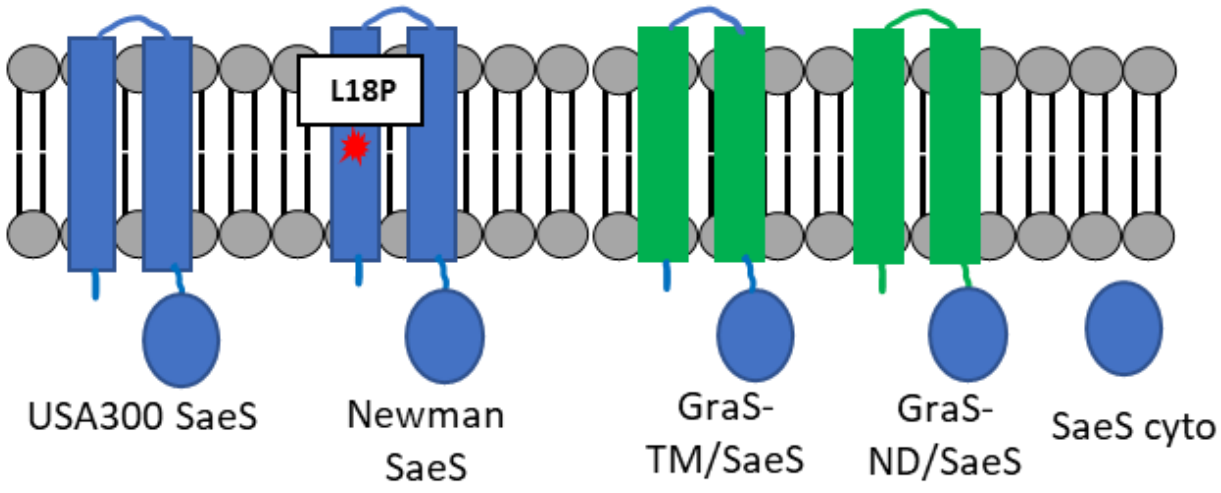
L18P
USA300 SaeS
Newman SaeS
GraS-TM/SaeS
GraS-ND/SaeS
SaeS cyto

Figure 4.5

Figure 4.5. Graphical representation of the different SaeS constructs used in this study. Blue indicates SaeS domains and green indicates GraS domains. Blue indicates SaeS portions of of the chimera and green indicates GraS portions of the chimera.

(SaeS^{cyto}). This construct removes the transmembrane domains and extracytoplasmic linker peptide from SaeS, leaving only the cytoplasmic portion of SaeS, including the HAMP and histidine kinase domains intact. Since these constructs exchange portions native SaeS protein with another sensor kinase, we first wanted to test if the GraS system itself would respond to fatty acid treatment when grown under our conditions. To do this, we tested the activity of the *mprF* promoter which has been shown to be a target gene for the GraRS system using a P_{mprF}-*lux* reporter plasmid (pGYLux::*mprF*) [141]. We found a modest decrease in expression of the *mprF* promoter when cells were grown in the presence of 31μM oleic acid under our conditions (Figure 4.11). This response, however, occurred even in a strain harboring a transposon insertion into the RR of the GraRS system *graR* indicating it was independent of the sensor GraS.

Next, we tested how the GraS/SaeS chimeras and SaeS^{cyto} strains responded to growth in the presence of oleic acid under our conditions. The chimera expression vectors were integrated into both Newman Δ*sae* and USA300 Δ*saeRS* strains, respectively. SaeRS activity was measured via P_{coa}-*gfp* expression (using pYJ335) [219] in strain Newman (Figure 4.6A) and P_{coa}-*lacZ* (using pJB1051) activity in strain USA300 (Figure 4.6B). Both 31 μM and 314 μM oleic acid reduced the expression of P_{coa}-*gfp* activity to below background levels (media blank) in the presence of wild-type SaeS, as anticipated. Next, the response of the coagulase promoter activity to oleic acid was assessed when chimeric GraS-ND/SaeS, GraS-TM/SaeS, and SaeS^{cyto} were expressed. The presence of 31 μM and 314 μM oleic acid did not decrease coagulase promoter activity when either of the three SaeS constructs were expressed (Figure 4.6A). In contrast to native USA300 SaeS, coagulase promoter activity in the GraS-TM/SaeS chimera strains was actually increased when grown in both 31 μM and 314 μM oleic acid, whereas coagulase promoter activity was increased in the strains expressing GraS-ND/SaeS and SaeS^{cyto} in the presence of 314 μM. Similar results

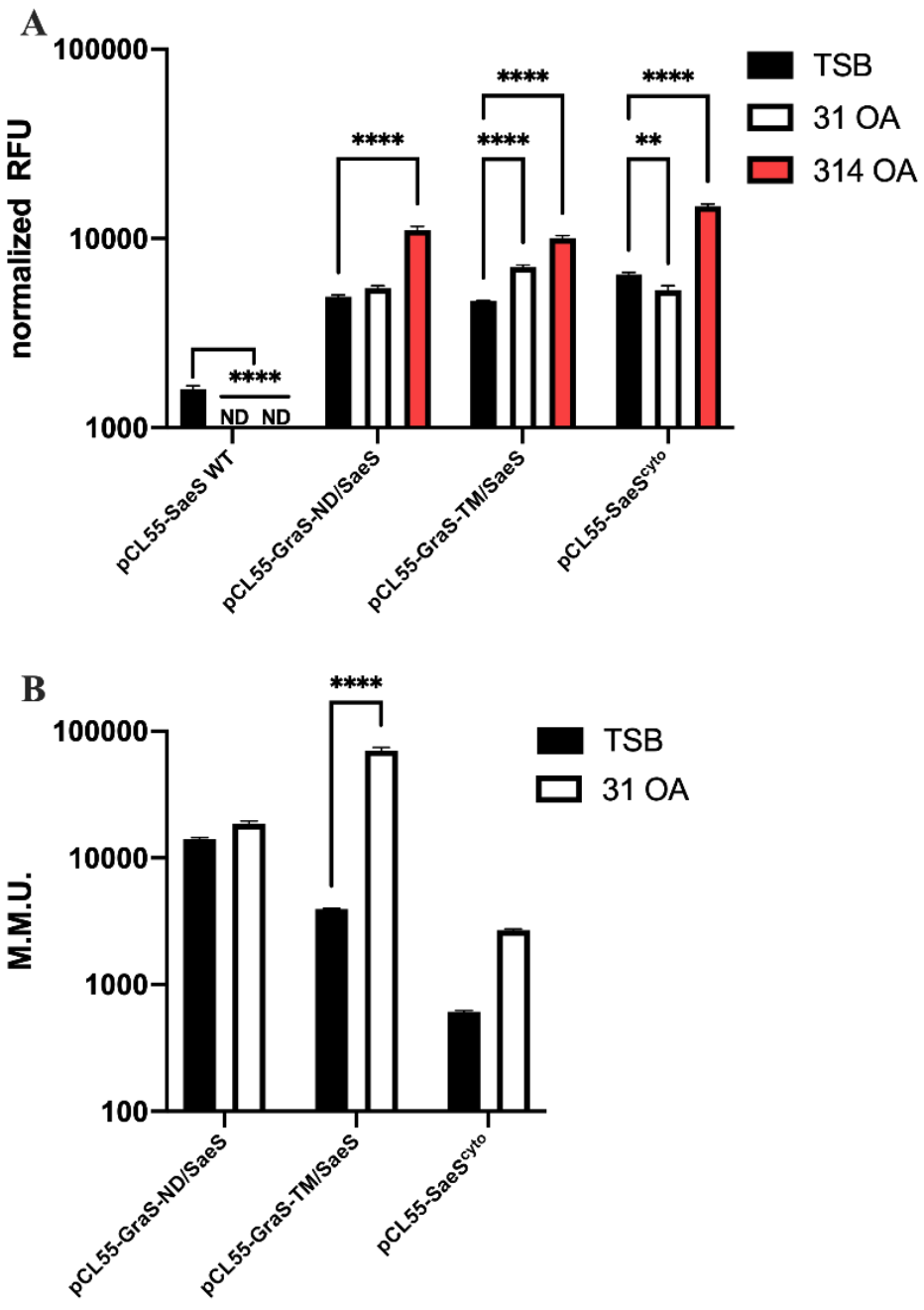
A
100000
10000
1000
normalized RFU
TSB
31 OA
314 OA
****
****
****
****
**
ND ND
pCL55-SaeS WT
pCL55-GraS-ND/SaeS
pCL55-GraS-TM/SaeS
pCL55-SaeS^cyto
B
100000
10000
1000
100
M.M.U.
TSB
31 OA
****
pCL55-GraS-ND/SaeS
pCL55-GraS-TM/SaeS
pCL55-SaeS^cyto

Figure 4.6

Figure 4.6. Replacement or removal of native SaeS transmembrane domains desensitizes SaeRS to fatty acid (μM) treatment. Strains were grown to exponential phase (six hours) in TSB supplemented with oleic acid (μM). **A)** Expression of chimeric GraS/SaeS or $SaeS^{cyto}$ in Newman Δ*sae* background. Activity was measured via *Pcoa-gfp.* Data are represented as relative fluorescent units normalized to OD600. **B)** Expression of chimeric GraS/SaeS or $SaeS^{cyto}$ in AH1263 Δ*saeRS* background. Activity was measured via *Pcoa-lacZ.* Data are represented as Modified Miller Units (M.M.U.). Data are representative of multiple experiments (n=3). Data were analyzed via Ordinary one-way ANOVA (Prism). $^{**}p<0.01$, $^{****}p<0.0001$.

were observed when the chimeras were expressed in the USA300 Δ*saeRS* strain (Figure 4.6B). In conclusion, replacement of the transmembrane domains of SaeS with GraS, as well as complete removal of the N-terminal domain of SaeS, did not result in the expected decrease in SaeS activity in the presence of oleic acid suggesting that free fatty acids are negatively impacting USA300 SaeS at the membrane.

Discussion

Work investigating SaeRS activation and inactivation signals has yielded a few interesting results. Current hypotheses suggest that SaeS, along with other intramembrane HKs, senses membrane stress where the stress (i.e., treatment with cell-wall targeting antibiotics [224]) would induce conformational changes in the protein, referred to as a "trip-wire" model. What is known is that the neutrophil-produced HNP-1, which targets and damages membranes, affects SaeS activity dependent on the amino acid sequence of the extracytoplasmic linker peptide of SaeS [219]. Treatment of *S. aureus* with SDS, a membrane-disrupting detergent, also impacts the activity of SaeS and is currently thought to be predicated on the allele of the transmembrane domains of SaeS [221]. Fatty acids have recently been identified as negative regulator of SaeS activity in *S. aureus* at concentrations that are not inhibitory to growth [148, 149]. ExoFAs, particularly oleic acid, also induce changes in SaeS activity below concentrations where the fatty acid is used for phospholipid synthesis [222]. Antimicrobial fatty acids are a part of the innate immune system, primarily playing a role in limiting bacterial growth on skin tissue. Specific fatty acids, particularly unsaturated fatty acids, are toxic to bacteria. Like antimicrobial peptides and some antibiotics, fatty acids exert their effects on bacteria by affecting membrane stability, respiratory disruption, and altered activity of membrane-associated proteins [225].

We were interested in identifying a potential relationship between different concentrations of fatty acids and their impact on both respiratory and SaeRS activity. There appears to be no correlation between concentrations of fatty acids that impact both SaeRS and respiration. We found that oleic acid (C18:1 *cis*) is highly effective at decreasing SaeRS activity at levels as low as 3 μM while not dereasing respiration. Both Linoleic acid (C18:2 *cis*) and linoelaidic acid (C18:2 *trans*) were also effective at lower concentrations. Oleic acid (C18:1 *cis*) and linoleic acid (C18:2 *trans*) are major components of fatty acids found on human skin [80] and potentially serve as a signaling molecules for the host environment. Our previous data suggest that oleic acid is not inserted into phospholipids at concentrations of 31 μM [222]. We presume even lower concentrations of oleic acid would similarliy not be incorporated. If oleic acid is not being utilized for phospholipid synthesis at low levels, given the inability of *S. aureus* to degrade fatty acids, it is likely that growth in the presence of unsaturated fatty acids serves as a signal of stress. Inactivation of the fatty acid kinase *fakA* results in the accumulation of fatty acids in the cell and the the ability to grow better in the presence of unsaturated fatty acids compared to wild-type *S. aureus* [160]. This growth advantage was dependent on the stress-associated sigma factor, *σB*, as it is needed for the increased resistance [160]. The presence of fatty acids that are not being utilized for phospholipid synthesis, either in a *fakA* mutant or when present at below-incorporation levels in the environment, likely induce a stress response that is at least partially dependent on *σB*. Stress responses generally have pleiotropic effects. For example, a transcriptomic study revealed global changes in gene expression, particularly for *σB*-dependent target genes, 20 minutes after exposure of *S. aureus* to 100 μM linoleic acid (C18:2 *cis*) [179]. Similar studies should be done to assess how other fatty acids, and possibly combinations of various fatty acids, alter gene expression and protein levels.

It was possible that fatty acids were detrimental to the normal expression of *saeR* and *saeS* and could be responsible for the inhibition. Basal expression of *saeR* and *saeS* is driven by the constitutive *P3* promoter located upstream of *saeR* and we found that expression of this promoter was not affected by growth in the presence of oleic acid. In theory, fatty acids could be overstimulating SaeRS to an extent where the *P1* promoter would become active due to extremely high levels of P~SaeR. This would result in expression of SaeP and SaeQ, resulting in decreased SaeS activity. To overcome this potential negative-feedback loop, we replaced the low-affinity *P1* promoter of the *saePQRS* operon with a leaky $P_{xyl/tetO}$. Using either the wild type *P1* promoter or the $P_{xyl/tetO}$, oleic acid decreased activity of SaeRS independently of SaeP and SaeQ. This result suggests that fatty acids affect the kinase activity of SaeS rather than the phosphatase activity.

The USA300 and Newman allele of SaeS dictates the SaeS response to membrane-targeting moleucles such as SDS. Fatty acids (such as oleic acid) target and localize to the membrane alter it's structure and function [222]. We hypothesized that USA300 SaeS would be sensitive while Newman SaeS would not be, similar to their relationship with SDS [221]. Expression of *hla* using a P_{hla}-*lacZ* fusion indicated that fatty acid treatment did not impact expression of low-affinity targets of P~SaeR (Figure 4.4A). Similar to what was observed with SDS treatment [221], fatty acids decreased SaeRS activity in strain USA300 but increased activity in strain Newman (Figure 4.4B). This response appears regardless of strain background, as the introduction of the USA300 substitution into strain Newman significantly sensitizes SaeS to fatty acids. SaeRS activity in strain Newman was increased by the presence of oleic acid. Our data support that the USA300 allele of *saeS* is uniquely sensitive to fatty acid treatment. We predict that the consequence of the substitution mutation in strain Newman renders SaeS insensitive to potential protein structural changes that occur when membranes are damaged by either SDS or fatty acids.

To expand on this, we used chimeric versions of SaeS [219]. These constructs were comprised of the N-terminal domains of GraS, another intramembrane HK found in *S. aureus*. We found that, in contrast to wild type SaeRS, both the ND and TM chimeras of GraS/SaeS were not negatively impacted by fatty acid treatment. Instead, the activity of these constructs was induced by fatty acid treatment, like the wild-type strain Newman. We wanted to make sure that GraS was not sensitive to fatty acid treatment. It could be possible that the chimeric GraS is sensitive to fatty acid treatment under our growth conditions and the chimeras would be capable of transducing a GraS signal. This was not that case, as fatty acid treatment did not greatly impact P_{mprF}*::lux* activity under our growth conditions. Additionally, the cytoplasmic only portion of SaeS was slightly decreased in the presence of 31 μM oleic acid but significantly increased in 314μM. Our expression patterns for these constructs grown under our conditions is like previously reported data, which indicated that these constructs are constitutively on and not responsive to HNP-1 activation [219]. Thus, constitutively active SaeS constructs, whether it be the Newman allele of SaeS, the GraS/SaeS chimeras, or the cytoplasmic only portion of SaeS is insensitive to fatty acid treatment. GraS is an intramembrane HK and senses cell-wall targeting antimicrobial peptides, it is relatively surprising that it is not impacted by fatty acids the same a SaeS. It is possible that the conformation of GraS is better able to withstand fatty acid treatment compared to SaeS. It is also possible that the intramembrane HKs respond differently to different stimuli and under different environmental conditions. Further work examining how free fatty acids and other membrane-targeting molecules impact individual intramembrane HKs is needed. The combination of the GraS/SaeS chimera data and the cytoplasmic only portion of SaeS and their insensitivity to fatty acid treatment strongly suggests that the USA300 allele of SaeS is uniquely sensitive to fatty acids.

The results of this study and other studies strongly support a model whereby fatty acids inhibit SaeS at the site of the transmembrane domains and not the cytoplasmic portion of SaeS.

The presence of free fatty acids has been shown to impact transcription in other organisms [226-229], including *Listeria monocytogenes.* The response in *L. monocytogenes* includes regulatory targets of the maser regulatory protein PrfA [230]. Evidence has implicated free fatty acids in altering the expression of PrfA-dependent genes [230]. Recently, it was shown that free fatty acids are able to prevent activated PrfA from binding DNA [231]. This data suggests that fatty acids could prevent other regulatory proteins from binding DNA, such as SaeR. Our data, however, provide evidence that this is not the case for SaeRS, as replacement or removal of the transmembrane domains of SaeS rendered the system on. If free fatty acids interrupted P~SaeR from binding DNA it would occur downstream of changes to SaeS. It appears that free fatty acids can impact transcription of target genes by different mechanisms in different organisms.

Our data support a model where free fatty acids induce membrane stress and is sensed by SaeS at the membrane (Figure 4.7). This data also show that fatty acids can impact SaeRS activity at levels that do not hinder respiratory activity. For oleic acid, SaeRS activity is altered regardless of changes in respiration. It is unclear if respiratory activity itself is directly impacting SaeRS activity, or if they are independent events. We hypothesize that fatty acid-induced membrane stress, particularly due to unsaturated fatty acids like oleic acid (C18:1 *cis*) and linoleic acid (C18:2 *cis*) alters the confirmation of SaeS. Activation of the system by HNP-1 appeared to partially overcome inactivation by fatty acids. This, along with our chimera GraS/SaeS data, suggest fatty acids and HNP-1 affect SaeS in different manners. Our data indicate that this response is due in part to the transmembrane domains of SaeS as replacement of native SaeS transmembrane domains with

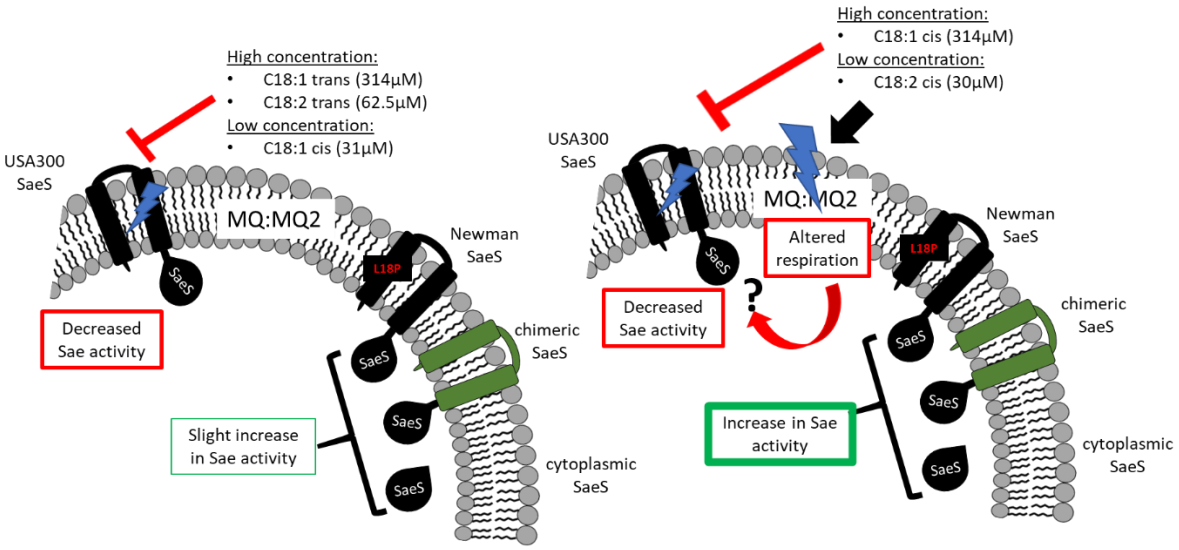
High concentration:
• C18:1 trans (314µM)
• C18:2 trans (62.5µM)
Low concentration:
• C18:1 cis (31µM)
USA300 SaeS
MQ:MQ2
Newman SaeS
L18P
chimeric SaeS
cytoplasmic SaeS
SaeS
Decreased Sae activity
Slight increase in Sae activity
High concentration:
• C18:1 cis (314µM)
Low concentration:
• C18:2 cis (30µM)
USA300 SaeS
MQ:MQ2
Altered respiration
Decreased Sae activity
?
Newman SaeS
L18P
chimeric SaeS
Increase in Sae activity
cytoplasmic SaeS
SaeS

Figure 4.7

Figure 4.7. Working model for how fatty acid impacts SaeRS activity. **(A)** In the presence of low concentrations of C18:1 cis (oleic acid) and high concentrations of C18:1 trans (elaidic acid), SaeRS activity in USA300 is decreased independent of effect on respiration. SaeRS activity in strain Newman and GraS/SaeS chimeras are slightly increased. **(B)** In the presence of high concentrations of C18:1 cis (oleic acid) and low concentrations of C18:2 cis (linoleic acid) and C18:2 trans (linoelaidic acid), SaeRS activity in USA300 and respiratory activity is decreased. SaeRS is strain Newman and GraS/SaeS chimera is significantly increased.

another HK desensitizes SaeS. Since GraS was dramatically altered by the presence of oleic acid under our growth conditions, it is interesting to consider that different intramembrane HKs sense membrane stress via different mechanisms or in different environmental conditions. Introduction of the USA300 allele into strain Newman was enough to sensitize the system to fatty acids. We speculate that this residue is essential for the conformational integrity of SaeS when stress at the membrane is sensed.

Material and methods

Bacterial strains, plasmids, and growth conditions. Bacterial strains and plasmids used in this study are listed in Table 1. *S. aureus* was grown in tryptic soy broth (TSB) or tryptic soy agar supplemented with chloramphenicol (5 or10 μg mL^{-1}), erythromycin (5 μg mL^{-1}), tetracycline (10 μg mL^{-1}), or kanamycin (250 μg mL^{-1}) when necessary. Media used for all experiments was TSB without glucose. Glucose was added to TSB at a final concentration of 14mM and was filter-sterilized using 0.22μm filter units. All experiments, except for fatty acid growth curves in Figure 4.8, were grown as follows unless otherwise noted. Cultures were grown at 37°C, shaking at 250RPM, at a 1:10 media to flask volume ratio at an initial optical density at 600 nm (OD600) of 0.1 in TSB. TSB was supplemented with lauric acid (Acros Organics), myristelaidc acid (Cayman Chemicals), palmitic acid (MP Biomedical), palmitoleic acid (Acros Organics), stearic acid (MP Biomedical), oleic acid (Alfa Aesar), elaidic acid (Acros Organics), linoleic acid (Acros Organics) and linoelaidic acid (Cayman Chemical) by adding fatty acid from stocks (dissolved in ethanol, methanol or chloroform) to 45 mL TSB in a 50 mL Falcon tube. The TSB with fatty acid was then vortexed vigorously prior to aliquoting to flasks. The fatty acid growth curves in Figure 4.8 were performed using a plate reader as previously described [160]. Briefly, overnight cultures were diluted to an OD600 of 0.01 in 200μl TSB supplemented with fatty acid in a 96-well plate. The

fatty acid was added to TSB as described above. The cultures were grown in a Spark 10M plate reader (Tecan Group) with orbital shaking at 37˚C and OD600 was read every 15 minutes.

Transposon mutants were obtained from BEI Resources and transduced via Φ-11 bacteriophage into AH1263 as previously described [204]. All bacterial plasmids were propagated in DH5α *Escherichia coli* and electroporated into *S. aureus* strain RN4220. Φ-11 bacteriophage was then used to transduce the plasmid into its recipient *S. aureus* strain. Primers were synthesized by Integrated DNA Technologies (Coralville, IA). Plasmids were purified using Wizard Plus SV Minipreps DNA purification (Promega Corporation, Madison, WI). Restriction and ligation enzymes were purchased from New England BioLabs (Beverly, MA), and DNA fragments were cleaned and purified using DNA Clean and Concentrator-5 kit (Zymo Research, Orange, CA).

CTC staining. Electron transport chain activity (respiratory activity) was determined using the *Bac*Light RedoxSensor CTC Vitality Kit (Molecular Probes, Invitrogen) [170] as previously described [222]. Bacteria were grown for 6 hrs in TSB supplemented with indicated fatty acid. Cultures were diluted to an OD_{600} = 0.1 in 650 μL PBS. One sample was diluted in 70% ethanol as a negative control. 65 μL of 50 mM CTC was added to each sample, except for a no stain control. The samples were then incubated in the dark at 37˚C for 30 minutes and analyzed using a Tecan Spark 10M plate reader (Excitation 485+/-20nm and Emission 645+/-40nm).

Construction of pJB1051 and pJB1054. The P_{coa}-*lacZ* from pJB1018 was digested and ligated into pCN34 and pCN36. pJB1018, pC34, and pCN36 were digested with EcoR1 and Sph1. The digested product from pJB1018 (the P_{coa}-*lacZ* fragment) was ligated into digest pCN34 and pCN36 and transformed in DC10b *E. coli* and plated on LB + ampicillin (100μg/mL) + x-gal (5-bromo-4-chloro-3-indolyl-β-D-galactopyranoside) (40μg/mL). Blue colonies were then confirmed via

digestion with EcoR1 and Sph1, resulting in pJB1051 and pJB1054. The plasmids were then moved into RN4220 via electroporation and plated on TSA + kanamycin (250ug/mL) for pJB1051 or TSA + tetracycline (5μg/mL) for pJB1054. Each plasmid was then moved into recipient strains via bacteriophage transduction and confirmed via digestion.

B-galactosidase assay. β-galactosidase activity was determined as previously described [189]. Briefly, one mL of bacterial culture was collected after six hours of growth. Cells were pelleted, resuspended in 1.2 mL Z-buffer (60 mM Na_2HPO_4, 40 mM NaH_2PO_4, 10 mM KCl, 1 mM $MgSO_4$, and 3.4 mL β-mercaptoethanol) and lysed using a FastPrep-24 5G homogenizer (MP Biomedicals), according to the manufacturer's recommended settings for *S. aureus* cells. β-galactosidase activity was determined by adding 140 μL of *ortho*-nitrophenyl-β-galactosidase (ONPG) (4 mg mL^{-1} [wt/vol]) to 700 μL of cell lysates and allowing reaction to turn slightly yellow at 37°C. The reaction was stopped with 200 μL of 1 M sodium bicarbonate and then absorbance was measured at 420 nm. The β-galactosidase activity was determined based on protein concentration using a Bradford assay with Bio-Rad protein concentration reagent and reported as Modified Miller Units (M.M.U.).

Construction of USA300 GraS/SaeS chimera strains. Bacteriophage Φ11 was used to transduce the integration plasmid pCL55 containing each GraS/SaeS constructs from the Newman strains into JLB331 recipient strain and plated on TSA + chloramphenicol (5 μg mL^{-1}). Colonies were re-struck on TSA + chloramphenicol (5 μg mL^{-1}) for lysogeny. Non-lysogenic colonies were then spotted on 0.5% rabbit blood agar plates to confirm the gain of alpha-hemolysin activity. Integration of each pCL55 construct into the lipase (*geh*) gene was confirmed using primers ZD66 and ZD67 specific for the 3`-end of the lipase gene.

Construction of ΔsaeRS, ΔsaeP, ΔsaeQ strains. In-frame deletion strains were created using pJB38 as previously described [232]. For deletion of *saeR* and saeS, upstream of *saeR* was amplified using primers JBKU132 and JBKU133 and downstream of *saeS* was amplified using primers JBKU131 and JBKU132 from the chromosome of AH1263. The PCR products were cleaned and digested with EcoR1 and Kpn1 (upstream fragment) and Knp1 and Sal1 (downstream fragment) and pJB38 was digested with EcoR1 and Sal1. The three fragments were ligated and transformed into DH5α *E. coli*, resulting in pJB1048.

To delete *saeP*, upstream of *saeP* was amplified using primers CKN29 and CNK30 and downstream of *saeP* was amplified using CNK31 and CNK32. The PCR products were cleaned and digested with EcoR1 and Kpn1 (upstream fragment) and Kpn1 and Sal1 (downstream fragment). pJB38 was digested with EcoR1 and Sal1. The three fragments were ligated and transformed in DH5α *E. coli*, resulting in pCK20.

To delete *saeQ*, upstream of *saeQ* gene was amplified using primers CKN34 and CNK35 and downstream of *saeP* gene was amplified using CNK36 and CNK37. The PCR products were cleaned and digested with EcoR1 and Kpn1 (upstream fragment) and Kpn1 and Sal1 (downstream fragment). pJB38 was digested with EcoR1 and Sal1. The three fragments were ligated and transformed in DH5α *E. coli*, resulting in pCK21. Each plasmid was electroporated into *S. aureus* strain RN4220 and subsequently moved into *S. aureus* strain AH1263 via bacteriophage transduction. Deletion of *saeRS*, *saeP*, and *saeQ* from the chromosome of *S. aureus* were confirmed via sequencing.

Construction of $P1_{xyl/tetO}$-sae and $P1_{xyl/tetO}$-sae ΔsaePQ strains. To generate a strain that had an inducible tetracycline promoter in front of the P3 promoter but was also missing *saePQ*, the native

P1 promoter or *sae* was removed using allelic exchange of pMP1. To make pMP1, primers JBKU83 and JBKU84 were used to amplify the upstream fragment and JBKU85 and JBKU86 were used to amplify the downstream fragment. The upstream fragment was digested with EcoR1 and BamHI, the downstream fragment was digested with BamH1 and Sal1, and the vector (pCL10) was digested with EcoR1 and Sal1. The three digests were ligated and transformed into DH5α and the plasmid was confirmed via sequencing, resulting in pMP1. The $P_{xyl/tet}$ promoter was amplified using primers MP1 and MP2 from pJB38. These PCR products were digested, ligated into pMP1, and transformed into DH5α. The plasmid was confirmed via sequencing, resulting in pMP2. pMP2 was then electroporated into RN4220 *S. aureus* and transduced into AH1263. Allelic exchange was then performed according to protocol, resulting in strain JLB155.

Next, *saeP* and *saeQ* were deleted from the chromosome of strain JLB155. First made a plasmid that would delete *saePQ* up to the *P3* promoter (pMP5) in the background of an allelic exchange plasmid (pCL10) and inserted that into a strain that contained the inducible tetracycline promoter in front of the *sae P1* promoter. To generate pMP5, primers MP19 and MP20 (up-stream portion- used pMP2 as the template DNA) and MP21 and MP22 (down-stream portion- used AH1263 chromosomal DNA as the template). The up-stream PCR product was digested with EcoRI and KpnI. The down-stream PCR product was digested with KpnI and SalI. The background plasmid pCL10 was digested with EcoRI and SalI. These digested products were then ligated. The ligated plasmid was transformed into DH5α and confirmed via sequencing, resulting in pMP5. The pMP5 plasmid was then electroporated into RN4220 and transduced into JLB155. pMP5 (the *saePQ* deletion plasmid) was exchanged into the chromosome of JLB155 according to protocol [232]. This generated JLB304, which has an inducible tetracycline promoter in front of the SaeP3 promoter but *saePQ* were removed from the chromosome.

Luciferase activity assay. Luciferase activity for P_{mprF} was determined using empty vector pGYLux and pGYLux::*mprF* similarly as previously described [141]. AH1263 and JLB157 (*mprF*::Tn) carrying pGYLux::*mprF* were grown for 6 hours in 12.5 mL TSB (125 mL flask) with and without 31μM oleic acid for 6 hours. 200μL of each culture was added to white 96-well flat bottom plate in quadruplicates. 20μL of decanal solution (60% H_2O, 40% ethanol, 0.1% decanal) was added to each well and luminescence was measuring using a Tecan 10M Spark plate reader. Luminescence was normalized to OD600.

GFP reporter assay. To determine P_{coa} activity using pYJ335 [219], Newman *Δsae* strains harboring integrated pCL55 constructs and pYJ335 were grown in 12.5 mL TSB (125 mL flask) supplemented with 31μM or 314 μM oleic acid for 6 hours. 100 μL of culture was added to a black 96-well flat bottom plate (in triplicate) and fluorescence was determined using a Tecan 10M Spark plate reader (excitation 485 nm +/- 20 nm, emission 538 nm +/- 20 nm). The fluorescence value of a TSB media control was subtracted from the fluorescence value of each well and then normalized to the OD600 from each culture.

Table 4.1

Strain or plasmid	Relevant characteristics[a]	Reference
Strain name		
RN4220	Restriction-deficient *S. aureus* strain	[209]
AH1263	*S. aureus* wild-type USA300	[86]
CYL5876	*S. aureus* wild-type Newman	[233]
CYL11481	*S. aureus* Newman SaeS^{P18L}	[234]
JLB29	AH1263 SaeS^{L18P}	[148]
JLB331	AH1263 Δ*saeRS*	This study
JLB137	AH1263 Δ*saeQ*	This study
JLB140	AH1263 Δ*saeP*	This study
JLB155	AH1263 P$_{xyl/tetO}$-*sae*	This study
JLB304	AH1263 P$_{xyl/tetO}$-*sae* Δ*saePQ*	This study
KUTB1	Newman Δ*sae* pCL55-SaeRS WT	[219]
KUTB2	Newman Δ*sae* pCL55-SaeRS saeS ND	[219]
KUTB3	Newman Δ*sae* pCL55-SaeRS saeS^{cyto}	[219]
KUTB4	Newman Δ*sae* pCL55-SaeRS saeS TM	[219]
JLB341	JLB331 pCL55-SaeRS SaeS TM	This study
JLB342	JLB331 pCL55-SaeRS SaeS ND	This study
JLB343	JLB331 pCL55-SaeRS SaeS^{cyto}	This study
JLB320	AH1263 *graR*::erm	This study
CFS18	AH2216 - pEPSA5-SOD(WT)saeS-T7	[235]
CFS41	AH2216 - pEPSA5-SOD(C50S/C56S)saeS-T7	[235]

Strain or plasmid	Relevant characteristics[a]	Reference
JLB15	AH1263 *saeR*::ΦNΣ	[148]
JLB17	AH1263 *saeS*::ΦNΣ	[148]
NE481	Source of *graR* transposon mutation	[210]
Plasmids		
pCL10	Temp-sensitive Amp^R, Cm^R, Tet^R exchange vector	[236]
pJB38	Temp-sensitive Amp^R, Cm^R exchange vector	[237]
pMP1	Plasmid containing upstream and downstream P1 *sae* operon (pCL10)	This study
pMP2	pMP1 containing $P_{xyl\text{-}tet}$ promoter.	This study
pMP5	Deletion plasmid for *saePQ* (pCL10)	This study
pCK20	Deletion plasmid for *saeP* (pJB38)	This study
pCK21	Deletion plasmid for *saeQ* (pJB38)	This study
pJB1018	P_{coa}-*lacZ* reporter, Cm^R	[148]
pJB1051	P_{coa}-*lacZ* reporter, Kan^R	This study
pJB1054	P_{coa}-*lacZ* reporter, Tet^R	This study
pCL55-SaeRS	pCL55 with USA300 SaeR and SaeS	[219]
pQL147	pCL55-SaeRS TM chimera	[219]
pQL91	pCL55-SaeRS ND chimera	[219]
pQL20	pCL55-SaeRS cyto	[219]
pCN34	Kan^R vector plasmid to make pJB1051	[238]
pCN36	Tet^L vector plasmid to make pJB1054	[238]

Table 4.1. Bacterial strains and plasmids used in this study. [a] Antibiotic resistance abbreviations used: amp^R, ampicillin resistance; erm^R, erythromycin resistance; tet^L or tet^R, tetracycline resistance; cm^r, chloramphenicol resistance.

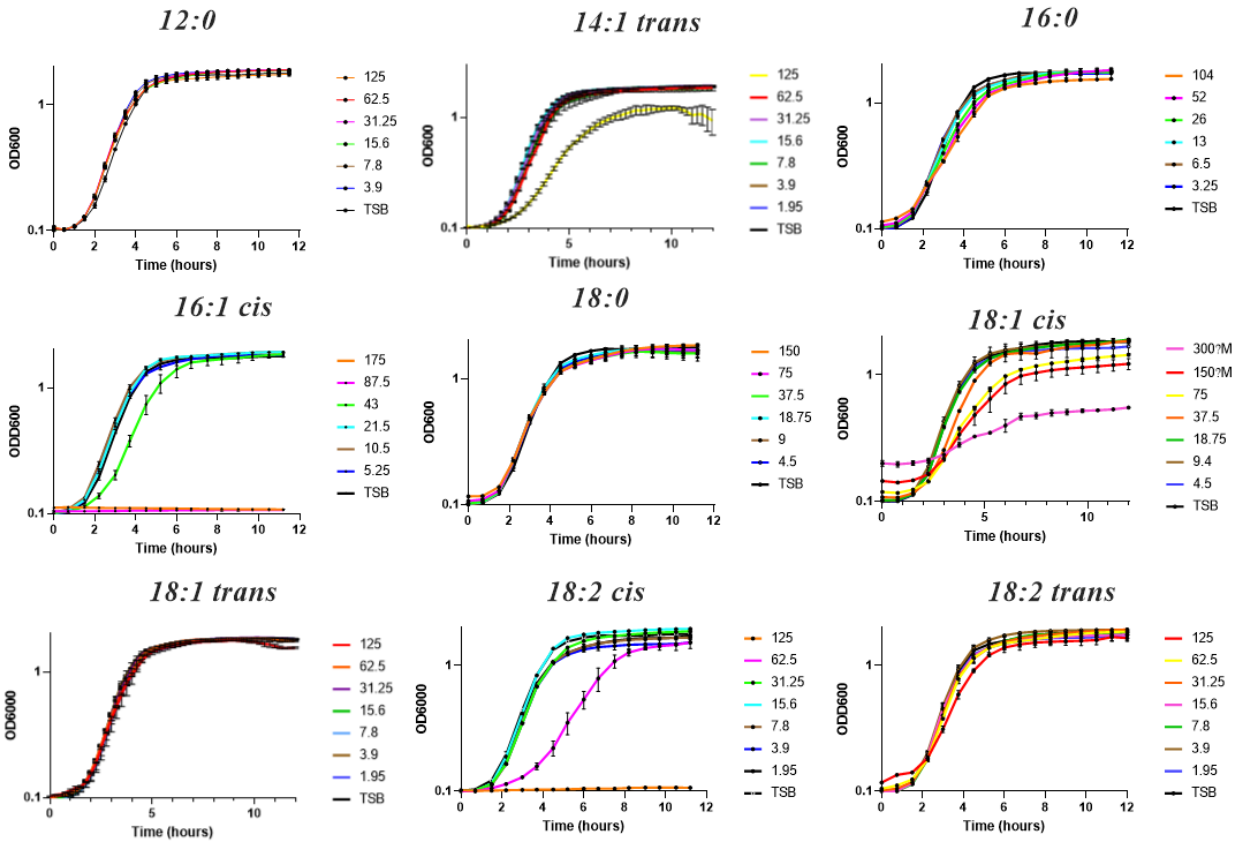
12:0
OD600
Time (hours)
125
62.5
31.25
15.6
7.8
3.9
TSB
14:1 trans
OD600
Time (hours)
125
62.5
31.25
15.6
7.8
3.9
1.95
TSB
16:0
OD600
Time (hours)
104
52
26
13
6.5
3.25
TSB
16:1 cis
OD600
Time (hours)
175
87.5
43
21.5
10.5
5.25
TSB
18:0
OD600
Time (hours)
150
75
37.5
18.75
9
4.5
TSB
18:1 cis
OD600
Time (hours)
300?M
150?M
75
37.5
18.75
9.4
4.5
TSB
18:1 trans
OD6000
Time (hours)
125
62.5
31.25
15.6
7.8
3.9
1.95
TSB
18:2 cis
OD6000
Time (hours)
125
62.5
31.25
15.6
7.8
3.9
1.95
TSB
18:2 trans
OD600
Time (hours)
125
62.5
31.25
15.6
7.8
3.9
1.95
TSB

Figure 4.8

Figure 4.8. Growth of *S. aureus* strain AH1263 in TSB supplemented with the indicated fatty acid (μM). Data are representative of multiple experiments (n=4).

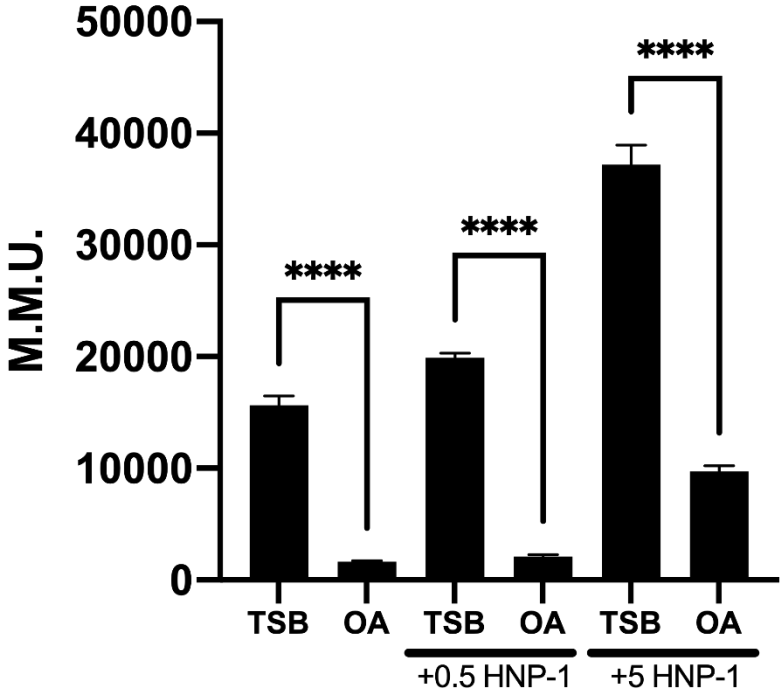
50000
40000
30000
20000
10000
0
M.M.U.
****
****
****
TSB
OA
TSB
OA
TSB
OA
+0.5 HNP-1
+5 HNP-1

Figure 4.9

Figure 4.9. P_{coa}-*lacZ* was determined for wild type USA300 *S. aureus* when grown in TSB to exponential phase (six hours) supplemented with human neutrophil peptide 1 (HNP-1 in μg/mL) and oleic acid (OA in μM). Data are presented as Modified Miller Units (M.M.U.) and representative of multiple experiments (n=3). Data were analyzed using one-way Ordinary ANOVA (Prism). ****$p<0.0001$.

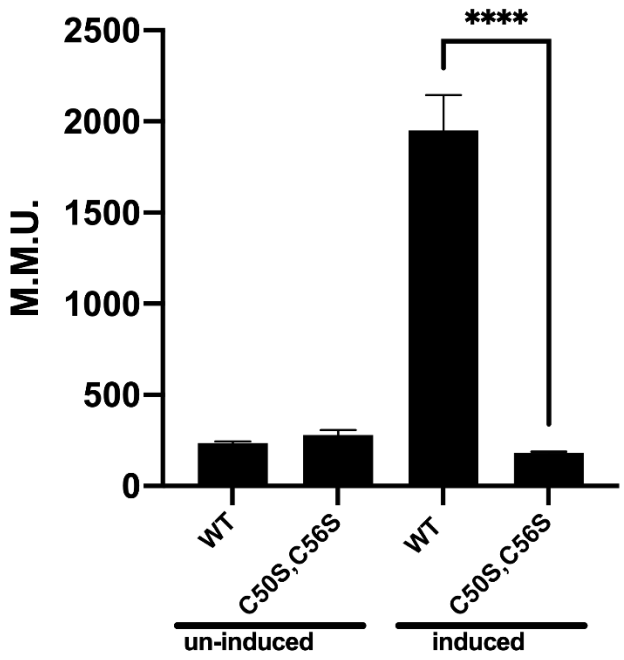
****
2500
2000
1500
1000
500
0
M.M.U.
WT
C50S,C56S
WT
C50S,C56S
un-induced
induced

Figure 4.10

Figure 4.10. P_{coa}-*lacZ* was determined in *saeS*::Tn mutant *S. aureus* when either wild type (WT) *saeS* or the cysteine residues in the second transmembrane domain of *saeS* (C50S, C56S) was induced via xylose (6mM). Data are representative of multiple experiments (n=3). Data are presented as Modified Miller Units (M.M.U.) and analyzed via one-way Ordinary ANOVA (Prism). ****$p<0.0001$.

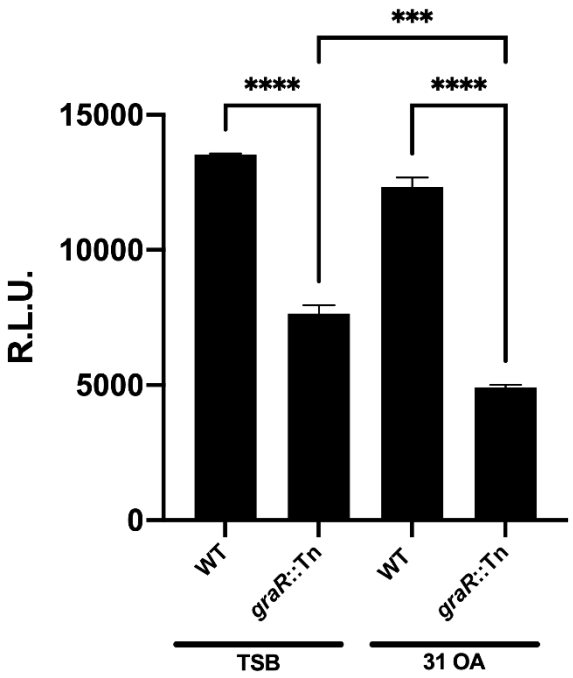

Figure 4.11

Figure 4.11. P_{mprF}-*lux* was determined in *graR*::Tn mutant *S. aureus* grown in TSB supplemented with oleic acid (μM) to exponential phase (six hours). Data is representative of multiple experiments (n=4). Data are presented as relative luminescence units (R.L.U.) and was normalized to media blank and OD600. Data was analyzed via one-way Ordinary ANOVA (Prism). ***p<0.0005, ****p<0.0001.

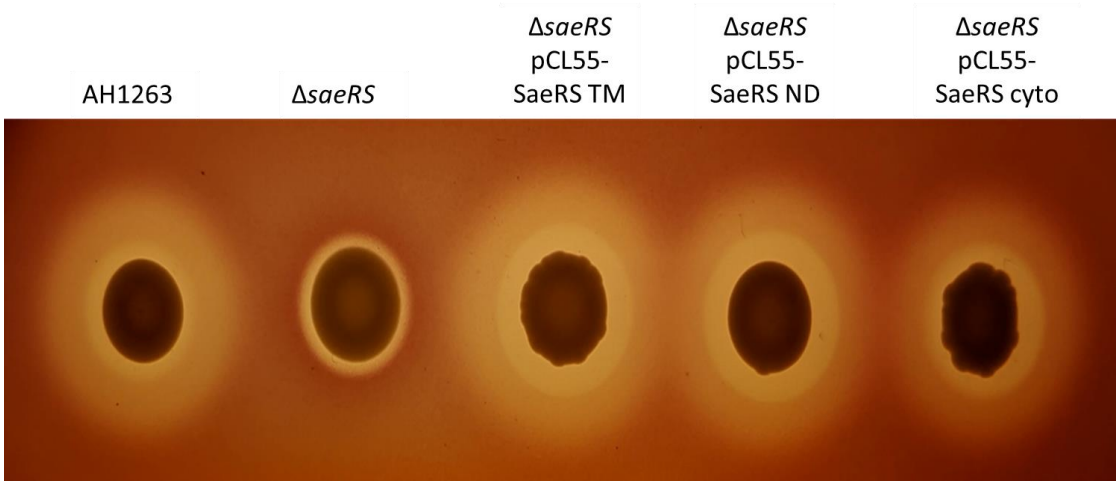
AH1263
ΔsaeRS
ΔsaeRS pCL55-SaeRS TM
ΔsaeRS pCL55-SaeRS ND
ΔsaeRS pCL55-SaeRS cyto

Figure 4.12

Figure 4.12. GraS/SaeS and SaeRS cytoplasmic only domain restores hemolysis of *saeR*::Tn mutant. Wild-type AH1263, *saeR*::Tn, *saeR*::Tn pCL55-SaeRS TM, ND, and cytoplasmic were grown on rabbit's blood (0.5%) agar plate.

Concluding Remarks

Staphylococcus aureus has been studied intensly for years. Nonetheless, the understanding of some of the basic mechanism this bacterium uses to become a successful pathogen remains unresolved. These basic mechanisms involve how the bacterium acquires nutrients and building blocks from the host and how it can sense its environment and adjust its response accordingly. The quintessential building blocks for cellular organisms are phospholipids and the fatty acids that comprise them. These phospholipids form the phospholipid membrane, demarcating the inside from the outside of the cell. The phospholipid membrane also houses machinery for cellular processes. The electron transport chain of bacteria, which is located within the membrane, is at the mercy of membrane integrity and homeostasis. Bacterial sensors, such as histidine kinases (HK), are also embedded in the phospholipid membrane and their activity is impacted by chemical agents that target the membrane.

The importance of the phospholipid membrane in cellular life obviously presents the synthesis of the membrane as a intriguing therapeutic target for bacterial pathogens. Bacteria utilize the fatty acid synthesis type II (FASII) system to synthesize fatty acids, the building blocks of phospholipids. The FASII system differs from the mammalian mechanism for fatty acid synthesis, suggesting that small molecules can be developed to specifically target and inhibit bacterial FASII. Indeed, there are numerous bacterial FASII inhibitors identified. Intense debate over whether these inhibitors are effective antimicrobials against Gram-positive pathogens has been hashed out in the literature. After the identification of FASII inhibitors, many Gram-positive pathogens have been found to overcome this inhibition via the utilization of exogenous fatty acids (exoFAs). In 2009, Brinster et al published that FASII inhibitors were ineffective at inhibiting Gram-positive pathogen growth (including *S. aureus*) when free fatty acids or human serum were added to the growth

media [239]. In 2010, a direct response to this publication by Balemans *et al.* argued that FASII is essential in *S. aureus* and is valid therapeutic target due to different mechanisms of fatty acid synthesis in different Gram-positive pathogens [62]. In Streptococci, FASII is repressed in the presence of free fatty acids while in *S. aurues* free fatty acids do not repress FASII [164]. This results in streptococci being able to overcome FASII inhibition while *S. aureus* is not. In contrast to Streptococci, *S. aureus* primarily inserts exoFAs into only one position (*sn*-1) of the phosopholipid moleucle [156]. This prevents *S. aureus* from solely relying on exoFAs for phospholipid synthesis . Despite these *in vitro* findings, exoFAs have been suggested to induce the emergence of FASII-resistant clones [67, 68]. Clearly, a more thorough understanding of how bacteria utilize exoFAs, their impact on phospholipid synthesis and homeostasis, and how they impact bacterial virulence and physiology is needed. The role that the exoFA utilization system (the fatty acid kinase (Fak) system) plays in *S. aureus* is limited to its sole role in acquiring exoFAs for phospholipid synthesis. How the inactivation of the Fak system changes the total composition and function of the membrane and systems that are reliant on the membrane, would greatly enhance the understanding and the efficacy of FASII inhibition as a strategic therapeutic target.

S. aureus commonly interacts with free fatty acids when colonizing and infecting host skin tissues. The data in this dissertation has helped move the research field forward by identifying previously unknown roles for the Fak system in maintaining metabolic and phospholipid membrane homeostasis. Further, it has created a better understanding of how fatty acids impact the activity of SaeRS and virulence factor production. The results from this dissertation also creates more questions: how do fatty acids and the Fak system impact the activity of the electron transport chain in *S. aureus*? Where do unutilized free fatty acids localize within the cell? Do free fatty acids interfere with the structural integrity of SaeS and, thus, impact its activity?

The Fak system includes the fatty acid kinase, FakA, and the fatty acid-binding proteins FakB1 and FakB2. Free fatty acids in the environment are thought to passively diffuse into the phospholipid membrane where FakB1 (specific for saturated fatty acids) or FakB2 (specific for unsaturated fatty acids) removes them from the membrane. This allows for FakA to phosphorylate the free fatty acid, which can then be utilized as a substrate for phospholipid synthesis. Aside from phospholipid synthesis, the Fak system impacts virulence factor production through the two-component system SaeRS. Free fatty acids accumulate in the cell in a *fakA* mutant, which decreases the activity of SaeRS and thus, a decrease in secreted virulence factors. A clear mechanism for this Fak-dependent and fatty acid-dependent impact on virulence factor production is unknown. My research project sought to answer the following outstanding questions in the *S. aureus* field: 1) how exoFAs and FakA impact membrane composition and membrane-related properties, 2) how fatty acid metabolism and FakA impact cellular metabolism, and 3) how fatty acids contribute to SaeRS activity suppression.

Connection between exogenous fatty acid metabolism and central metabolism.

The results of these studies identified that genetic inactivation of the fatty acid kinase *fakA* alters several metabolic pathwyas in *S. aureus* and results in longer phospholipids and increases the abundance of SCFA in the cell. A mechanistic explanation for this phenomenon is still unknown. During a recent study, an RNA helicase CshA, a part of the RNA degradosome responsible for the bacterial response to cold shock, provided evidence for a relationship between membrane changes and metabolic homeostasis. One mRNA target for CshA is the transcript of pyruvate dehydrogenase, *pdh*. In wild-type *S. aureus* cells, CshA activity is increased upon cold-shock (25˚C) resulting in degradation of *pdh* transcript [240]. This results in decreased flow of carbon through acetyl-CoA and acetate and decreases the ratio of SCFA:BCFA in phospholipids as

compared to normal conditions. We hypothesize that the more rigid membranes observed in the *fakA* mutant resembles how bacterial membranes are altered in a *cshA* mutant (i.e. more SCFA containing phospholipids). One possible explanation could be decreased activity of CshA in the *fakA* mutant, increasing transcript levels of *pdh*, and increasing the pool of acetyl-CoA that could be used for SCFA biosynthesis. Studies addressing global transcriptional and proteomic analysis in the absence of *fakA* is needed to better understand how changes in membrane composition affect cellular processes.

An additional hypothesis for how FakA and metabolism are connected is that fatty acid accumulation in the *fakA* mutant alters membrane function. We discovered that inactivating the Fak system resulted in a glucose and aeration-dependent growth advantage as compared to wild type. This was due to an increase in acetate production and consumption as compared to wild type. We also identified global changes in the metabolic status of the *fakA* mutant cells including altered urea cycle activity and amino acid consumption. An increase in respiratory activity in the *fakA* mutant compared to that of wild type was also observed, which results in a more oxidized cellular environment. It is intriguing to speculate where and how the free fatty acids accumulate within the cell. The free fatty acids may accumulate within the phospholipid membrane and act in a similar manner as surfactant molecules (such as SDS). This could also impact many other cellular processes since the electron transport chain (ETC) and membrane bound HK proteins, in addition to many other cellular proteins and processes, are dependent on the maintenance of integrity, structure, and charge in and across the membrane. The activity of the ETC was increased in the *fakA* mutant compared to wild type. The balance of NAD/NADH and NADP/NADPH were also altered. This mutant also grew better and produced and consumed acetate at a faster rate than wild type. Since these observations were oxygen and glucose-dependent, we hypothesize that free fatty

acids accumulate within the *fakA* mutant, leading to membrane structural and functional changes that culminate in metabolic changes. Altered ETC activity could result in altered ratios of NAD+/NADH and NADP+/NADPH. These altered ratios would ultimately impact the rate at which is glucose is consumed and acetate was produced and then re-consumed. An additional hypothesis would be that free fatty acids accumulated within the *fakA* mutant interact and inhibit protein function within the cell. For example unsaturated fatty acids like linoleic acid (C18:2 *cis*) and oleic acid (C18:1 *cis*) acid alter enzymatic activity of citrate synthase from pig heart and glucose-6-phoshpate of yeast, respectively [241]. Fatty acids could affect protein activity through allosteric interactions [242] or through disrupting substrate-enzyme interactions. Further studies are needed to clearly define how the Fak system and free fatty acids impact metabolism.

Fatty acids as signals for SaeRS.

We found that free fatty acids can induce transcriptional changes at concentrations that were below those needed for phospholipid synthesis. Fatty acids, in particularly oleic and linoleic acid, are found in abundance in human serum and on the skin, indicating that they serve as a host-environment signal. Growth in the presence of 31 μM oleic acid did not result in the FA being incorporated into phospholipids while it did induce changes in the activation of the two-component system SaeRS. Additionally, the accumulation of free fatty acids in a *fakA* mutant are responsible for inactivation of SaeRS [149]. Other membrane targeting molecules, such as β-lactam antibiotics [224] or SDS [221], also alter SaeRS activity in a SaeS allele-dependent manner. We predict that that free fatty acids impact SaeRS activity in a similar manner as SDS. USA300 SaeS was negatively impact and Newman SaeS (L18P) was positively impacted, similar to the previous finding with SDS. Complete removal of the transmembrane domains of SaeS desensitized SaeRS

to fatty acid treatment, regardless of strain background. These results all indicate that the membrane spanning domains of SaeS are responsible for the sensitivity of SaeS to fatty acids.

We hypothesize that SaeS of *S. aureus* is being affected at the membrane by fatty acids due to the fatty acid's impact on membrane structure. This could possibly be due to the instability of SaeS in the membrane when treated with free fatty acids, particularly at concentrations when the fatty acid is not used for phospholipid synthesis. The *S. aureus* genome encodes four intramembrane HKs. In general, all of them are responsive to membrane stress [139, 140, 243]. One could hypothesize that sensing signals at the membrane and transmembrane domains of the intramembrane HKs is a common mechanism for all these systems. Our data suggests that this may not be the case, as GraRS activity did not appear to be affected by fatty acid treatment under our growth conditions tested. We hypothesize that compared to other intramembrane HK, SaeS is uniquely sensitive to fatty acid treatment. It is also more sensitive to oleic acid than other fatty acids tested. HKs form homodimers and is required for activity of the HK. It is possible that altered membrane function and composition results in a destabilization of SaeS homodimers in the membrane, resulting in decreased activity. It is also possible that different intramembrane HKs have varying levels of stability in phospholipid membranes of different compositions. Studies trying to decipher the differences and similarities between these HKs and their unique responses requires further study and could help illuminate a mechanism for signal transduction for these unique signaling proteins. Employing a biophysical approach would greatly increase our understanding of how these fatty acids impact phospholipid membrane structure and function. For example, the increased capacity to utilize biomimetic phospholipid bilayers and the ability of x-ray and neutron reflectometry to interrogate phospholipid membrane structure. These powerful tools would shed light on exactly how free fatty acids (like unsaturated fatty acids), staphyloxanthin in *S. aureus*, cholesterol in other

bacteria, and any other membrane associated molecules, alter the characteristics of the membrane. It is likely that fatty acids are observed as a stress to bacteria either in the cytoplasm or due to changes to the phospholipid membrane. Previous work by our lab showed that the stress-associated sigma factor *sigB* was necessary for resistance to growth in the presence of fatty acids [160].

S. aureus commonly interacts with free fatty acids when colonizing and infection host skin tissues, creating a need for better understanding the complex interactions of the bacterium with these molecules. While studies have interrogated the global transcriptional response to fatty acids has been done, my work in the Bose lab has helped move the research field forward by identifying previously unknown roles for the Fak system in maintaining metabolic and phospholipid membrane homeostasis. My work has also created a better understanding of how fatty acids impact the activity of SaeRS and virulence production. Despite the advances made from these studies, there are still many questions that remain in the study of fatty acids and *S. aureus*. Some of these outstanding questions include: how do fatty acids and the Fak system impact the activity of the electron transport chain in *S. aureus*? Where do unutilized free fatty acids localize within the cell? Do free fatty acids interfere with the structural integrity of SaeS and, thus, impact its activity? The results from my studies in the Bose lab have laid a foundation for the assessment of these questions that future work will help uncover.

Literature Cited

1. Ogston, A., *"On Abscesses".* Clinical Infectious Diseases, 1984. **6**(1): p. 122-128.
2. Lowy, F.D., *Staphylococcus aureus Infections.* New England Journal of Medicine, 1998. **339**(8): p. 520-532.
3. Fleming, A., *Penicillin.* BMJ, 1941. **2**(4210): p. 386-386.
4. Wertheim, H.F., et al., *The role of nasal carriage in Staphylococcus aureus infections.* Lancet Infect Dis, 2005. **5**(12): p. 751-62.
5. David, M.Z. and R.S. Daum, *Community-associated methicillin-resistant Staphylococcus aureus: epidemiology and clinical consequences of an emerging epidemic.* Clin Microbiol Rev, 2010. **23**(3): p. 616-87.
6. Lee, B.Y., et al., *The economic burden of community-associated methicillin-resistant Staphylococcus aureus (CA-MRSA).* Clin Microbiol Infect, 2013. **19**(6): p. 528-36.
7. Ray, G.T., J.A. Suaya, and R. Baxter, *Microbiology of skin and soft tissue infections in the age of community-acquired methicillin-resistant Staphylococcus aureus.* Diagnostic Microbiology and Infectious Disease, 2013. **76**(1): p. 24-30.
8. Otto, M., *Community-associated MRSA: What makes them special?* International Journal of Medical Microbiology, 2013. **303**(6-7): p. 324-330.
9. Knox, J., A.C. Uhlemann, and F.D. Lowy, *Staphylococcus aureus infections: transmission within households and the community.* Trends Microbiol, 2015. **23**(7): p. 437-44.
10. Pallin, D.J., et al., *Increased US emergency department visits for skin and soft tissue infections, and changes in antibiotic choices, during the emergence of community-associated methicillin-resistant Staphylococcus aureus.* Ann Emerg Med, 2008. **51**(3): p. 291-8.
11. Moran, G.J., et al., *Methicillin-Resistant S. aureus Infections among Patients in the Emergency Department.* New England Journal of Medicine, 2006. **355**(7): p. 666-674.
12. Frazee, B.W., et al., *High Prevalence of Methicillin-Resistant Staphylococcus aureus in Emergency Department Skin and Soft Tissue Infections.* Annals of Emergency Medicine, 2005. **45**(3): p. 311-320.
13. Panton, P.N. and F.C.O. Valentine, *Staphylococcal toxin.* Lancet, 1932. **1**: p. 506-508.
14. Peschel, A. and M. Otto, *Phenol-soluble modulins and staphylococcal infection.* Nature Reviews Microbiology, 2013. **11**(10): p. 667-673.
15. Seidl, K., et al., *Effect of a glucose impulse on the CcpA regulon in Staphylococcus aureus.* BMC Microbiol, 2009. **9**: p. 95.
16. Rose, I.A., et al., *Enzymatic phosphorylation of acetate.* J Biol Chem, 1954. **211**(2): p. 737-56.
17. Brown, T.D., M.C. Jones-Mortimer, and H.L. Kornberg, *The enzymic interconversion of acetate and acetyl-coenzyme A in Escherichia coli.* J Gen Microbiol, 1977. **102**(2): p. 327-36.
18. Richardson, A.R., S.J. Libby, and F.C. Fang, *A nitric oxide-inducible lactate dehydrogenase enables Staphylococcus aureus to resist innate immunity.* Science, 2008. **319**(5870): p. 1672-6.

19. Ferreira, M.T., et al., *Effect of oxygen on glucose metabolism: utilization of lactate in Staphylococcus aureus as revealed by in vivo NMR studies.* PLoS One, 2013. **8**(3): p. e58277.
20. Starai, V.J. and J.C. Escalante-Semerena, *Acetyl-coenzyme A synthetase (AMP forming).* Cell Mol Life Sci, 2004. **61**(16): p. 2020-30.
21. Wolfe, A.J., *The acetate switch.* Microbiol Mol Biol Rev, 2005. **69**(1): p. 12-50.
22. Schurig-Briccio, L.A., et al., *Characterization of the type 2 NADH:menaquinone oxidoreductases from Staphylococcus aureus and the bactericidal action of phenothiazines.* 2014. **1837**(7): p. 954-963.
23. Kerscher, S., et al., *The Three Families of Respiratory NADH Dehydrogenases*. Springer Berlin Heidelberg. p. 185-222.
24. Heikal, A., et al., *Structure of the bacterial type II NADH dehydrogenase: a monotopic membrane protein with an essential role in energy generation.* 2014. **91**(5): p. 950-964.
25. Sellamuthu, S., et al., *Type-II NADH Dehydrogenase (NDH-2): a promising therapeutic target for antitubercular and antibacterial drug discovery.* Expert Opin Ther Targets, 2017. **21**(6): p. 559-570.
26. Schurig-Briccio, L.A., et al., *Role of respiratory NADH oxidation in the regulation of Staphylococcus aureus virulence.* EMBO Rep, 2020: p. e45832.
27. Hammer, N.D., et al., *Two Heme-Dependent Terminal Oxidases Power Staphylococcus aureus Organ-Specific Colonization of the Vertebrate Host.* mBio, 2013. **4**(4): p. e00241-13-e00241.
28. Schlag, S., et al., *Characterization of the oxygen-responsive NreABC regulon of Staphylococcus aureus.* J Bacteriol, 2008. **190**(23): p. 7847-58.
29. Richardson, A.R., P.M. Dunman, and F.C. Fang, *The nitrosative stress response of Staphylococcus aureus is required for resistance to innate immunity.* Mol Microbiol, 2006. **61**(4): p. 927-39.
30. Machado, H., et al., *A defined minimal medium for systems analyses of Staphylococcus aureus reveals strain-specific metabolic requirements.* Appl Environ Microbiol, 2019.
31. Nuxoll, A.S., et al., *CcpA regulates arginine biosynthesis in Staphylococcus aureus through repression of proline catabolism.* PLoS Pathog, 2012. **8**(11): p. e1003033.
32. Richardson, A.R., G.A. Somerville, and A.L. Sonenshein, *Regulating the Intersection of Metabolism and Pathogenesis in Gram-positive Bacteria.* Microbiol Spectr, 2015. **3**(3).
33. Pohl, K., et al., *CodY in Staphylococcus aureus: a regulatory link between metabolism and virulence gene expression.* J Bacteriol, 2009. **191**(9): p. 2953-63.
34. Goerke, B. and J. Stulke, *Carbon catabolite repression in bacteria: many ways to make the most out of nutrients.* Nature Reviews Microbiology, 2008. **6**(8): p. 613-624.
35. Sonenshein, A.L., *Control of key metabolic intersections in Bacillus subtilis.* Nat Rev Microbiol, 2007. **5**(12): p. 917-27.
36. Deutscher, J., et al., *Protein kinase-dependent HPr/CcpA interaction links glycolytic activity to carbon catabolite repression in gram-positive bacteria.* Mol Microbiol, 1995. **15**(6): p. 1049-53.
37. Deutscher, J., et al., *P-Ser-HPr--a link between carbon metabolism and the virulence of some pathogenic bacteria.* Biochim Biophys Acta, 2005. **1754**(1-2): p. 118-25.
38. Sadykov, M.R., et al., *CcpA coordinates central metabolism and biofilm formation in Staphylococcus epidermidis.* Microbiology, 2011. **157**(Pt 12): p. 3458-68.

39. Lopez, J.M. and B. Thoms, *Role of sugar uptake and metabolic intermediates on catabolite repression in Bacillus subtilis.* J Bacteriol, 1977. **129**(1): p. 217-24.
40. Nuxoll, A.S., et al., *CcpA Regulates Arginine Biosynthesis in Staphylococcus aureus through Repression of Proline Catabolism.* Plos Pathogens, 2012. **8**(11).
41. Halsey, C.R., et al., *Amino Acid Catabolism in Staphylococcus aureus and the Function of Carbon Catabolite Repression.* MBio, 2017. **8**(1).
42. Seidl, K., et al., *Staphylococcus aureus CcpA affects virulence determinant production and antibiotic resistance.* Antimicrob Agents Chemother, 2006. **50**(4): p. 1183-94.
43. Ratnayake-Lecamwasam, M., et al., *Bacillus subtilis CodY represses early-stationary-phase genes by sensing GTP levels.* Genes Dev, 2001. **15**(9): p. 1093-103.
44. Brinsmade, S.R., et al., *Regulation of CodY activity through modulation of intracellular branched-chain amino acid pools.* J Bacteriol, 2010. **192**(24): p. 6357-68.
45. Brinsmade, S.R., *CodY, a master integrator of metabolism and virulence in Gram-positive bacteria.* Curr Genet, 2017. **63**(3): p. 417-425.
46. Roux, A., et al., *CodY-mediated regulation of the Staphylococcus aureus Agr system integrates nutritional and population density signals.* J Bacteriol, 2014. **196**(6): p. 1184-96.
47. Montgomery, C.P., et al., *CodY deletion enhances in vivo virulence of community-associated methicillin-resistant Staphylococcus aureus clone USA300.* Infect Immun, 2012. **80**(7): p. 2382-9.
48. Majerczyk, C.D., et al., *Staphylococcus aureus CodY negatively regulates virulence gene expression.* J Bacteriol, 2008. **190**(7): p. 2257-65.
49. Majerczyk, C.D., et al., *Direct targets of CodY in Staphylococcus aureus.* J Bacteriol, 2010. **192**(11): p. 2861-77.
50. Sun, F., et al., *AirSR, a [2Fe-2S] cluster-containing two-component system, mediates global oxygen sensing and redox signaling in Staphylococcus aureus.* J Am Chem Soc, 2012. **134**(1): p. 305-14.
51. Hall, J.W., et al., *The Staphylococcus aureus AirSR Two-Component System Mediates Reactive Oxygen Species Resistance via Transcriptional Regulation of Staphyloxanthin Production.* Infect Immun, 2017. **85**(2).
52. Pragman, A.A., et al., *Characterization of virulence factor regulation by SrrAB, a two-component system in Staphylococcus aureus.* J Bacteriol, 2004. **186**(8): p. 2430-8.
53. James, K.L., et al., *Interplay of Nitric Oxide Synthase (NOS) and SrrAB in Modulation of Staphylococcus aureus Metabolism and Virulence.* Infection and Immunity, 2018. **87**(2).
54. Ulrich, M., et al., *The staphylococcal respiratory response regulator SrrAB induces ica gene transcription and polysaccharide intercellular adhesin expression, protecting Staphylococcus aureus from neutrophil killing under anaerobic growth conditions.* Mol Microbiol, 2007. **65**(5): p. 1276-87.
55. Mashruwala, A.A. and J.M. Boyd, *The Staphylococcus aureus SrrAB Regulatory System Modulates Hydrogen Peroxide Resistance Factors, Which Imparts Protection to Aconitase during Aerobic Growth.* PLOS ONE, 2017. **12**(1): p. e0170283.
56. Marrakchi, H., Y.M. Zhang, and C.O. Rock, *Mechanistic diversity and regulation of Type II fatty acid synthesis.* 2002. **30**(6): p. 1050-1055.
57. Hara, Y., et al., *Involvement of PlsX and the acyl-phosphate dependent sn-glycerol-3-phosphate acyltransferase PlsY in the initial stage of glycerolipid synthesis in Bacillus subtilis.* 2008. **83**(6): p. 433-442.

58. White, S.W., et al., *The Structural Biology of Type II Fatty Acid Biosynthesis.* Annual Review of Biochemistry, 2005. **74**(1): p. 791-831.
59. Parsons, J.B. and C.O. Rock, *Bacterial lipids: metabolism and membrane homeostasis.* Prog Lipid Res, 2013. **52**(3): p. 249-76.
60. Sen, S., et al., *Growth-Environment Dependent Modulation of Staphylococcus aureus Branched-Chain to Straight-Chain Fatty Acid Ratio and Incorporation of Unsaturated Fatty Acids.* PLOS ONE, 2016. **11**(10): p. e0165300.
61. Singh, V.K., et al., *Insertional inactivation of branched-chain alpha-keto acid dehydrogenase in Staphylococcus aureus leads to decreased branched-chain membrane fatty acid content and increased susceptibility to certain stresses.* Appl Environ Microbiol, 2008. **74**(19): p. 5882-90.
62. Balemans, W., et al., *Essentiality of FASII pathway for Staphylococcus aureus.* Nature, 2010. **463**(7279): p. E3; discussion E4.
63. Wang, Y. and S. Ma, *Recent Advances in Inhibitors of Bacterial Fatty Acid Synthesis Type II (FASII) System Enzymes as Potential Antibacterial Agents.* 2013: p. n/a-n/a.
64. Parsons, J.B. and C.O. Rock, *Is bacterial fatty acid synthesis a valid target for antibacterial drug discovery?* 2011. **14**(5): p. 544-549.
65. Parsons, J.B., et al., *Identification of a two-component fatty acid kinase responsible for host fatty acid incorporation by Staphylococcus aureus.* Proc Natl Acad Sci U S A, 2014. **111**(29): p. 10532-7.
66. Bose, J.L., et al., *Identification of the Staphylococcus aureus vfrAB operon, a novel virulence factor regulatory locus.* Infect Immun, 2014. **82**(5): p. 1813-22.
67. Morvan, C., et al., *Environmental fatty acids enable emergence of infectious Staphylococcus aureus resistant to FASII-targeted antimicrobials.* 2016. **7**: p. 12944.
68. Morvan, C., et al., *The Staphylococcus aureus FASII bypass escape route from FASII inhibitors.* Biochimie, 2017. **141**: p. 40-46.
69. Kuhn, S., C.J. Slavetinsky, and A. Peschel, *Synthesis and function of phospholipids in Staphylococcus aureus.* Int J Med Microbiol, 2015. **305**(2): p. 196-202.
70. Ratledge, C. and S.G. Wilkinson, *Microbial lipids*. 1988: London: Academic Press.
71. Oku, Y., et al., *Characterization of the Staphylococcus aureus mprF gene, involved in lysinylation of phosphatidylglycerol.* Microbiology, 2004. **150**(Pt 1): p. 45-51.
72. Koprivnjak, T., et al., *Characterization of Staphylococcus aureus Cardiolipin Synthases 1 and 2 and Their Contribution to Accumulation of Cardiolipin in Stationary Phase and within Phagocytes.* 2011. **193**(16): p. 4134-4142.
73. Tsai, M., et al., *Staphylococcus aureus requires cardiolipin for survival under conditions of high salinity.* BMC Microbiol, 2011. **11**: p. 13.
74. Chandler, C.E. and R.K. Ernst, *Bacterial lipids: powerful modifiers of the innate immune response.* F1000Research, 2017. **6**: p. 1334.
75. Nguyen, M.T. and F. Gotz, *Lipoproteins of Gram-Positive Bacteria: Key Players in the Immune Response and Virulence.* Microbiol Mol Biol Rev, 2016. **80**(3): p. 891-903.
76. Peschel, A., et al., *Staphylococcus aureus Resistance to Human Defensins and Evasion of Neutrophil Killing via the Novel Virulence Factor Mprf Is Based on Modification of Membrane Lipids with l-Lysine.* The Journal of Experimental Medicine, 2001. **193**(9): p. 1067-1076.

77. Jiang, J.-H., et al., *Antibiotic resistance and host immune evasion in Staphylococcus aureus mediated by a metabolic adaptation.* Proceedings of the National Academy of Sciences, 2019. **116**(9): p. 3722-3727.
78. Dowds, C.M., et al., *Lipid antigens in immunity.* 2014. **395**(1).
79. Liu, Y., et al., *Gram-Positive Bacterial Extracellular Vesicles and Their Impact on Health and Disease.* Frontiers in Microbiology, 2018. **9**.
80. Kiezel-Tsugunova, M., A.C. Kendall, and A. Nicolaou, *Fatty acids and related lipid mediators in the regulation of cutaneous inflammation.* Biochem Soc Trans, 2018. **46**(1): p. 119-129.
81. Lampe, M.A., et al., *Human stratum corneum lipids: characterization and regional variations.* J Lipid Res, 1983. **24**(2): p. 120-30.
82. McDevitt, D., et al., *Characterization of the Interaction Between the Staphylococcus Aureus Clumping Factor (ClfA) and Fibrinogen.* 1997. **247**(1): p. 416-424.
83. Que, Y.-A., et al., *Fibrinogen and fibronectin binding cooperate for valve infection and invasion in Staphylococcus aureus experimental endocarditis.* 2005. **201**(10): p. 1627-1635.
84. Patti, J.M., et al., *Molecular characterization and expression of a gene encoding a Staphylococcus aureus collagen adhesin.* J Biol Chem, 1992. **267**(7): p. 4766-72.
85. Gries, C.M., et al., *Staphylococcus aureus fibronectin binding protein A mediates biofilm development and infection.* Infect Immun, 2020.
86. Boles, B.R., et al., *Identification of genes involved in polysaccharide-independent Staphylococcus aureus biofilm formation.* PLoS One, 2010. **5**(4): p. e10146.
87. Mashruwala, A.A., et al., *SaeRS Is Responsive to Cellular Respiratory Status and Regulates Fermentative Biofilm Formation in Staphylococcus aureus.* Infect Immun, 2017. **85**(8): p. IAI.00157-17.
88. Laarman, A.J., et al., *Staphylococcus aureus metalloprotease aureolysin cleaves complement C3 to mediate immune evasion.* J Immunol, 2011. **186**(11): p. 6445-53.
89. Drapeau, G.R., Y. Boily, and J. Houmard, *Purification and properties of an extracellular protease of Staphylococcus aureus.* J Biol Chem, 1972. **247**(20): p. 6720-6.
90. Shaw, L., et al., *The role and regulation of the extracellular proteases of Staphylococcus aureus.* Microbiology, 2004. **150**(Pt 1): p. 217-28.
91. Paharik, A.E., et al., *The Spl Serine Proteases Modulate Staphylococcus aureus Protein Production and Virulence in a Rabbit Model of Pneumonia.* mSphere, 2016. **1**(5): p. e00208-16.
92. Kolar, S.L., et al., *Extracellular proteases are key mediators of Staphylococcus aureus virulence via the global modulation of virulence-determinant stability.* MicrobiologyOpen, 2013. **2**(1): p. 18-34.
93. Cunningham, L., B.W. Catlin, and M.P. De Garilhe, *A Deoxyribonuclease of Micrococcus pyogenes.* Journal of the American Chemical Society, 1956. **78**(18): p. 4642-4645.
94. Olson, M.E., et al., *Staphylococcus aureus Nuclease Is an SaeRS-Dependent Virulence Factor.* 2013. **81**(4): p. 1316-1324.
95. Holland, K.T., D. Taylor, and A.M. Farrell, *The effect of glycerol monolaurate on growth of, and production of toxic shock syndrome toxin-1 and lipase by, Staphylococcus aureus.* J Antimicrob Chemother, 1994. **33**(1): p. 41-55.

96. Delekta, P.C., et al., *Staphylococcus aureus Utilizes Host-Derived Lipoprotein Particles as Sources of Fatty Acids.* Journal of Bacteriology, 2018. **200**(11).
97. Miale, J.B., *The Role of Staphylocoagulase in Blood Coagulation.* Blood, 1949. **4**(9): p. 1039-1048.
98. Lehman, M.K., et al., *Protease-Mediated Growth of Staphylococcus aureus on Host Proteins Is opp3 Dependent.* mBio, 2019. **10**(2).
99. Hartleib, J., et al., *Protein A is the von Willebrand factor binding protein on Staphylococcus aureus.* Blood, 2000. **96**(6): p. 2149-2156.
100. Forsgren, A. and P.G. Quie, *Effects of staphylococcal protein A on heat labile opsonins.* J Immunol, 1974. **112**(3): p. 1177-80.
101. Falugi, F., et al., *Role of Protein A in the Evasion of Host Adaptive Immune Responses by Staphylococcus aureus.* 2013. **4**(5): p. e00575-13-e00575.
102. Veldkamp, K.E., et al., *Modulation of neutrophil chemokine receptors by Staphylococcus aureus supernate.* Infect Immun, 2000. **68**(10): p. 5908-13.
103. Postma, B., et al., *Chemotaxis Inhibitory Protein of Staphylococcus aureus Binds Specifically to the C5a and Formylated Peptide Receptor.* The Journal of Immunology, 2004. **172**(11): p. 6994-7001.
104. Rooijakkers, S.H.M., et al., *Immune evasion by a staphylococcal complement inhibitor that acts on C3 convertases.* Nature Immunology, 2005. **6**(9): p. 920-927.
105. Inoshima, I., et al., *A Staphylococcus aureus pore-forming toxin subverts the activity of ADAM10 to cause lethal infection in mice.* Nat Med, 2011. **17**(10): p. 1310-4.
106. Wilke, G.A. and J.B. Wardenburg, *Role of a disintegrin and metalloprotease 10 in Staphylococcus aureus -hemolysin-mediated cellular injury.* Proceedings of the National Academy of Sciences, 2010. **107**(30): p. 13473-13478.
107. Walev, I., et al., *Selective killing of human monocytes and cytokine release provoked by sphingomyelinase (beta-toxin) of Staphylococcus aureus.* Infect Immun, 1996. **64**(8): p. 2974-9.
108. Marshall, M.J., G.A. Bohach, and D.F. Boehm, *Characterization of Staphylococcus aureus beta-toxin induced leukotoxicity.* J Nat Toxins, 2000. **9**(2): p. 125-38.
109. Katayama, Y., et al., *Beta-hemolysin promotes skin colonization by Staphylococcus aureus.* J Bacteriol, 2013. **195**(6): p. 1194-203.
110. Coleman, D.C., et al., *Staphylococcus aureus bacteriophages mediating the simultaneous lysogenic conversion of beta-lysin, staphylokinase and enterotoxin A: molecular mechanism of triple conversion.* J Gen Microbiol, 1989. **135**(6): p. 1679-97.
111. Goerke, C., J. Koller, and C. Wolz, *Ciprofloxacin and trimethoprim cause phage induction and virulence modulation in Staphylococcus aureus.* Antimicrob Agents Chemother, 2006. **50**(1): p. 171-7.
112. Alonzo, F., 3rd and V.J. Torres, *The bicomponent pore-forming leucocidins of Staphylococcus aureus.* Microbiol Mol Biol Rev, 2014. **78**(2): p. 199-230.
113. Alonzo, F., 3rd, et al., *Staphylococcus aureus leucocidin ED contributes to systemic infection by targeting neutrophils and promoting bacterial growth in vivo.* Mol Microbiol, 2012. **83**(2): p. 423-35.
114. Dumont, A.L., et al., *Characterization of a new cytotoxin that contributes to Staphylococcus aureus pathogenesis.* Molecular Microbiology, 2011. **79**(3): p. 814-825.
115. Spaan, A.N., et al., *The staphylococcal toxin Panton-Valentine Leukocidin targets human C5a receptors.* Cell Host Microbe, 2013. **13**(5): p. 584-594.

116. Smith, M.L. and S.A. Price, *Staphylócoceus γ Haemolysin.* The journal of pathology and bacteriology, 1938. **47**(3): p. 379-393.
117. DuMont, A.L., et al., *Staphylococcus aureus LukAB cytotoxin kills human neutrophils by targeting the CD11b subunit of the integrin Mac-1.* Proc Natl Acad Sci U S A, 2013. **110**(26): p. 10794-9.
118. Mehlin, C., C.M. Headley, and S.J. Klebanoff, *An inflammatory polypeptide complex from Staphylococcus epidermidis: isolation and characterization.* J Exp Med, 1999. **189**(6): p. 907-18.
119. Wang, R., et al., *Identification of novel cytolytic peptides as key virulence determinants for community-associated MRSA.* Nature Medicine, 2007. **13**(12): p. 1510-1514.
120. Surewaard, B.G., et al., *Inactivation of staphylococcal phenol soluble modulins by serum lipoprotein particles.* PLoS Pathog, 2012. **8**(3): p. e1002606.
121. Surewaard, B.G., et al., *Staphylococcal alpha-phenol soluble modulins contribute to neutrophil lysis after phagocytosis.* Cell Microbiol, 2013. **15**(8): p. 1427-37.
122. Periasamy, S., et al., *How Staphylococcus aureus biofilms develop their characteristic structure.* Proceedings of the National Academy of Sciences, 2012. **109**(4): p. 1281-1286.
123. Novick, R.P., et al., *The agr P2 operon: An autocatalytic sensory transduction system in Staphylococcus aureus.* Molecular and General Genetics MGG, 1995. **248**(4): p. 446-458.
124. Novick, R.P., *Autoinduction and signal transduction in the regulation of staphylococcal virulence.* Molecular Microbiology, 2003. **48**(6): p. 1429-1449.
125. Thoendel, M. and A.R. Horswill, *Identification of Staphylococcus aureus AgrD Residues Required for Autoinducing Peptide Biosynthesis.* Journal of Biological Chemistry, 2009. **284**(33): p. 21828-21838.
126. Boisset, S., et al., *Staphylococcus aureus RNAIII coordinately represses the synthesis of virulence factors and the transcription regulator Rot by an antisense mechanism.* Genes Dev, 2007. **21**(11): p. 1353-66.
127. Bronesky, D., et al., *Staphylococcus aureus RNAIII and Its Regulon Link Quorum Sensing, Stress Responses, Metabolic Adaptation, and Regulation of Virulence Gene Expression.* Annu Rev Microbiol, 2016. **70**: p. 299-316.
128. Cheung, A.L., et al., *Regulation of virulence determinants in vitro and in vivo in Staphylococcus aureus.* FEMS Immunol Med Microbiol, 2004. **40**(1): p. 1-9.
129. Bayer, M.G., J.H. Heinrichs, and A.L. Cheung, *The molecular architecture of the sar locus in Staphylococcus aureus.* Journal of bacteriology, 1996. **178**(15): p. 4563-4570.
130. Chien, Y.-T., et al., *SarA, a Global Regulator of Virulence Determinants inStaphylococcus aureus, Binds to a Conserved Motif Essential for sar-dependent Gene Regulation.* Journal of Biological Chemistry, 1999. **274**(52): p. 37169-37176.
131. Chien, Y.-T. and A.L. Cheung, *Molecular Interactions between Two Global Regulators,sarandagr, inStaphylococcus aureus.* Journal of Biological Chemistry, 1998. **273**(5): p. 2645-2652.
132. Zielinska, A.K., et al., *sarA-mediated repression of protease production plays a key role in the pathogenesis of Staphylococcus aureus USA300 isolates.* Mol Microbiol, 2012. **86**(5): p. 1183-96.
133. Loughran, A.J., et al., *Impact of individual extracellular proteases on Staphylococcus aureus biofilm formation in diverse clinical isolates and their isogenic sarA mutants.* Microbiologyopen, 2014. **3**(6): p. 897-909.

134. Cheung, A.L., K. Nishina, and A.C. Manna, *SarA of Staphylococcus aureus binds to the sarA promoter to regulate gene expression.* J Bacteriol, 2008. **190**(6): p. 2239-43.
135. Villanueva, M., et al., *Sensory deprivation in Staphylococcus aureus.* Nature Communications, 2018. **9**(1).
136. Fedtke, I., et al., *The nitrate reductase and nitrite reductase operons and the narT gene of Staphylococcus carnosus are positively controlled by the novel two-component system NreBC.* J Bacteriol, 2002. **184**(23): p. 6624-34.
137. Dubrac, S., et al., *New Insights into the WalK/WalR (YycG/YycF) Essential Signal Transduction Pathway Reveal a Major Role in Controlling Cell Wall Metabolism and Biofilm Formation in Staphylococcus aureus.* Journal of Bacteriology, 2007. **189**(22): p. 8257-8269.
138. Delaune, A., et al., *The WalKR system controls major staphylococcal virulence genes and is involved in triggering the host inflammatory response.* Infect Immun, 2012. **80**(10): p. 3438-53.
139. Pietiainen, M., et al., *Transcriptome analysis of the responses of Staphylococcus aureus to antimicrobial peptides and characterization of the roles of vraDE and vraSR in antimicrobial resistance.* BMC Genomics, 2009. **10**: p. 429.
140. Falord, M., et al., *Investigation of the Staphylococcus aureus GraSR Regulon Reveals Novel Links to Virulence, Stress Response and Cell Wall Signal Transduction Pathways.* PLoS ONE, 2011. **6**(7): p. e21323.
141. Flannagan, R.S., et al., *Staphylococcus aureus Uses the GraXRS Regulatory System To Sense and Adapt to the Acidified Phagolysosome in Macrophages.* MBio, 2018. **9**(4).
142. Rogasch, K., et al., *Influence of the Two-Component System SaeRS on Global Gene Expression in Two Different Staphylococcus aureus Strains.* Journal of Bacteriology, 2006. **188**(22): p. 7742-7758.
143. Giraudo, A.T., et al., *Characterization of a Tn551-mutant of Staphylococcus aureus defective in the production of several exoproteins.* Can J Microbiol, 1994. **40**(8): p. 677-81.
144. Giraudo, A.T., et al., *The sae locus of Staphylococcus aureus encodes a two-component regulatory system.* FEMS Microbiol Lett, 1999. **177**(1): p. 15-22.
145. Jeong, D.-W., et al., *The auxiliary protein complex SaePQ activates the phosphatase activity of sensor kinase SaeS in the SaeRS two-component system of Staphylococcus aureus.* 2012. **86**(2): p. 331-348.
146. Jeong, D.W., et al., *Identification of the P3 Promoter and Distinct Roles of the Two Promoters of the SaeRS Two-Component System in Staphylococcus aureus.* Journal of Bacteriology, 2011. **193**(18): p. 4672-4684.
147. Mainiero, M., et al., *Differential Target Gene Activation by the Staphylococcus aureus Two-Component System saeRS.* Journal of Bacteriology, 2010. **192**(3): p. 613-623.
148. Krute, C.N., K.C. Rice, and J.L. Bose, *VfrB Is a Key Activator of the Staphylococcus aureus SaeRS Two-Component System.* J Bacteriol, 2017. **199**(5).
149. Ericson, M.E., et al., *Role of Fatty Acid Kinase in Cellular Lipid Homeostasis and SaeRS-Dependent Virulence Factor Expression in Staphylococcus aureus.* MBio, 2017. **8**(4).
150. Tong, S.Y., et al., *Staphylococcus aureus infections: epidemiology, pathophysiology, clinical manifestations, and management.* Clin Microbiol Rev, 2015. **28**(3): p. 603-61.

151. Klevens, R.M., *Invasive Methicillin-Resistant Staphylococcus aureus Infections in the United States.* JAMA, 2007. **298**(15): p. 1763.
152. Ernst, C.M. and A. Peschel, *MprF-mediated daptomycin resistance.* International Journal of Medical Microbiology, 2019.
153. Lu, H. and P.J. Tonge, *Inhibitors of FabI, an Enzyme Drug Target in the Bacterial Fatty Acid Biosynthesis Pathway.* 2008. **41**(1): p. 11-20.
154. Omura, S., *The antibiotic cerulenin, a novel tool for biochemistry as an inhibitor of fatty acid synthesis.* Bacteriol Rev, 1976. **40**(3): p. 681-97.
155. Wang, J., et al., *Platensimycin is a selective FabF inhibitor with potent antibiotic properties.* Nature, 2006. **441**(7091): p. 358-361.
156. Parsons, J.B., et al., *Incorporation of extracellular fatty acids by a fatty acid kinase-dependent pathway inStaphylococcus aureus.* Molecular Microbiology, 2014. **92**(2): p. 234-245.
157. Kaiser, J.C., et al., *The role of two branched-chain amino acid transporters inStaphylococcus aureusgrowth, membrane fatty acid composition and virulence.* Molecular Microbiology, 2016. **102**(5): p. 850-864.
158. Krute, C.N., K.C. Rice, and J.L. Bose, *VfrB is a key activator of the Staphylococcus aureus SaeRS two-component system.* 2016: p. JB.00828-16.
159. DeMars, Z. and J.L. Bose, *Redirection of Metabolism in Response to Fatty Acid Kinase in Staphylococcus aureus.* J Bacteriol, 2018. **200**(19).
160. Krute, C.N., et al., *Inactivation of the exogenous fatty acid utilization pathway leads to increased resistance to unsaturated fatty acids in Staphylococcus aureus.* Microbiology, 2019. **165**(2): p. 197-207.
161. Alnaseri, H., et al., *DNA Binding and Sensor Specificity of FarR, a Novel TetR Family Regulator Required for Induction of the Fatty Acid Efflux Pump FarE in Staphylococcus aureus.* Journal of Bacteriology, 2018. **201**(3).
162. Bligh, E.G. and W.J. Dyer, *A RAPID METHOD OF TOTAL LIPID EXTRACTION AND PURIFICATION.* Canadian Journal of Biochemistry and Physiology, 1959. **37**(8): p. 911-917.
163. Ernst, C.M., et al., *The Bacterial Defensin Resistance Protein MprF Consists of Separable Domains for Lipid Lysinylation and Antimicrobial Peptide Repulsion.* 2009. **5**(11): p. e1000660.
164. Parsons, J.B., et al., *Metabolic basis for the differential susceptibility of Gram-positive pathogens to fatty acid synthesis inhibitors.* 2011. **108**(37): p. 15378-15383.
165. Braungardt, H. and V.K. Singh, *Impact of Deficiencies in Branched-Chain Fatty Acids and Staphyloxanthin in Staphylococcus aureus.* BioMed Research International, 2019. **2019**: p. 1-8.
166. Subczynski, W.K. and A. Wisniewska, *Physical properties of lipid bilayer membranes: relevance to membrane biological functions.* Acta Biochim Pol, 2000. **47**(3): p. 613-25.
167. Gruszecki, W.I. and K. Strzałka, *Carotenoids as modulators of lipid membrane physical properties.* Biochimica et Biophysica Acta (BBA) - Molecular Basis of Disease, 2005. **1740**(2): p. 108-115.
168. Mishra, N.N., et al., *Carotenoid-Related Alteration of Cell Membrane Fluidity Impacts Staphylococcus aureus Susceptibility to Host Defense Peptides.* 2011. **55**(2): p. 526-531.

169. Mogen, A.B., et al., *Staphylococcus aureus nitric oxide synthase (saNOS) modulates aerobic respiratory metabolism and cell physiology.* Mol Microbiol, 2017. **105**(1): p. 139-157.
170. Lewis, A.M., et al., *Examination of theStaphylococcus aureusnitric oxide reductase (saNOR) reveals its contribution to modulating intracellular NO levels and cellular respiration.* Molecular Microbiology, 2015. **96**(3): p. 651-669.
171. Hayami, M., et al., *Lipid Composition ofStaphylococcus aureusand Its Derived L-forms.* 1979. **23**(6): p. 435-442.
172. Mishra, N.N. and A.S. Bayer, *Correlation of Cell Membrane Lipid Profiles with Daptomycin Resistance in Methicillin-Resistant Staphylococcus aureus.* Antimicrobial Agents and Chemotherapy, 2013. **57**(2): p. 1082-1085.
173. Mukhopadhyay, K., et al., *In vitro susceptibility of Staphylococcus aureus to thrombin-induced platelet microbicidal protein-1 (tPMP-1) is influenced by cell membrane phospholipid composition and asymmetry.* Microbiology, 2007. **153**(4): p. 1187-1197.
174. Parsons, J.B., et al., *Membrane Disruption by Antimicrobial Fatty Acids Releases Low-Molecular-Weight Proteins from Staphylococcus aureus.* Journal of Bacteriology, 2012. **194**(19): p. 5294-5304.
175. Lopez, M.S., et al., *Host-derived fatty acids activate type VII secretion in Staphylococcus aureus.* Proc Natl Acad Sci U S A, 2017. **114**(42): p. 11223-11228.
176. Tiwari, K., C. Gatto, and B. Wilkinson, *Interrelationships between Fatty Acid Composition, Staphyloxanthin Content, Fluidity, and Carbon Flow in the Staphylococcus aureus Membrane.* Molecules, 2018. **23**(5): p. 1201.
177. Unden, G. and J. Bongaerts, *Alternative respiratory pathways of Escherichia coli: energetics and transcriptional regulation in response to electron acceptors.* Biochimica et Biophysica Acta (BBA) - Bioenergetics, 1997. **1320**(3): p. 217-234.
178. Neumann, Y., et al., *The effect of skin fatty acids on Staphylococcus aureus.* 2015. **197**(2): p. 245-267.
179. Kenny, J.G., et al., *The Staphylococcus aureus Response to Unsaturated Long Chain Free Fatty Acids: Survival Mechanisms and Virulence Implications.* PLoS ONE, 2009. **4**(2): p. e4344.
180. Devaiah, S.P., et al., *Quantitative profiling of polar glycerolipid species from organs of wild-type Arabidopsis and a phospholipase Dalpha1 knockout mutant.* Phytochemistry, 2006. **67**(17): p. 1907-24.
181. Welti, R., et al., *Profiling membrane lipids in plant stress response.* J Biol Chem, 2002. **277**: p. 31994-32002.
182. Narayanan, S., et al., *Wheat leaf lipids during heat stress: I. High day and night temperatures result in major lipid alterations.* Plant Cell Environ, 2016. **39**(4): p. 787-803.
183. Brugger, B., et al., *Quantitative analysis of biological membrane lipids at the low picomole level by nano-electrospray ionization tandem mass spectrometry.* Proc Natl Acad Sci U S A, 1997. **94**(6): p. 2339-44.
184. Welti, R., et al., *Profiling membrane lipids in plant stress responses. Role of phospholipase D alpha in freezing-induced lipid changes in Arabidopsis.* J Biol Chem, 2002. **277**(35): p. 31994-2002.

185. Singh, V.K., et al., *Roles of pyruvate dehydrogenase and branched-chain α-keto acid dehydrogenase in branched-chain membrane fatty acid levels and associated functions in Staphylococcus aureus.* Journal of Medical Microbiology, 2018. **67**(4): p. 570-578.
186. Lowy, F.D., *Staphylococcus aureus infections.* N Engl J Med, 1998. **339**(8): p. 520-32.
187. Somerville, G.A., *At the Crossroads of Bacterial Metabolism and Virulence Factor Sythesis in Staphylocci.* 2009.
188. Mlynek, K.D., et al., *Nutritional regulation of the Sae two-component system by CodY in Staphylococcus aureus.* J Bacteriol, 2018.
189. Krute, C.N., K.C. Rice, and J.L. Bose, *VfrB is a key activator of the Staphylococcus aureus SaeRS two-component system.* J Bacteriol, 2016.
190. Sabirova, J.S., et al., *Fatty acid kinase A is an important determinant of biofilm formation in Staphylococcus aureus USA300.* BMC Genomics, 2015. **16**: p. 861.
191. Thomas, V.C., et al., *A central role for carbon-overflow pathways in the modulation of bacterial cell death.* PLoS Pathog, 2014. **10**(6): p. e1004205.
192. Sadykov, M.R., et al., *Inactivation of the Pta-AckA pathway causes cell death in Staphylococcus aureus.* J Bacteriol, 2013. **195**(13): p. 3035-44.
193. Somerville, G.A., et al., *Correlation of acetate catabolism and growth yield in Staphylococcus aureus: implications for host-pathogen interactions.* Infect Immun, 2003. **71**(8): p. 4724-32.
194. Heath, R.J., S.W. White, and C.O. Rock, *Lipid biosynthesis as a target for antibacterial agents.* Progress in Lipid Research, 2001. **40**(6): p. 467-497.
195. Atkinson, D.E. and G.M. Walton, *Adenosine triphosphate conservation in metabolic regulation. Rat liver citrate cleavage enzyme.* J Biol Chem, 1967. **242**(13): p. 3239-41.
196. Sonenshein, A.L., *CodY, a global regulator of stationary phase and virulence in Gram-positive bacteria.* Curr Opin Microbiol, 2005. **8**(2): p. 203-7.
197. Kaiser, J.C., et al., *Repression of branched-chain amino acid synthesis in Staphylococcus aureus is mediated by isoleucine via CodY, and by a leucine-rich attenuator peptide.* PLoS Genet, 2018. **14**(1): p. e1007159.
198. Enjalbert, B., et al., *Acetate fluxes in Escherichia coli are determined by the thermodynamic control of the Pta-AckA pathway.* Sci Rep, 2017. **7**: p. 42135.
199. Lei, T., J. Yang, and Y. Ji, *Determination of essentiality and regulatory function of staphylococcal YeaZ in branched-chain amino acid biosynthesis.* Virulence, 2015. **6**(1): p. 75-84.
200. Lei, T., et al., *The essentiality of staphylococcal Gcp is independent of its repression of branched-chain amino acids biosynthesis.* PLoS One, 2012. **7**(10): p. e46836.
201. Parsons, J.B., et al., *Metabolic basis for the differential susceptibility of Gram-positive pathogens to fatty acid synthesis inhibitors.* Proc Natl Acad Sci U S A, 2011. **108**(37): p. 15378-83.
202. Onal Okyay, T. and D. Frigi Rodrigues, *High throughput colorimetric assay for rapid urease activity quantification.* J Microbiol Methods, 2013. **95**(3): p. 324-6.
203. Stuart, C.A., E. Vanstratum, and R. Rustigian, *Further Studies on Urease Production by Proteus and Related Organisms.* Journal of Bacteriology, 1945. **49**(5): p. 437-444.
204. Krausz, K.L. and J.L. Bose, *Bacteriophage Transduction in Staphylococcus aureus: Broth-Based Method.* Methods Mol Biol, 2016. **1373**: p. 63-8.

205. Livak, K.J. and T.D. Schmittgen, *Analysis of relative gene expression data using real-time quantitative PCR and the 2(-Delta Delta C(T)) Method.* Methods, 2001. **25**(4): p. 402-8.
206. Lewis, A.M. and K.C. Rice, *Quantitative Real-Time PCR (qPCR) Workflow for Analyzing Staphylococcus aureus Gene Expression.* Methods Mol Biol, 2016. **1373**: p. 143-54.
207. Moormeier, D.E., et al., *Use of Microfluidic Technology To Analyze Gene Expression during Staphylococcus aureus Biofilm Formation Reveals Distinct Physiological Niches.* Applied and Environmental Microbiology, 2013. **79**(11): p. 3413-3424.
208. Mogen, A.B., et al., *Staphylococcus aureus nitric oxide synthase (saNOS) modulates aerobic respiratory metabolism and cell physiology.* Mol Microbiol, 2017.
209. Kreiswirth, B.N., et al., *The toxic shock syndrome exotoxin structural gene is not detectably transmitted by a prophage.* Nature, 1983. **305**(5936): p. 709-712.
210. Fey, P.D., et al., *A genetic resource for rapid and comprehensive phenotype screening of nonessential Staphylococcus aureus genes.* MBio, 2013. **4**(1): p. e00537-12.
211. Lehman, M.K., et al., *Identification of the amino acids essential for LytSR-mediated signal transduction in Staphylococcus aureus and their roles in biofilm-specific gene expression.* Mol Microbiol, 2015. **95**(4): p. 723-37.
212. Suaya, J.A., et al., *Incidence and cost of hospitalizations associated with Staphylococcus aureus skin and soft tissue infections in the United States from 2001 through 2009.* 2014. **14**(1): p. 296.
213. Tiwari, S., et al., *Two-Component Signal Transduction Systems of Pathogenic Bacteria As Targets for Antimicrobial Therapy: An Overview.* Frontiers in Microbiology, 2017. **8**.
214. Wang, S., *Bacterial Two-Component Systems: Structures and Signaling Mechanisms, Protein Phosphorylation in Human Health.* InTech 2012.
215. Li, M., et al., *Gram-positive three-component antimicrobial peptide-sensing system.* Proc Natl Acad Sci U S A, 2007. **104**(22): p. 9469-74.
216. Kuroda, M., et al., *Two-component system VraSR positively modulates the regulation of cell-wall biosynthesis pathway in Staphylococcus aureus.* 2004. **49**(3): p. 807-821.
217. Bhate, M.P., et al., *Structure and Function of the Transmembrane Domain of NsaS, an Antibiotic Sensing Histidine Kinase in Staphylococcus aureus.* Journal of the American Chemical Society, 2018. **140**(24): p. 7471-7485.
218. Geiger, T., et al., *The Virulence Regulator Sae of Staphylococcus aureus: Promoter Activities and Response to Phagocytosis-Related Signals.* Journal of Bacteriology, 2008. **190**(10): p. 3419-3428.
219. Liu, Q., et al., *The Extracytoplasmic Linker Peptide of the Sensor Protein SaeS Tunes the Kinase Activity Required for Staphylococcal Virulence in Response to Host Signals.* 2015. **11**(4): p. e1004799.
220. Steinhuber, A., et al., *Molecular architecture of the regulatory Locus sae of Staphylococcus aureus and its impact on expression of virulence factors.* J Bacteriol, 2003. **185**(21): p. 6278-86.
221. Makgotlho, P.E., et al., *SDS Interferes with SaeS Signaling of Staphylococcus aureus Independently of SaePQ.* PLoS ONE, 2013. **8**(8): p. e71644.
222. DeMars, Z., V.K. Singh, and J.L. Bose, *Exogenous Fatty Acids Remodel Staphylococcus aureus Lipid Composition through Fatty Acid Kinase.* J Bacteriol, 2020. **202**(14).

223. Galbraith, H. and T.B. Miller, *Effect of long chain fatty acids on bacterial respiration and amino acid uptake.* J Appl Bacteriol, 1973. **36**(4): p. 659-75.
224. Kuroda, H., et al., *Subinhibitory concentrations of β-lactam induce haemolytic activity in Staphylococcus aureus through the SaeRS two-component system.* FEMS Microbiology Letters, 2007. **268**(1): p. 98-105.
225. Yoon, B.K., et al., *Antibacterial Free Fatty Acids and Monoglycerides: Biological Activities, Experimental Testing, and Therapeutic Applications.* Int J Mol Sci, 2018. **19**(4).
226. Chatterjee, A., P.K. Dutta, and R. Chowdhury, *Effect of Fatty Acids and Cholesterol Present in Bile on Expression of Virulence Factors and Motility of Vibrio cholerae.* Infection and Immunity, 2007. **75**(4): p. 1946-1953.
227. Marques, C., D. Davies, and K. Sauer, *Control of Biofilms with the Fatty Acid Signaling Molecule cis-2-Decenoic Acid.* Pharmaceuticals, 2015. **8**(4): p. 816-835.
228. Plecha, S.C. and J.H. Withey, *Mechanism for Inhibition of Vibrio cholerae ToxT Activity by the Unsaturated Fatty Acid Components of Bile.* 2015. **197**(10): p. 1716-1725.
229. Golubeva, Y.A., et al., *Intestinal Long-Chain Fatty Acids Act as a Direct Signal To Modulate Expression of the Salmonella Pathogenicity Island 1 Type III Secretion System.* mBio, 2016. **7**(1): p. e02170-15.
230. Sternkopf Lillebaek, E.M., et al., *Antimicrobial medium- and long-chain free fatty acids prevent PrfA-dependent activation of virulence genes in Listeria monocytogenes.* Res Microbiol, 2017. **168**(6): p. 547-557.
231. Dos Santos, P.T., et al., *Free fatty acids interfere with the DNA binding activity of the virulence regulator PrfA of Listeria monocytogenes.* J Bacteriol, 2020.
232. Lehman, M.K., J.L. Bose, and K.W. Bayles, *Allelic Exchange.* Methods Mol Biol, 2016. **1373**: p. 89-96.
233. Cue, D., et al., *SaeRS-Dependent Inhibition of Biofilm Formation in Staphylococcus aureus Newman.* PLOS ONE, 2015. **10**(4): p. e0123027.
234. Luong, T.T., et al., *Staphylococcus aureus ClpC Divergently Regulates Capsule via sae and codY in Strain Newman but Activates Capsule via codY in Strain UAMS-1 and in Strain Newman with Repaired saeS.* Journal of Bacteriology, 2011. **193**(3): p. 686-694.
235. Flack, C.E., et al., *Differential regulation of staphylococcal virulence by the sensor kinase SaeS in response to neutrophil-derived stimuli.* 2014. **111**(19): p. E2037-E2045.
236. Malachowa, N., et al., *Characterization of a Staphylococcus aureus Surface Virulence Factor That Promotes Resistance to Oxidative Killing and Infectious Endocarditis.* Infection and Immunity, 2011. **79**(1): p. 342-352.
237. Bose, J.L., P.D. Fey, and K.W. Bayles, *Genetic tools to enhance the study of gene function and regulation in Staphylococcus aureus.* Appl Environ Microbiol, 2013. **79**(7): p. 2218-24.
238. Charpentier, E., et al., *Novel Cassette-Based Shuttle Vector System for Gram-Positive Bacteria.* Applied and Environmental Microbiology, 2004. **70**(10): p. 6076-6085.
239. Brinster, S., et al., *Type II fatty acid synthesis is not a suitable antibiotic target for Gram-positive pathogens.* Nature, 2009. **458**(7234): p. 83-6.
240. Khemici, V., et al., *The DEAD-box RNA helicase CshA is required for fatty acid homeostasis in Staphylococcus aureus.* PLOS Genetics, 2020. **16**(7): p. e1008779.
241. Pande, S.V. and J.F. Mead, *Inhibition of enzyme activities by free fatty acids.* J Biol Chem, 1968. **243**(23): p. 6180-5.

242. Tippett, P.S. and K.E. Neet, *An allosteric model for the inhibition of glucokinase by long chain acyl coenzyme A.* Journal of Biological Chemistry, 1982. **257**(21): p. 12846-12852.
243. Jordan, S., et al., *Regulation of LiaRS-Dependent Gene Expression in Bacillus subtilis: Identification of Inhibitor Proteins, Regulator Binding Sites, and Target Genes of a Conserved Cell Envelope Stress-Sensing Two-Component System.* Journal of Bacteriology, 2006. **188**(14): p. 5153-5166.